

3-11-2011

Biological investigation of the stimulated flapping motions of the moth, *Manduca sexta*

Travis B. Tubbs

Follow this and additional works at: <https://scholar.afit.edu/etd>

Part of the [Aerodynamics and Fluid Mechanics Commons](#)

Recommended Citation

Tubbs, Travis B., "Biological investigation of the stimulated flapping motions of the moth, *Manduca sexta*" (2011). *Theses and Dissertations*. 1360.

<https://scholar.afit.edu/etd/1360>

This Thesis is brought to you for free and open access by the Student Graduate Works at AFIT Scholar. It has been accepted for inclusion in Theses and Dissertations by an authorized administrator of AFIT Scholar. For more information, please contact richard.mansfield@afit.edu.



**BIOLOGICAL INVESTIGATION OF
THE STIMULATED FLAPPING MOTIONS OF THE MOTH, *MANDUCA SEXTA***

THESIS

Travis B. Tubbs, Captain, USAF

AFIT/GSS/ENY/11-M04

**DEPARTMENT OF THE AIR FORCE
AIR UNIVERSITY**

AIR FORCE INSTITUTE OF TECHNOLOGY

Wright-Patterson Air Force Base, Ohio

APPROVED FOR PUBLIC RELEASE; DISTRIBUTION UNLIMITED

The views expressed in this thesis are those of the author and do not reflect the official policy or position of the United States Air Force, Department of Defense, or the United States Government. This material is declared a work of the U.S. Government and is not subject to copyright protection in the United States.

AFIT/GSS/ENY/11-M04

**BIOLOGICAL INVESTIGATION OF
THE STIMULATED FLAPPING MOTIONS OF THE MOTH, *MANDUCA SEXTA***

THESIS

Presented to the Faculty

Department of Aeronautics and Astronautics

Graduate School of Engineering and Management

Air Force Institute of Technology

Air University

Air Education and Training Command

In Partial Fulfillment of the Requirements for the

Degree of Master of Science (Space Systems)

Travis B. Tubbs, BS

Captain, USAF

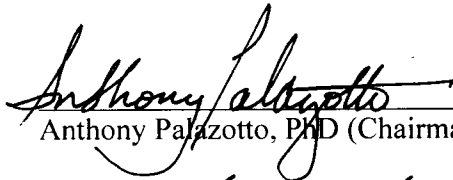
March 2011

APPROVED FOR PUBLIC RELEASE; DISTRIBUTION UNLIMITED

BIOLOGICAL INVESTIGATION OF
THE STIMULATED FLAPPING MOTIONS OF THE *MANDUCA SEXTA*

Travis B. Tubbs, BS
Captain, USAF

Approved:




Anthony Palazotto, PhD (Chairman)

3-4-11
Date



Richard Cobb, PhD (Member)

3-4-11
Date



Mark Willis, PhD (Member)

3-4-11
Date

Abstract

An investigation was conducted assessing the possibility and feasibility of reproducing the biological flapping motion of the wings of the moth, *Manduca sexta* (hawkmoth) by artificially stimulating the flight muscles for Micro Air Vehicle research. Electromyographical signals were collected using bipolar intramuscular fine wire electrodes inserted into the primary flight muscles, the dorsal longitudinal and dorsal ventral muscles, of the adult *M.sexta*. These signals were recorded and associated with wing movement using high speed video. The signals were reapplied into the corresponding muscle groups with the intention of reproducing similar flapping motion. A series of impulse signals were also directed into the primary flight muscles as a means of observing muscle response through measured forewing angles. This study pioneered electromyographic research on *M.sexta* at the Air Force Institute of Technology with tests conducted with pupal implants and fine wire electrodes. Through this process, the research showed the deformational structural changes that take place when a wing is removed from an insect and proved that muscular stimulation is a viable means of measuring wing movement while still attached to the moth. This study also assisted in developing an understanding related to the role that a thorax-like fuselage could play in future micro aircraft designs. This study has shown that partial neuromuscular control of the primary flight muscles a *Manduca sexta* is possible with electrical stimulants which could be used to directly control insect flight.

AFIT/GSS/ENY/11-M04

To Father, Mother, Wife, and Children

Acknowledgements

I am truly grateful for the many people who made this work possible. I would first like to thank all the professors that helped with the research. Most important is Dr. Anthony Palazotto for his trust and willingness to let me pursue the research that I was interested in. His excitement about the research was inspiring; I hope to be like him someday. To Dr. Mark Willis, for taking the time to train me in the ways of *Manduca* raising and biological research, and for always being willing to lend his help and reassurance. To Dr. Richard Cobb who provided clear guidance and Matlab expertise throughout this entire process. To our sponsors Dr Doug Smith (AFOSR) and Dr Richard Snyder (AFRL) for providing the monetary support needed to make this research possible.

Many non-professor people made this work come together and they must be thanked. To Lt Jonathan Climber who's ninja like Matlab skills enabled me to gather data. To Mrs. Heidi Cahoon, who deftly converted my rambling into compete sentences, her attention to detail is beyond compare. And to Lt Nathaniel DeLeon and Maj Ryan O'Hara, who were always stepping up with ideas and support when needed.

My closest ally in this effort has always been and always will be my wonderful wife. Her patience while raising a colony of hawkmoths in our house and my unconventional approach to the subject is extraordinary. She provided inspiring insight and wisdom. Without her help I could accomplish nothing.

Lastly I must acknowledge God in all things and in all thing give him praise. Many prayers were offered throughout my time at AFIT (usually during exams) and the fact that this thesis is complete is a testament to His support. I thank God for all that I am:

“Therefore, let us glory, yea, we will glory in the Lord; yea, we will rejoice, for our joy is full; yea, we will praise our God forever. Behold, who can glory too much in the Lord? Yea, who can say too much of his great power, and of his mercy, and of his long-suffering towards the children of men?” (Alma 26:16.)

Table of Contents

	Page
AFIT/GSS/ENY/11-M04	iv
Abstract	iv
AFIT/GSS/ENY/11-M04	v
Acknowledgements	vi
List of Figures	x
List of Tables	xiv
List of Acronyms	xv
I. Introduction	1
Objective	1
Background	2
Natural Template	5
Iterative Research Process	7
<i>M.sexta</i> Flight Muscles	8
What is Electromyography?.....	9
History of Electromyography	10
Electrical Signals Controlling Animals	12
<i>M.sexta</i> Flight Muscles	13
EMG in <i>M.sexta</i>	15
Biological Flapping Mechanism	16
Research Overview	18
Document Overview	19
II. Theory	21
The Biological Process	21
Neural Signals	22
Recording the Muscular Potential Difference.....	27
The EMG Signal	29
Signal Sampling	32
Theoretical Summary.....	33
III. Experimentation	34
Experimenting with Living Organisms.....	34
Pilot Study.....	34
Initial Development	38

	Page
The Implant.....	39
Electromyography and <i>M. sexta</i>	39
Initial Failures	41
Rising Moths	43
Better Implant Methodology.....	43
Fine Wire Implants	46
EMG and Flapping Motion.....	49
High Speed Wing Angles.....	50
Potential Energy Process.....	53
Experimental Summary	57
IV. Results and Discussion.....	58
Implant Results	58
Fine Wire EMG.....	60
Natural Unstimulated Flapping Angle	62
EMG Signal Analysis	64
Transmitted EMG Signal	66
Transmitted Impulse Signals to Individual Muscles.....	67
Transmitted Impulse Signals to DLMs and DVMs	71
Faster Transmitted Signals.....	73
Clear Frequency Response.....	78
Voltage Response.....	80
Pulse Width Modulation	82
Results Summary	83
V. Summary and Conclusion	85
Flapping Angle Data	85
EMG Signals	86
Reapplying the EMG Signal	87
Transmitting Impulse Signals	88
Experimental Limitations.....	88
Sample Size Limitations	89
Relevance of the Current Investigation.....	89
Final Statement	91
Appendix A.....	92
Scientific Instrument Used.....	92
NI USB 6229	92
HP 3312A 15MHZ Function Generator.....	92

	Page
Instruments Division-Signal Conditioning Amplifier 2310.....	93
Eyeclips	93
Lux Thermostat	94
Repticare Heat Emitter	94
Tektronix TDS 420 A.....	94
Microsoft LifeCam.....	95
Stemi SV 6 Zeiss	95
Casio Exilim EX-FC 150	96
The Implant FFC to BNC Adapter.....	96
Appendix B.....	97
Manduca Sexta Background	97
Eggs.....	98
Larvae.....	98
Pupae	99
Adults (Manduca sexta)	100
Preparation	101
Hatching Chamber.....	101
Rearing Chamber.....	102
Pupating Chamber	102
Moth Cage	103
Bibliography	104

List of Figures

Figure	Page
1. “Pine hawkmoth sitting on conifer bark” (Sauer, n.d)	4
2. <i>M.sexta</i> feeding at dusk, this species is also known as the hummingbird moth because of its rapid agile flight (Hinterwirth, 2010)	4
3. A fossilized Pterodactyl (unknown, n.d); prehistoric fossils provide valuable insight into how flight was first achieved	5
4. An adult female <i>Manduca Sexta</i> (hawkmoth) from the colony of Dr. Mark Willis at Case Western University	6
5. A flow chart depicting the iterative process used to improve Micro Air Vehicle, designs based off of biological attributes	7
6. A cross-sectional view of a <i>M.sexta</i> thorax showing the primary flight muscles: A) DVM contracting, causing an up-stroke; B) DVM relaxing, while the DLM begins to contract; C) DLM contracting, causing a down-stroke.....	9
7. Animals that have responded to applied electrical signals: A) <i>Manduca Sexta</i> , Hawkmoth; B) <i>Blaberus discoidalis</i> , Cockroach; C) <i>Mecynorrhina torquata</i> , Flower Beetle; D) <i>Rattus norvegicus</i> , Rat; E) <i>Columba livia</i> , Pigeon.....	12
8. X-ray cross section of <i>M.sexta</i> thorax indicating the 5 muscle fiber bundles of each of the DLMs.....	13
9. Cross-section of <i>M.sexta</i> showing the primary flight muscles, DVM (green) and DLM (red)	13
10. A graphical picture of the different muscle units and the neurons that are associated with them (Kondoh & Obara, 1982)	14
11. Side view depiction showing the motoneuron (MN1-4 solid and MN5 dashed) placement in the muscle.	14
12. Sequence of images demonstrating muscular control through implants: A) The pupae implant connection to <i>M.sexta</i> ; B) Resting posture; C) Signal supplied to DVM inducing upstroke reaction; D) Signal supplied to DLM to induce down-stroke reaction.....	16
13. Images taken from time-lapse video showing the structural changes of two severed wings over time, one in the foreground and one in the background	17
14. One example of a flapping mechanism that removed the wing from the thorax before testing (Sims, Palazotto, & Norris, 2010)	17
15. Graphical representation of an EMG backpack designed for <i>M.sexta</i>	21
16. A cartoon representation of the resting condition of muscle cells; There is a negative potential difference inside the cell due to the concentration of sodium ions outside the cell membrane	22
17. Idealized depiction of the changes of membrane voltage over time, due to ion changes caused by the Action Potential, with specific characteristics labeled.....	23
18. A depiction of how the Action Potential (AP), seen in yellow, is related to electrical signals: A) The AP moves across the membrane changing the polarity while the inset graph shows the voltage increasing; B) As the AP reaches an ion channel, Na ⁺ diffuses in, rapidly making the cell more positive; C) The AP then causes the K ⁺ channel to open so that potassium leaves the cell, causing a rapid drop in voltage; D) The AP moves on to activate more cells, and the normal cell processes restore the resting potential	25

	Page
19. A depiction of how an insect muscle responds to neurological signals; this single muscle is composed of two different muscle units, each innervated with the axons of a different mononeuron; as a signal travels, it uses the transverse tubular system to activate multiple areas of the muscle to induce contraction	26
20. Ionic potential difference is collected and amplified; the difference between the two electrodes, the differential output, is recorded as EMG	27
21. EMG signal processing techniques	29
22. (A-C): Personal Medical EMG recordings of the first dorsal interosseous muscle (muscle between the thumb and forefinger on the back of the hand) taken by Dr. Joshua Alpers, MD, to demonstrate EMG signals: A) Signal from a single motor neuron with nearly relaxed muscle; B) Increased motor neuron signals activated through increased contractions; C) Multiple motor neurons recorded at maximum muscle contraction.....	31
23. Power Spectral Density recorded from the Right Dorsal Longitudinal Muscle of the <i>M.sexta</i>	33
24. A) Fellow research student, Nate Deleon, observing the dissection of a <i>M.sexta</i> larvae; B) Tubules; C) Ganglia; D) Nervous System; E) Brain (indicated by arrow).....	35
25. A) Dr. Mark Willis, demonstrating proper implant techniques; B) Applying dental wax to fix an implanted electrode; C) Inserting second pair of electrodes into Left Dorsal Longitudinal Muscle.....	37
26. EMG signals from a <i>M.sexta</i> , using fine wire implants; the recorded signals are superimposed below the picture	37
27. A) Computer Tomography of a <i>M.sexta</i> ; B) Side view showing the Dorsal Longitudinal Muscle; C) Cross section showing the Dorsal Longitudinal Muscles (DLMs) and Dorsal Ventral Muscles (DVMs).....	38
28. Rapid prototype of the CT scan of the <i>M.sexta</i>	39
29. Pupae implant, based on Dr. Bozkurt's design; the fly-out shows the tip at 200x magnification	39
30. Computer simulated depiction of the pupae implant location on the adult <i>M.sexta</i> after emerging from the pupal stage; the components used for testing are listed	41
31. Improvised implant tool used to consistently produce small holes in the <i>M.sexta</i> exoskeleton at a consistent separation distance apart; B) The tool is overlaid on top of an implant to ensure proper tip spacing	43
32. Surgically puncturing the pupae shell with the implant tool	44
33. The only successful emergence of a <i>M.sexta</i> with the pupae implant attached.....	44
34. A closer view of where the implant is being inserted.....	44
35. Only successful moth to emerge attached to FFC.....	45
36. Cross section of a pupae that failed to emerge, the black portion is evidence of muscle decay.....	45
37. Multiple pupae were implanted with very limited success	45
38. Attempting to record EMG signals using pupae implant	45
39. Screen shots of <i>M.sexta</i> flight using a Casio Exilim FC-150 HS camera	46
40. Implanted <i>M.sexta</i> in the DLM (red arrows) and DVM (green) using 0.008" silver fine wires coated with Teflon.....	47
41. Diagram used by Dr. Willis to demonstrate proper DVM implant location.....	47
42. The silver fine wire used to collect EMG signals; fly-out shows a close up of the actual wire and the Teflon coating at 400x magnification.....	47

	Page
43. Simulink used to record EMG signals from <i>M.sexta</i>	48
44. Simulink used to transmit EMG signals to <i>M.sexta</i>	48
45. EMG signal collection and transmission process.....	49
46. Four sequences of images being processed through Adobe After Effects and Matlab; A) Lowest point in the down-stroke; B) Moving through the up-stroke; C) Highest point on up-stroke; D) Moving through the down-stroke.....	52
47. Centroid of wing found using Matlab.....	53
48. Two images superimposed to find the wing angle (α) associated with tergum displacement as indicated by red arrow	54
49. A graphical representation of the calculated triangles and the associated lengths to determine the centroid displacement	55
50. Chart depicting implant mortality rate.....	58
51. Matlab graph showing the only EMG recording made with a pupae implant, the highlighted area in red can be seen in the ‘Zoomed In’ section of the graph.....	59
52. A photograph of the surviving pupae implant moth while the signals are being recorded	59
53. One complete recording of EMG signals. Two periods of flapping motion can be seen.....	61
54. <i>M.sexta</i> wing angles, the fly-out shows a closer view of one complete flapping cycle.	62
55. Overlay of found flapping angles with those found experimentally from Wilming and Elington.....	63
56. A chart indicating the frequency responsive components of the signals	64
57. The cropped EMG signals from the primary flight muscle of the <i>M.sexta</i>	65
58. Flapping angles found when stimulated with previously recorded EMG signals	66
59. 5V signal directed into the LDVM at a 1.9 second interval; the impulse was 0.19 seconds long	68
60. 5V signal directed into the LDLM at a 1.9 second interval; the impulse was 0.19 seconds long	69
61. 5V signal directed into the RDLM at a 1.9 second interval; the impulse was 0.19 seconds long	70
62. 5V signal directed into the RDVM at a 1.9 second interval; the impulse was 0.19 seconds long	71
63. Wing angle response with two different 5V signals, the DLM impulse signal was 180 degrees out of phase	72
64. Two different 5V signals supplied with a 0.756 second period and a 0.0756 second signal length; the red is supplied to the DVM and the green is supplied to the DLM	73
65. The natural flapping angle from the <i>M.Sexta</i> (blue) and the artificially stimulated signal (green), overlaid to show the differences.....	74
66. Two different 5V signals supplied with a .756 second period and a .0756 second signal length; the red is supplied to the DVM and the green is supplied to the DLM; during this test, the signals were randomly removed from the test subject to indicate that the supplied signal was in fact causing the motion.	75
67. Matlab’s spectrogram function showing the natural wing beat frequency over time	76
68. Matlab’s spectrogram function showing the artificially stimulated wing beat frequency over time	77
69. Incrementally increasing the transmitted frequency. The different colors were added using Photoshop to indicate the different frequencies. The numbers in the red box indicate the frequency in Hz associated with that color.	78

	Page
70. Matlab spectrogram depicting the frequencies transmitted to the DLMs by the function generator	79
71. Matlab spectrogram depicting the frequency response of the transmitted signal in Figure 70	79
72. The transmitted voltage incrementally increased and decreased and associated wing response	81
73. Pulse width modulation test, three different tests were conducted with all the variables consistent except the pulse width. The top transmitted signal had a pulse width of 0.0076 seconds; the middle transmitted signal had a pulse width of 0.0038 seconds; the bottom transmitted signal had a pulse width of 0.0023 seconds.....	82
74. <i>M.sexta</i> hatching from its egg at 400x magnification	98
75. Newly hatched <i>M.sexta</i> on the edge of a penny	98
76. <i>M.sexta</i> larvae becoming a pupae	99
77. Mature larvae eating hornworm diet	99
78. <i>M.sexta</i> pupae emerging as an adult	100
79. Adult <i>M.sexta</i> inflating its wings	101

List of Tables

Table	Page
1. MAV Design Requirements.....	6

List of Acronyms

AFIT-Air Force Institute of Technology

AP-Action Potential

BNC-Bayonet Neill-Concelman

EAPs-Electroactive Polymers

EMG-Electromyography

DARPA- Defense Advanced Research Projects Agency

DLM-Dorsal Longitudinal Muscle

DoD- Department of Defense

DVM-Dorsal Ventral Muscle

FFC-Flat Flex Cable

FPS-Frames Per Second

MAV- Micro Air Vehicle

MEMs-Micro-Electromechanical Systems

MU- Muscle Unit

MUAP-Muscle Unit Action Potentials

PSD-Power Spectral Density

PWM-Pulse Width Modulation

BIOLOGICAL INVESTIGATION OF THE STIMULATED FLAPPING MOTIONS OF THE MANDUCA SEXTA

I. Introduction

Objective

The primary objective of this thesis is to determine the possibility and benefits of reproducing the biological flapping motion of a hawkmoth, *M.sexta*, with artificial stimulation for the purpose of Micro Air Vehicle (MAV) development. An examination will be conducted of the electromyographical¹ (EMG) signals produced by the dorsal longitudinal muscles (DLMs) and dorsal ventral muscles (DVMs) in the adult *M.sexta* using a bipolar intramuscular fixed wire implant. A pupal stage implant was also investigated with inconclusive results. The EMG signals were recorded, and an attempt was made to associate the signals with wing movement using high speed video. The recorded EMG signals were then reapplied into the corresponding muscle group with the intention of reproducing similar flapping motion. Additional impulse signals were then applied to determine the resulting wing response.

This investigation will shed additional light on the biomechanics of insect flight and provide information that could be utilized directly for bioelectric muscle control of an insect, or could be extrapolated for future MAV designs based on of the biological response characteristics. An additional aspect of this research is the possibility of using *M.sexta* as a “living” flapping mechanism, which would allow wing movement to be studied with the insect’s natural boundary conditions intact. The ability to induce desired

¹ Electromyography is a technique for evaluating and recording the electrical activity of muscles

wing movements through electro-muscular stimulation has the potential to greatly advance biologically inspired MAV research specifically with respect to control design.

Background

The desire of those involved in clandestine activity, to be the proverbial “fly on the wall,” is rapidly and intentionally becoming a reality. There is a concerted effort being made by the Department of Defense (DoD) and Defense Advanced Research Projects Agency (DARPA) to design and develop aircraft that are not only very small in scale, but also function and perform in a manner similar to flying animals found in nature. This departure from standard flight design offers many great benefits, but it is still in its infancy.

Micro Air Vehicles (MAVs) are being pursued as future technological platforms for conducting missions and providing invaluable data to not only the immediate tactical soldier, but also to operational and strategic military leaders. This technology is developing quickly and will clearly be available in the future. To ensure that the United States is on the forefront of MAV research and development, DARPA is providing requirements (Table 1), funding, and a goal of insect size MAV development by 2030.

MAVs have obvious military applications, but they could also provide significant assistance in the civilian sector in areas such as: scientific research, police situations, or to assist with search and rescue operations. A small flying robot can be used in many dangerous situations, such as searching through collapsed tunnels and mines, or buildings damaged by earthquakes. MAVs could be used to provide valuable surveillance to counter hazardous criminal activities, such as police stand-offs or drug trafficking, could greatly reduce the risk to human life. MAVs could be used to gather data in places where

humans cannot go, such as at the sites of toxic chemical spills or damaged nuclear reactors (Alexander, 2002).

Dr. Mark Reeder, Editor-in-Chief of the *International Journal of Micro Air Vehicles*, explains that MAVs have a set of constraints which are considerably different from those of traditional aircraft, such as fast-response non-linear controls, nano-structures, integrated propulsion and lift mechanisms, highly flexible structures, and low Reynolds number aerodynamics (Reeder, 2009). The complexity of these mechanisms often forces different disciplines of research to cooperate in novel ways as they attempt to understand how to best address the challenges facing MAV flight (Reeder, 2009).

Biological-aerodynamics is one example of traditionally diverse areas of scientific research that has recently emerged due to the desire to understand and incorporate many of the biological aspects found in the numerous and highly successful MAVs found in nature. In the paper, *Biological Inspiration for Agile Autonomous Air Vehicles*, Johnny Evers accurately points out that biology, unlike many engineering fields, does not have a unified suite of mathematical formulas that clearly predicts animal behavior, which makes it seem to be observational, heuristic, and considered by many practicing physicists, chemists, and engineers to be a “soft” science. He further notes that biological studies help to bring about a much more complete picture of biological flight in relation to areas such as fluid dynamics, flight mechanics, control systems, and other studies performed by engineers because of their background in areas such as behavioral response characteristics, physiology, and even genetics.

An engineer may want to examine an insect to determine the optimal size of wings for high speed flight, but in nature there are many more factors that come into play. For example, the existing wing design for a particular species is really a compromise between camouflage (Figure 1), high speed and hovering flight modes (Figure 2). This is important to consider because, in nature characteristics are often optimized for more than one



Figure 1: “Pine hawkmoth sitting on conifer bark” (Sauer, n.d)

task. Natural selection says that animals have to be successful at many different and sometimes competing tasks. This means as humans, we should be careful about slavishly copying designs resulting from biological evolution. This example illustrates Evers’ argument for having a working partnership between the engineering and biological communities so that both parties could benefit from each other’s differing areas of expertise and view points.



Figure 2: *M.sexta* feeding at dusk, this species is also known as the hummingbird moth because of its rapid agile flight (Hinterwirth, 2010)

With regard to the study of biological flight and the human advancement in locomotion, Evers makes a very thought provoking statement:

“The study of biological locomotion seems to be a natural route to expansion of the capabilities of flying robots. Ironically then, the most universal technologies associated with human locomotion, the wheel, the rigid wing and the rotating propeller, are not found in nature. This irony provides a cautionary note that human engineered systems may have attributes and constraints that, ultimately, preclude biological solutions. (Evers, 2007)”

This statement captures the idea that it is possible that mankind may not be as advanced as we suppose when compared with nature. It also clearly impresses that despite humanities’ great accomplishments, it is important to keep in mind that there are likely alternate natural methods of functioning in the environment that have not been adequately researched and adapted to our needs.

Natural Template

“The unusual thing about *Manduca* is that it’s one of the most ordinary insects of all. The larvae is enormous. It has a very accessible nervous system and its organs are easy to isolate and dissect--that makes it a model organism of research. Entomologists call it ‘the white lab rat of insects.’ ”

Excerpt from the book, Ends of the Earth (Downs, 2009)

There are three main systems that are being examined in MAV research: fixed wing, flapping wing, and rotary wing movement. Under these main topics, there are many different models and approaches that are being pursued. Using nature as a template for development ensures that a working and functional model is used as a pattern for future decisions and procedures, such as



Figure 3: A fossilized Pterodactyl (unknown, n.d); prehistoric fossils provide valuable insight into how flight was first achieved

wing/fuselage development or testing the maximal lift capabilities in a given

environment. The four B's of biological flight are all being studied-namely, bats, birds, bugs and bones (Figure 3). Each group provides valuable insight about natural flight characteristics and helps scientists to better understand how nature has developed different flying mechanisms over time. The hope is that we as humans can use these systems to our benefit.

This thesis will focus on a specific biological system, the moth *M.sexta* (Figure 4). There is no question that *M.sexta* is a living Micro Air Vehicle that has developed through evolution for millions of years with the unique attributes that DARPA desires



Figure 4: An adult female *Manduca sexta* (hawkmoth) from the colony of Dr. Mark Willis at Case Western University

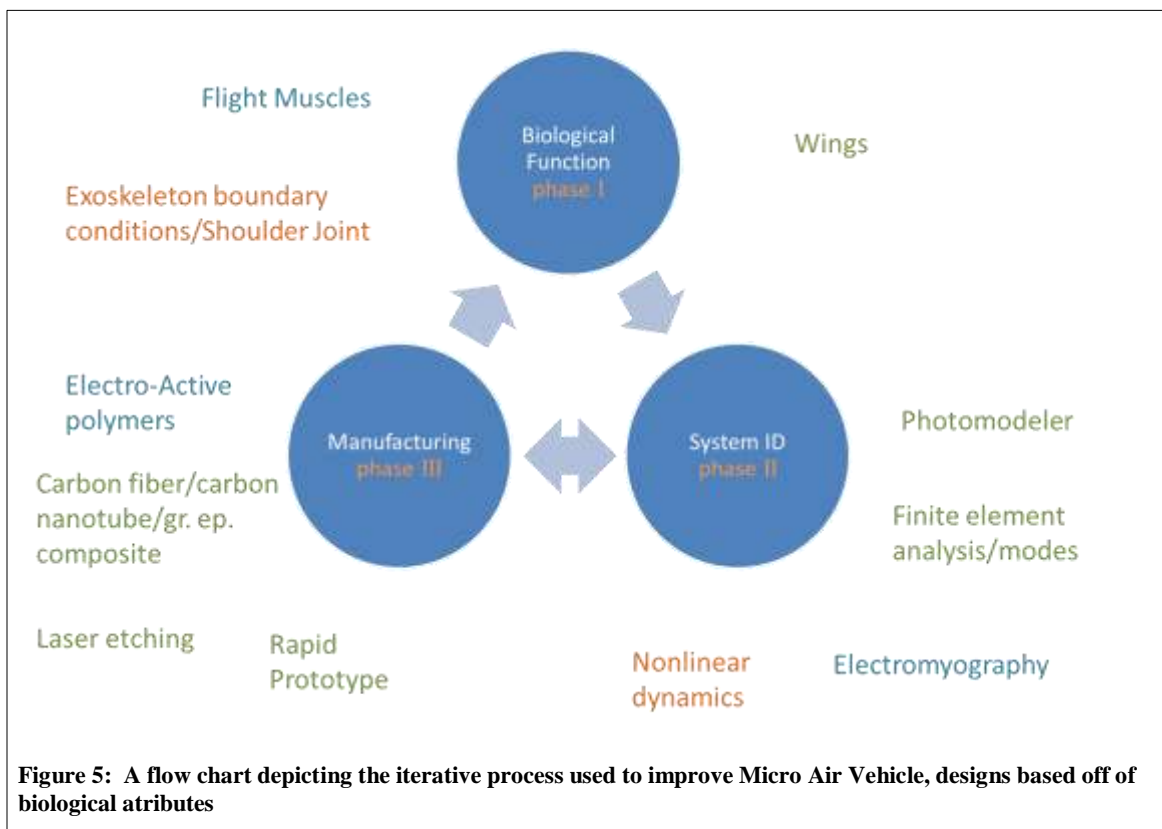
in MAVs by 2030 (Table 1). The qualities that enable functional flapping motion are of great interest, and will be examined at length with the intention of first understanding the biological process, next quantitatively determining the neuromuscular signals, and then experimentally associating flapping motion with signal inputs.

Table 1: MAV Design Requirements [Sims, 2009]

Specification	Requirements	Details
Size	< 15.24 cm	Maximum Dimension
Weight	~ 100 g	Gross Takeoff Weight
Range	1 to 10 km	Operational Range
Endurance	60 min	Loiter Time on Station
Altitude	< 150 m	Operational Ceiling
Speed	15 m/s	Maximum Flight Speed
Payload	20 g	Mission Dependent
Cost	\$1,500	Max Cost, 2009 (US Dollars)

Iterative Research Process

The overall objective of research, using bio-inspired technology and techniques, is to develop clear scientific understanding about some of the mechanisms that will facilitate the development of MAVs to meet DARPA specifications. To aid in this effort, a three phase iterative operational plan was developed for which the MAV research at AFIT, under Dr. Palazotto, can be characterized (Figure 5).



The intent of this plan is to chart the overall MAV research progress through the three phases of design and development. In the first phase, a specific biological function or characteristic is chosen from *M.sexta*. This phase focuses on determining which naturally occurring designs are available, and how they can be incorporated into a MAV

design. Some examples include wings, flight muscles, boundary conditions, and neurological signals.

The second phase identifies and focuses on the different methods available to collect or model experimental data. Selecting the best methodology is important for capturing the most useful information, which will provide greater insight into the biological processes, i.e. hovering, or the structure, i.e. the wing. This phase is also instrumental in validating manufactured materials from phase three.

The final phase focuses on manufacturing or designing some way of duplicating the original biological function of *M.sexta*. This is the proof of concept to verify that man is able to reproduce the biological response that was collected from the specimen. This also leads back into the biological phase because the manufactured product is compared to what is actually found in nature, ways to improve it are analyzed, and the process begins again to design an even better model that should more closely resemble the biological system. This is an iterative process, designed to improve understanding and development with each cycle.

***M.sexta* Flight Muscles**

As mentioned before, there are many different biological areas that need to be considered with regard to MAV flight. This research will focus primarily on the two major power producing muscles in flying insects, the dorsal longitudinal muscles (DLMs) and the dorsal ventral muscles (DVMs). Main power-producing muscles are stimulated by a single motor neuron, which means the total number of neurons controlling power production during flight is small (Willmott & Ellington, 1997).

The DVMs are the elevator muscles and indirectly cause the upward movement of the wings in all insects. This occurs because when the DVM muscles are contracted, they pull down the tergum (dorsal surface of the thorax), which moves the point of articulation of *M.sexta*'s wing down as well (Figure 6A) (Chapman, 1998). In most insects (including *M.sexta*), the downward wing (depression) is caused indirectly when the DLMs contract; then, the center of the tergum becomes bowed upward, and this moves the upper wing joint upward and the wing flaps down (Figure 6C) (Chapman, 1998).

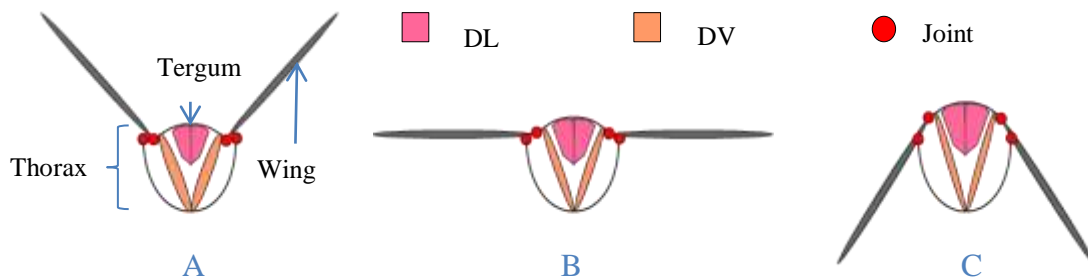


Figure 6: A cross-sectional view of a *M.sexta* thorax showing the primary flight muscles: A) DVM contracting, causing an up-stroke; B) DVM relaxing, while the DLM begins to contract; C) DLM contracting, causing a down-stroke

What is Electromyography?

The standard process of recording muscular contraction signals is Electromyography (EMG). EMG is a technique for evaluating and recording the electrical activity produced by muscles (Robertson, 2004). According to the National Library of Medicine, EMG is the measurement of the electrical potential generated by muscle cells when these cells are electrically or neurologically activated (Medicine, 2010). In insects, as well as vertebrates, biological signals are sent from the central nervous system through specialized cells, called motoneurons, to the muscles (Nation, 2002). When the muscles receive the electrical impulse, an ionic reaction known as the Action Potential (AP) is triggered. EMG is used to study this electrical impulse during

propagation through the muscle. Two electrical leads are used to measure the electrical AP of muscle fibers. This process will be discussed in greater detail in Chapter II.

History of Electromyography

The need to understand the physiological processes associated with flight are essential to accurately mimic biological specimens when designing MAVs. EMG has become the procedure of choice for gathering information about how the muscular system is activated to generate behavior. This process has been used for hundreds of years, and it is only becoming more useful as instruments and understanding improve.

Jan Swammerdam (1667) was the first to demonstrate that external stimulation of a nerve would result in muscle movement. He discovered that by stroking the nerve endings of a frog muscle, he was able to cause it to contract. In one version of Swammerdam's nerve muscle experiments, the nerve was suspended by a brass hook, which was then stroked with a silver wire; it is possible that this induced a small electrical current which would have been the first electrically stimulated muscular contraction (Cobb M. , 2002).

Francesco Redi's work in 1666 also dealt with electrical signals in muscles. He showed the exact muscle in the electric eel which generated electricity (Keithley, 1999). By 1773, in a letter to Benjamin Franklin, John Walsh showed that this same muscle tissue could generate a spark of electricity (Jungnickel & McCormach, 1999). One of the most important findings for this study was published in 1792 by Luigi Galvani, a physician who stumbled over the observation that electrical stimulation of a frog's leg

caused it to twitch. It was these results that caused a physicist named Alessandro Volta to study this phenomenon, and led to the discovery of electrical current (Keithley, 1999).

Nearly sixty years later, in 1849, Dubois-Raymond demonstrated (using frog muscles again) that electrical signals could be measured in muscle contractions (Braithwaite, 1853). The term electromyography was introduced by Etienne Marey when he made the first actual EMG recording of muscle contractions in 1890 (Dondelinger, 2011). In 1922, Gasser and Erlanger used an oscilloscope to show the electrical signals from muscles, but because of the nature of the signals and the low technology of the equipment that was being used, only rough information could be obtained from its observation. The capability of detecting electromyographic signals improved steadily from the 1930s throughout the 1950s, and researchers began to use improved electrodes more widely for the study of muscles (Dondelinger, 2011).

The advancement of EMG increased rapidly after the middle of the 1980s, when improvements in manufacturing enabled the mass production of fine wire² and amplifiers for medical purposes. The improved sensitivity and high quality equipment allowed much more refined recording techniques, and higher fidelity with the results (Zachry, 2004). Now, EMG has advanced far enough that many individuals use it as part of their personal workout routine for bodybuilding to maximize their strength training (Knight & Kinesiology, 2003).

² Thin wire electrodes which are inserted into the muscles, for this study 0.008” silver wire was used.

Electrical Signals Controlling Animals

Using electrical signals to stimulate animals into desired activity is not new. There are many examples of studies conducted using moths, cockroaches, beetles, rats, and even birds. Advanced micro-electromechanical systems (MEMS) allow integration with these living systems in order to exert some level of control over them. For example, Bozkurt et al. implanted microfabricated electrical probes at the pupal stage, which allowed direct electrical control over wing movement of a *M. sexta* moth (Figure 7a). The researchers were able to adjust flight direction of the moth by the actuation of down- and up-strokes of each wing with electrical impulses supplied to the moth's muscles (Bozkurt, Gilmour, & Lal, 2009). It has also been proven that it is possible to control the locomotor activity of a cockroach using brain nerve group stimulation (Figure 7b) (Watson & Ritzmann, 1995). Sato et al. demonstrated impressive control over beetle flight using an implanted and tetherless microsystem and electrical stimulation (Figure 7c) (Sato, et al., 2008).

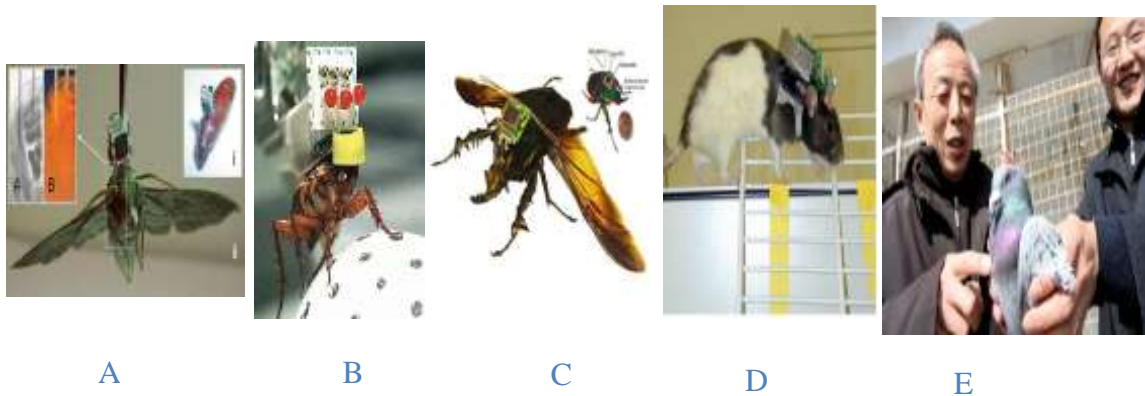


Figure 7: Animals that have responded to applied electrical signals: A) *Manduca Sexta*, Hawkmoth; B) *Blaberus discoidalis*, Cockroach; C) *Mecynorrhina torquata*, Flower Beetle; D) *Rattus norvegicus*, Rat; E) *Columba livia*, Pigeon

Higher animals have also proven susceptible to electrical stimuli. The ability to remotely control surgically implanted rats (Figure 7d) through mazes and over objects by using whisker sensations was demonstrated by Talwar et al. (Talwar, Xu, Hawley, Weiss, Moxon, & Chapin, 2002). It was also reported in the news that Chinese scientist Su Xuecheng was able to command a pigeon to fly right or left, and up or down, through an implant in the brain (Figure 7e) (Zhongying, 2007).

***M.sexta* Flight Muscles**

M.sexta is amongst the largest flying insects. Their flight is powered by two sets of synchronously activated muscles in the thorax (Figure 9). The DLMs are the largest muscles in the moth, comprising 5-8% of the total body mass (Tu & Daniel, 2004). The activation of these muscles can easily be detected with EMG because these synchronous muscles are usually activated only once in each wing stroke (Kammer, 1971). During flight, the DLM muscles function exclusively to generate the mechanical power used to depress the wings by compressing the

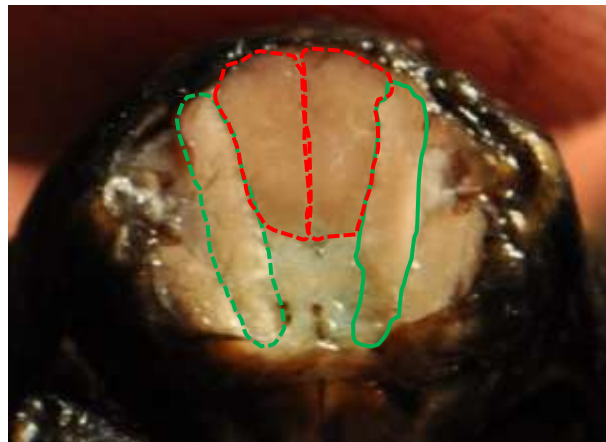


Figure 9: Cross-section of *M.sexta* showing the primary flight muscles, DVM (green) and DLM (red)

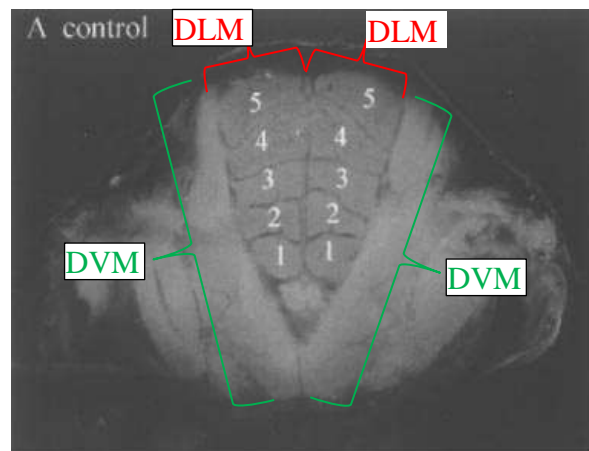


Figure 8: X-ray cross section of *M.sexta* thorax indicating the 5 muscle fiber bundles of each of the DLMs.

thorax, from the head to the abdomen (also known as the antero-posterior axis) (Tu & Daniel, 2004). The DVM compress the thorax in the orthogonal plane to power the wing up-stroke (Bertrand, Regnier, & Daniel, 2008).

The DLMs and DVMs, are made up of multiple muscle units (MU). The DLM has five muscle units or bundles (DLM 1-5) (Figure 8 and Figure 11). Motoneurons control the contraction of muscle fiber, and each of the DLM1–4 muscle fiber bundles are innervated by one of the four prothoracic motoneurons (MN1–4), are while DLM5 is innervated by the mesothoracic motoneuron, MN5 (Bayline, Duch, & Levine, 2001). The DVM has six muscle units (DVM 1a, 1b -5) (Figure 10). The DVMs are innervated by nine paired motoneurons and one UM-neurone (Kondoh & Obara, 1982). It is important to note that there is no overlap of innervation between muscle units (Keeley, n.d.). It is also important to understand the location of the muscle units and how they are innervated, because the number of motoneurons and their location determine

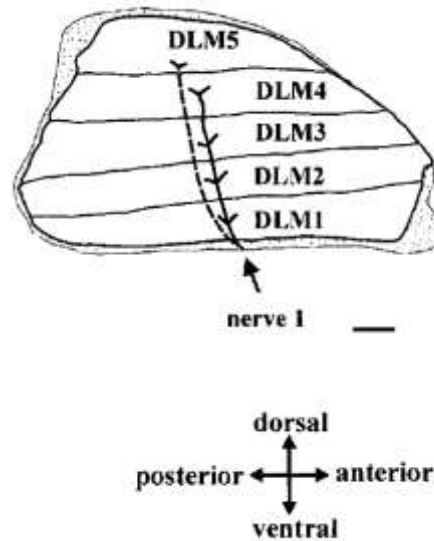


Figure 11: Side view depiction showing the motoneuron (MN1-4 solid and MN5 dashed) placement in the muscle.

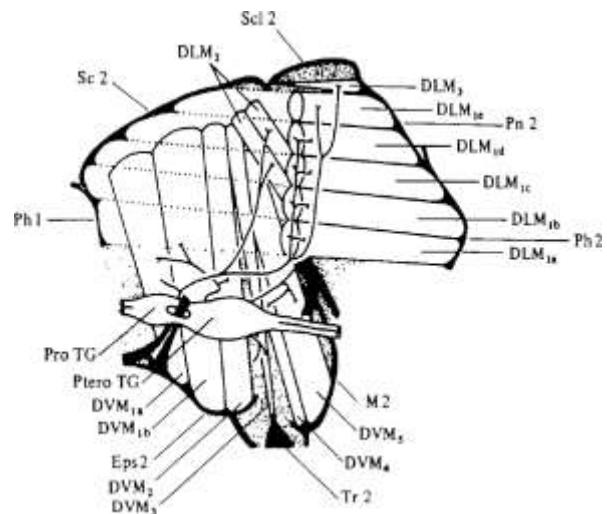


Figure 10: A graphical picture of the different muscle units and the neurons that are associated with them (Kondoh & Obara, 1982)

the EMG signals that are produced.

Another related fact is that in *M.sexta* and other insects there is a one-to-one correspondence between electrical potential recorded from the nervous system and the time it takes for the muscle to shorten and relax, which means that one signal produces one wing movement; this is not the case for insects that have asynchronous flight muscles (Chapman, 1998).

EMG in *M.sexta*

Using EMG on *M.sexta* muscular studies is not a new concept: Johnston and Levine have observed electromyographic activity of the leg muscles synchronized with video-taped recordings in the larval crawling and adult walking stages of *M.sexta* (Johnston & Levine, 1996). Wang, Ando, and Kanzaki used EMG to study the flight movement of the wings during free flight in a different species of hawkmoth (Wang, Ando, & Kanzaki, 2008), and Mohseni et al. studied the use of an ultralight biotelemetry backpack for recording EMG signals in *M.sexta* (Mohseni P. , Nagarajan, Ziaie, Najafi, & Crary, 2001).

The research herein is designed to provide an understanding of the signals that are required to induce natural wing movement. A portion of this study is based on research that was carried out by Alper Bozkurt at Cornell University, where surgical implants were directly placed into a *M.sexta*'s muscles during the pupal stage. Bozkurt's work demonstrated that EMG signals could be recorded and that electrical signals could be sent to the moth, altering movement and behavior (**Bozkurt, Gilmour, & Lal, 2009**). As stated earlier, the primary objective of this thesis is to determine what is required to

reproduce the biological flapping motion of *M.sexta* with artificial stimulation; as seen in Figure 12. Bozkurt has already demonstrated the ability to induce wing movement which demonstrates that *M.sexta* can be used as a biological MAV.

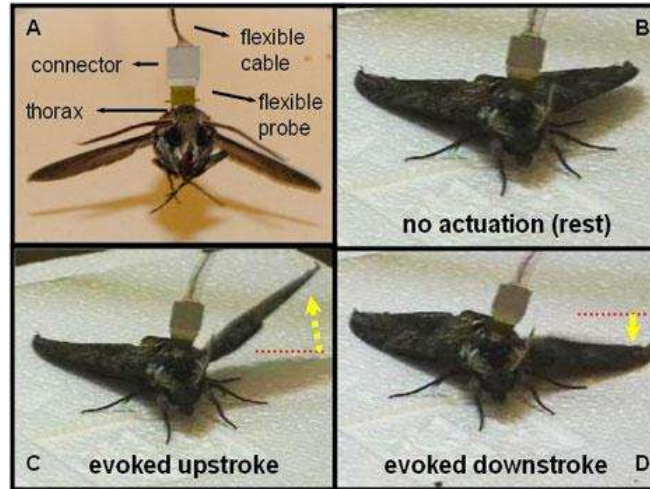


Figure 12: Sequence of images demonstrating muscular control through implants: A) The pupae implant connection to *M.sexta*; B) Resting posture; C) Signal supplied to DVM inducing upstroke reaction; D) Signal supplied to DLM to induce downstroke reaction

Biological Flapping Mechanism

An additional benefit for developing a method to quantitatively predict the flapping motion of the *M.sexta* is the ability to study the wing motion while maintaining the natural boundary conditions. The wing hinge is a complicated and difficult mechanical system that is currently impossible to duplicate and not well understood. Many researchers (Sims, Palazotto, & Norris, 2010) are simply removing *M.sexta* wings from the thorax and testing the wing properties separately. There are two fundamental problems with this approach. First, the properties are time dependent when removed from the body, and second, the boundary conditions are completely different from what is found naturally.

When removed, the wings begin to immediately desiccate (dry out), as seen in the time-lapse images shown in Figure 13. The most dramatic changes take place within the first three hours of removal, where the curvature of the wing becomes much more pronounced, and the structure becomes more brittle.

Despite the changes of the wing structure, the only way to correctly model the biological movement of *M.sexta* is to account for the boundary condition.

The current technique is to remove the wing and clamp it in some sort of flapping device (Figure 14) to

investigate the flapping properties of the wing. This induces a rigid boundary similar to a beam, while the physiological joint is much more complicated, involving many linkage systems and both direct and indirect muscles as seen in Figure 11.

The ability to study *M.sexta* wings under different flapping frequencies and movements, while eliminating the need to change the boundary conditions or remove the wings, would vastly improve the quality of the

data. Sending known signals into the appropriate muscles and receiving expected angular



Figure 13: Images taken from time-lapse video showing the structural changes of two severed wings over time, one in the foreground and one in the

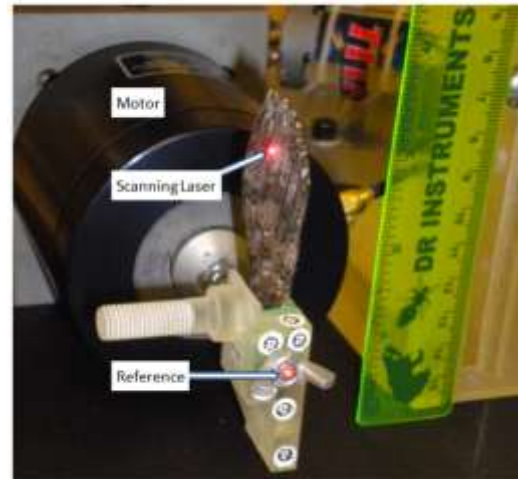


Figure 14: One example of a flapping mechanism that removed the wing from the thorax before testing (Sims, Palazotto, & Norris, 2010)

displacement would essentially transform the moth into a biological, flapping mechanism with all of the biological processes, mechanisms, and structures still accounted for.

Research Overview

The only way to accurately model the natural flapping motion of *M.sexta* is to correctly understand the neuromuscular impulses that induce specific wing movement. The electrical impulses that stimulate the flight muscles can be recorded and associated with specific forewing movement in *M.sexta*. The recorded EMG or impulse signals can then be reapplied to the flight muscles to generate predictive forewing movement.

This study will attempt to associate the signals produced by the indirect depressor (DLM) and levitator (DVM) muscles by examining the forewing motion of *M.sexta*. The bioelectrical impulses, which produce contraction of the DLMs and DVMs associated with the wing movement, will be recorded. Collecting EMG signals, while recording the flapping motion with high speed video cameras, will give an accurate picture of the flapping process of *M.sexta*. A correlation between the EMG and the wing movement will determine what signal induces a specific flapping motion. Knowing the signal and associated wing movement will increase understanding of how the moth is able to perform flight functions, and will shed additional light on what must be considered for MAV power generation to better mimic the natural species.

The recorded signals will then be reapplied to the respective muscles in an attempt to recreate the previously observed wing movement. The reapplication of previously recorded signals into a living specimen will enable verification of the wing response to specific stimuli. Being able to artificially produce predetermined wing

responses will have significant scientific applications regarding flight control, and could greatly increase experimental possibilities. Impulse signals will also be transmitted into the muscles to record the associated wing responses in an attempt to categorized what signals would be required to induce a specific movement.

The force required to generate wing elevation will be calculated based off the thoracic displacement and wing elevation. This will provide some idea of the forces needed to develop biologically similar MAV flight.

One possibility that should be considered as a means of force production for wing movement is the use of electroactive polymers (EAPs) in place of flight muscles (Tubbs, 2010). The data gathered provides a functional and observable template for possible qualities and forces that should be considered when attempting to mimic normal wing movements for flight.

Document Overview

The following four chapters are arranged in chronological order. Chapter II discusses the theory behind EMG, Action Potential, and signal processing. Chapter III explains the experimental work conducted at the Air Force Institute of Technology (AFIT) and at the Materials & Manufacturing Directorate of the Air Force Research Laboratory (AFRL). Chapter IV gives results and analysis. Chapter V reviews the highlights of each of the preceding chapters to present conclusions and opportunities for future endeavors.

The appendices follow Chapter V, and contain supplemental material from which one might gain further insight into the equipment used and instructions for those wishing

to conduct similar, future research, and general information outside the primary scope of this work. Finally, a bibliography contains the many different references used in preparation of this document.

II. Theory

“Electromyography is a seductive muse because it provides easy access to physiological processes that cause the muscle to generate force, produce movement, and accomplish the countless functions that allow us to interact with the world around us... To its detriment, electromyography is too easy to use and consequently too easy to abuse.” (De Luca, 1997)

The Biological Process

To determine the possibility and benefit of reproducing the biological flapping motion of a *M.sexta* with artificial stimulation, it is important to understand how biological signals are received in the flight muscles at a cellular level. This chapter will discuss how neural signals are transmitted to the appropriate flight muscles through the Action Potential. There are a number of options for how these signals are collected and processed. Accurate collection and processing of EMG signals is critical for providing information about normal wing motion in comparison with the wing movement produced with artificial stimulation for Micro Air Vehicle (MAV) development.

EMG signals have been recorded many times while studying *M.sexta*, both during the larval stage (Mezoff, Takesian, & Trimmer, 2004) and the adult stage (Wang, Ando, & Kanzaki, 2008). One DARPA funded study created an ultra-light EMG backpack (Figure 15) to record the moth's muscle signals during flight. Unfortunately, the EMG

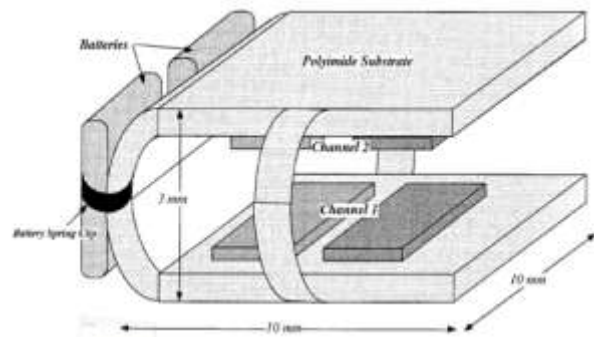


Figure 15: Graphical representation of an EMG backpack designed for *M.sexta*

backpack never actually worked successfully on a flying animal. (Mohseni P. , Nagarajan, Ziaie, Najafi, & Crary, 2001).

This study used fine wire implants because of the fixed nature of the implant process. This provided greater resistance to wire movement during wing flapping motions, and a clearer EMG signal than surface EMG (which is not as invasive, but is also less accurate for deeper muscle signals and more difficult to analyze due to overlapping signals) would have. Fine wires also provided the ability to directly redistribute the recorded signals into the very location from which they were received.

Neural Signals

Motor neurons receive signals from the brain, through the nervous system, which

cause muscle contractions. Muscle is an excitable tissue similar to neurons;

both have a membrane potential difference, which means there is a difference in voltage (or electrical potential difference) between the

interior and exterior of a cell. All electrically excitable cells maintain

voltage gradients across their membranes by means of metabolically driven ion pumps.

These ion pumps combine with ion channels embedded in the membrane to generate intracellular-versus-extracellular concentration differences of ions such as sodium,

potassium, chloride, and calcium (Figure 16). The Action Potential (AP) is the neural

messenger responsible for activating every segment of the muscle fiber so that the entire

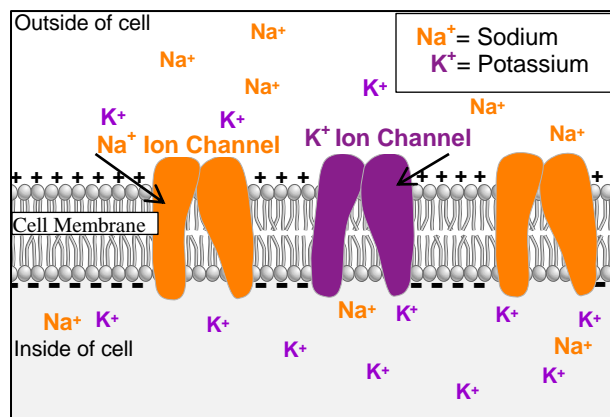


Figure 16: A cartoon representation of the resting condition of muscle cells; There is a negative potential difference inside the cell due to the concentration of sodium ions outside the cell membrane

muscle contracts in response to the neural signal. The AP arises because the cell's plasma membrane has specialized voltage-gated ion channels. These channels have gates that open and close in response to changes in the membrane potential (Cambell Neil A, Reece, & Mitchell, 1999).

To understand what EMG signals are and how they are generated it is important to discuss how muscle cells function.

When the muscle is unstimulated, the inside of an insect's muscle has an electrical potential between 30-70 mV, with the ions on the inside having a negative charge with respect to the outside of the cell (Chapman, 1998).

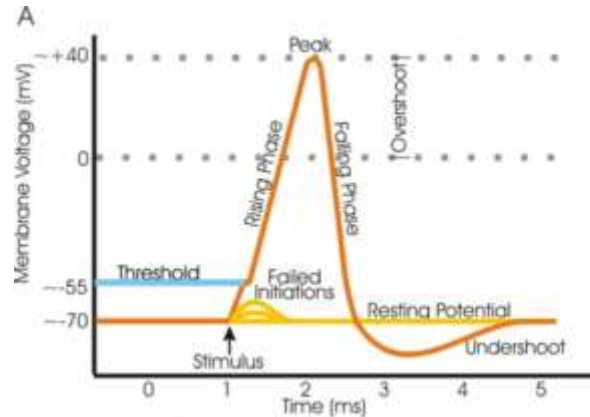


Figure 17: Idealized depiction of the changes of membrane voltage over time, due to ion changes caused by the Action Potential, with specific characteristics labeled

Every electrically active cell, like neurons and muscle, has a specific threshold of ionic balance. If the stimulus is too weak, then the membrane remains too polarized and the cellular ion pumps will work to reestablish the natural resting potential of the cell. If the stimulus is greater than the threshold, then the cell membrane depolarizes and fast responding sodium (Na^+) channels open, causing Na^+ ions to flow into the cell via Na^+ ions channels, making it much more positive, which then causes more Na^+ channels to open. This can be observed as the rising phase of a signal (Figure 17). The slow responding potassium (K^+) channels then open, allowing K^+ ions to flow out of the cell and causing a repolarization of the cell membrane and the falling phase of a signal. The relative slowness of the K^+ ion channel causes the signal to fall below the resting potential because the channel remains open after the cell has reached its resting potential.

The AP process begins with a change in the muscle fiber membrane's permeability to Na^+ (Figure 18a). Because these Na^+ ions are in relatively greater concentration outside the muscle fiber, any change in permeability results in an influx of Na^+ across the membrane (Figure 18b). Eventually, sufficient Na^+ ions enter the cell to reverse the polarity of the membrane potential, making the inside of the muscle fiber become positive (by about 30 mV) with respect to the surrounding extracellular medium (Figure 18c). As the membrane's potential polarity reverses, the permeability of the membrane to K^+ changes, causing K^+ to exit the cell. It is largely the outflow of K^+ ions that repolarizes the cell and restores the resting membrane potential (Figure 18d). The exchange between different ions across the cell membrane is measured by electrodes as a change in voltage. EMG is the process of measuring the voltage changes within neurological and muscle cells

In the meantime, as the AP spreads, it changes the membrane potential and opens adjacent sodium channels, allowing more sodium ions to enter. This changing from negative to positive and back to negative as each adjacent muscle fiber area is successively activated along the membrane is considered to be the muscle action potential. Muscular activation can be described as an electrical dipole traveling down a muscle fiber. Thus, if a pair of electrodes are placed close to or on an active muscle fiber, a measurement of the change in the membrane potential can be obtained.

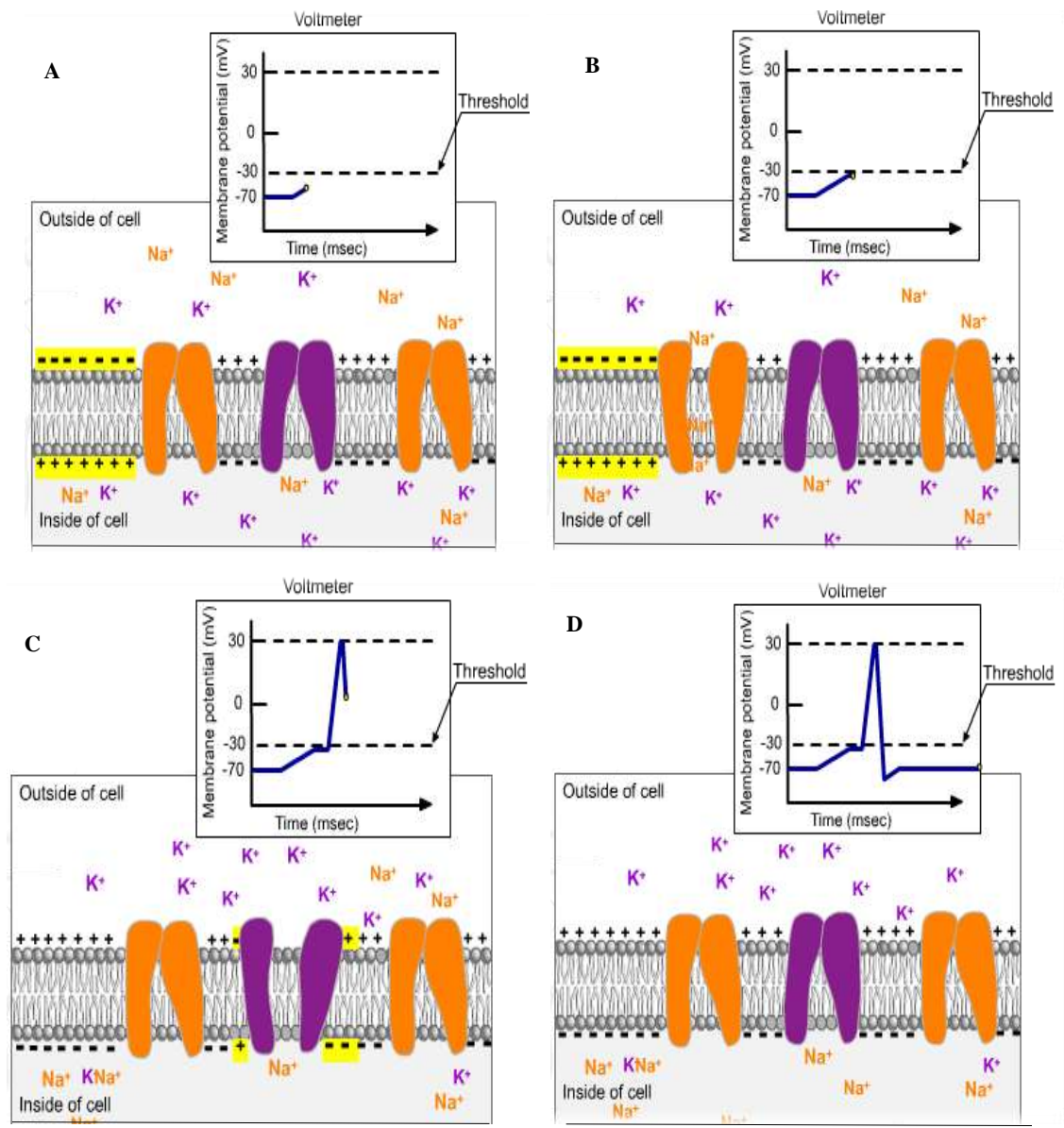


Figure 18: A depiction of how the Action Potential (AP), seen in yellow, is related to electrical signals: A) The AP moves across the membrane changing the polarity while the inset graph shows the voltage increasing; B) As the AP reaches an ion channel, Na^+ diffuses in, rapidly making the cell more positive; C) The AP then causes the K^+ channel to open so that potassium leaves the cell, causing a rapid drop in voltage; D) The AP moves on to activate more cells, and the normal cell processes restore the resting potential

The depolarization or electrical discharge of the muscle membrane is the basis of electromyography because the potential difference can be detected using fine wire implants. The signal originates at the axon connection site; insect muscles have multiple axon binding sites, and it is believed that the AP is distributed using the transverse tubular system, which is connected throughout the fiber (Chapman, 1998). The distributed AP stimulates the muscle contraction mechanism, causing a conformational change in the shape of the muscle (Figure 19).

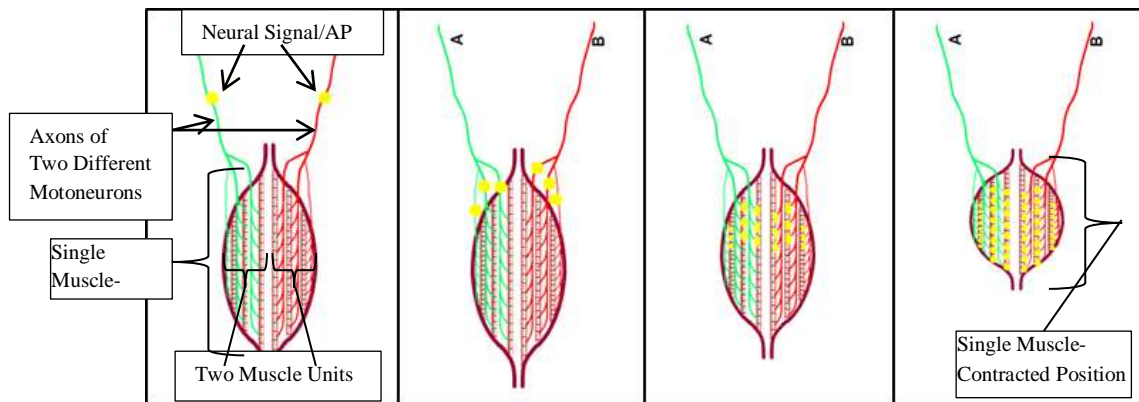


Figure 19: A depiction of how an insect muscle responds to neurological signals; this single muscle is composed of two different muscle units, each innervated with the axons of a different mononeuron; as a signal travels, it uses the transverse tubular system to activate multiple areas of the muscle to induce contraction

Action Potentials are said to be all-or-none since they either occur fully or they do not occur at all. This means that larger currents do not create larger APs. The amplitude of an AP is independent of the amount of current that produced it. In contrast, the frequency of an AP is what determines the intensity of a stimulus (Cambell Neil A, Reece, & Mitchell, 1999). This is very relevant to research conducted here because the AP threshold must be reached to stimulate the muscle with an electronic signal, but it is not just the amplitude of the signal that determines how the wings respond, it is also the frequency of the signal. This biological understanding provides valuable insight because

it indicates that large amplitude signals are not as important as changing the frequency of the signal in order to induce wing movement with artificial stimulation. It should also be insensitive to amplitude as long as it is above the threshold.

Recording the Muscular Potential Difference

EMG activity can be recorded using either a monopolar or a bipolar recording arrangement. This study will look at bipolar (or single differential) recordings, which are considerably more common because they produce higher frequency responses and more selectivity. In a bipolar recording arrangement, two electrodes are placed in the muscle. The signal is amplified and the difference between the two recording electrodes can then be obtained.

A simplified model of EMG signal collection can be seen in Figure 20. The triangular shape is a differential amplifier, and the Action Potential dipole travels from left to right down the idealized muscle fibers.

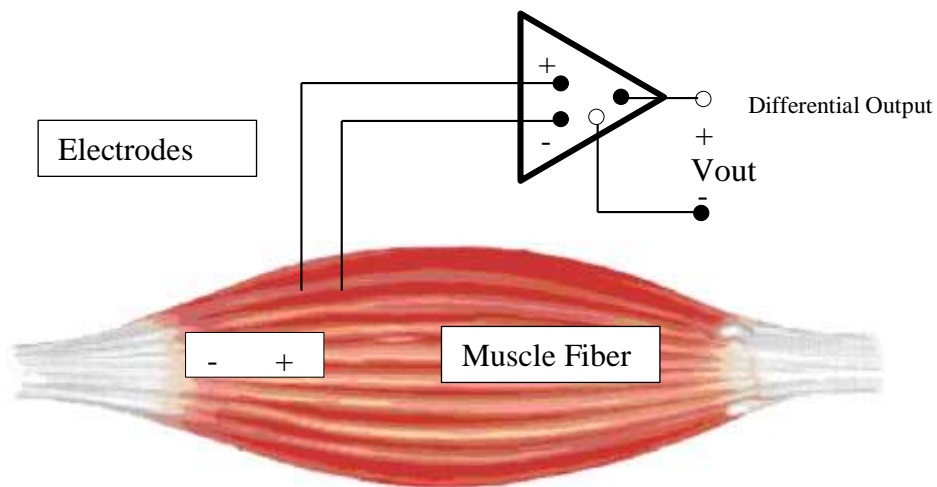


Figure 20: Ionic potential difference is collected and amplified; the difference between the two electrodes, the differential output, is recorded as EMG

The operational amplifier's output voltage will be proportional to the difference between the two electrodes. Differential voltage measurements are preferred to recording the actual signal because the relatively small magnitude of the EMG signal is around the same order of magnitude as electrical noise in the environment. By taking the difference between two electrodes, any noise common to both electrodes is canceled out, meaning that the differential output is a measure of the difference in voltage between two electrodes. The muscle membrane acts as a transducer, which transform biochemical signals into the electrical signals the electrodes record. In general, an EMG signal is the non-linear transduction of the activity of several muscle fibers near the electrodes.

When the positive portion of a signal reaches the first electrode, and because differential voltage is proportional to the difference between the second electrode relative to the first, the electrical difference increases. Then, the positive portion of the signal moves past the first electrode and approaches the second electrode, making it more positive. At the same time, while the positive portion of the signal approaches the second electrode, the negative portion of the signal has reached the first electrode and made it negative. Because one electrode is positive and the other electrode is negative, the difference between the two electrodes has greatly increased. Finally, the negative portion of the dipole passes near the second electrode and causes the differential output to become negative again, making the difference between the two signals very small. An EMG signal is a function of the distance between the two electrodes as well as the speed that the AP travels through the muscle fiber, for insects there are many APs to ensure that the signal is spread throughout the muscle.

EMG signal may be processed in a number of ways (Figure 21). The International Society of Electrophysiology and Kinesiology has been recommended the following technics for processing EMG data: full-wave rectification, in which the absolute value of the signal is taken; a linear envelope detector, which consists of full-wave rectification, followed by a low-pass filter (i.e., all the high frequencies are removed); integration of the linear envelope (taking the area under the curve); and a simple binary threshold detector, in which the muscle is

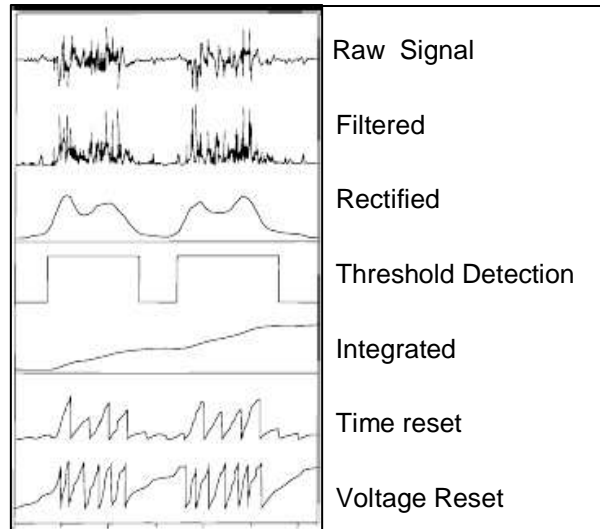


Figure 21: EMG signal processing techniques

designated to be either off or on (Vaughn, Davis, & O'Connor, 1992). Because this thesis is an initial study looking at primary flight muscles with respect to MAV research, the threshold detection was primarily used with phase variation of the differing muscle groups as well as signal length. This process is biologically significant because it mimics a clear neuromuscular AP signal over a given period of time. The intent was to establish a simple cause-and-react relationship between the EMG signal and the moth's wing angle for evaluation purposes.

The EMG Signal

The EMG signal is the summation of the discharges of all the motor units within the pick-up range of the electrode. During a sustained weak contraction, electrodes might detect two motor units discharging independently, at rates of about ten discharges per second. The EMG signal will consist of two distinct trains of Muscle Unit Action

Potentials (MUAPs). Most of the MUAPs will be clearly recognizable (Figure 22-A). Occasionally, the two motor units may discharge at nearly the same time, causing the two MUAPs to overlap one another (this is known as superposition). The resultant waveform can be either larger or smaller than the individual MUAPs, depending on whether the overlap results in constructive or destructive interference (McGill, Lateva, & Marateb, 2005). One of the benefits of using M.sexta is that there is little MUAP overlap.

During a somewhat stronger contraction, the EMG signal might contain MUAP trains from four to eight nearby motor units and several more distant ones, with discharge rates ranging up to fifteen discharges per second (Figure 22-B). The individual MUAPs will be difficult to sort out because of the high number of superpositions. The MUAPs from the nearby motor units can be enhanced by high-pass filtering. This accentuates their spikes, making them sharper and narrower. At the same time, high-pass filtering attenuates the duller, broader MUAPs from the more distant motor units. Even though the spikes from the nearby motor units are narrow, they tend to retain their individuality (McGill, Lateva, & Marateb, 2005).

The EMG signal from an even stronger contraction might contain so much activity that even after high-pass filtering, the individual MUAP trains cannot be identified with any degree of reliability (Figure 22-C). The complexity of an EMG signal depends on the strength of the contraction, on whether the strength remains constant or not, on whether the length of the muscle remains constant or not, and on the type of electrode used (McGill, Lateva, & Marateb, 2005).

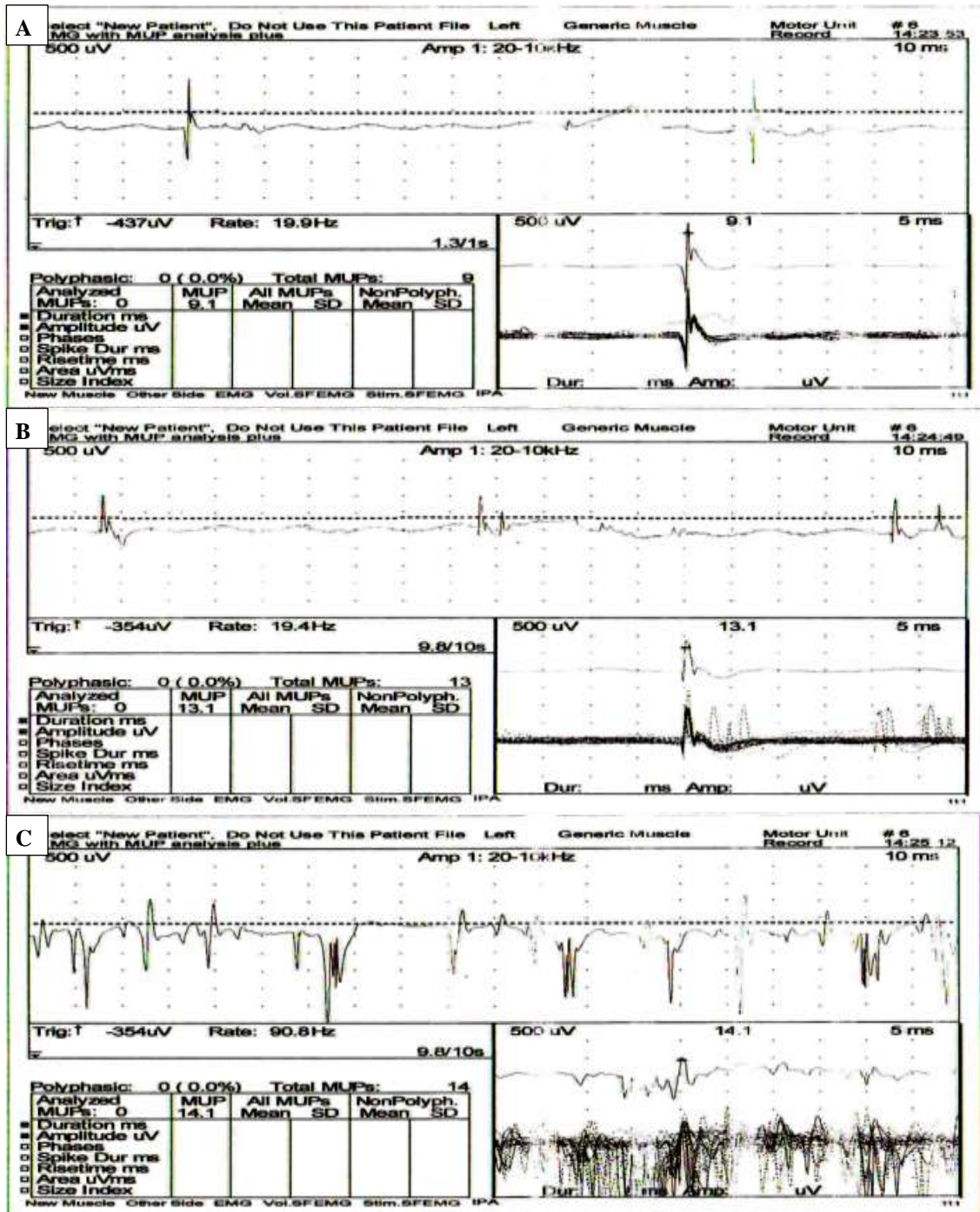


Figure 22(A-C): Personal Medical EMG recordings of the first dorsal interosseus muscle (muscle between the thumb and forefinger on the back of the hand) taken by Dr. Joshua Alpers, MD, to demonstrate EMG signals: A) Signal from a single motor neuron with nearly relaxed muscle; B) Increased motor neuron signals activated through increased contractions; C) Multiple motor neurons recorded at maximum muscle contraction

Signal Sampling

When recording electronic signals, Shannon's or Nyquist sampling theorem states that the signal must be sampled at a frequency greater than twice as high as the highest frequency present in the signal itself. This minimum sampling rate is called the *Nyquist sampling frequency* (f_n). In practice, most biomechanists usually sample 10x the highest frequency.

The signal can be expressed using Fourier series:

$$h(t) = a_0 + \sum [b_n \sin(2\pi f_n t) + c_n \cos(2\pi f_n t)] \quad (1)$$

The Fourier coefficients can be calculated using these formulas:

$$a_0 = \frac{1}{T} \int_0^T h(t) dt \quad (2)$$

$$b_n = \frac{2}{T} \int_0^T h(t) \sin(2\pi f_n t) dt \quad (3)$$

$$c_n = \frac{2}{T} \int_0^T h(t) \cos(2\pi f_n t) dt \quad (4)$$

The power spectral density (PSD) plot will be used to emphasize the frequencies that are most influential in creating the recorded waveform. The PSD shows which frequencies the energy of the signal is strongest and weakest (Figure 23).

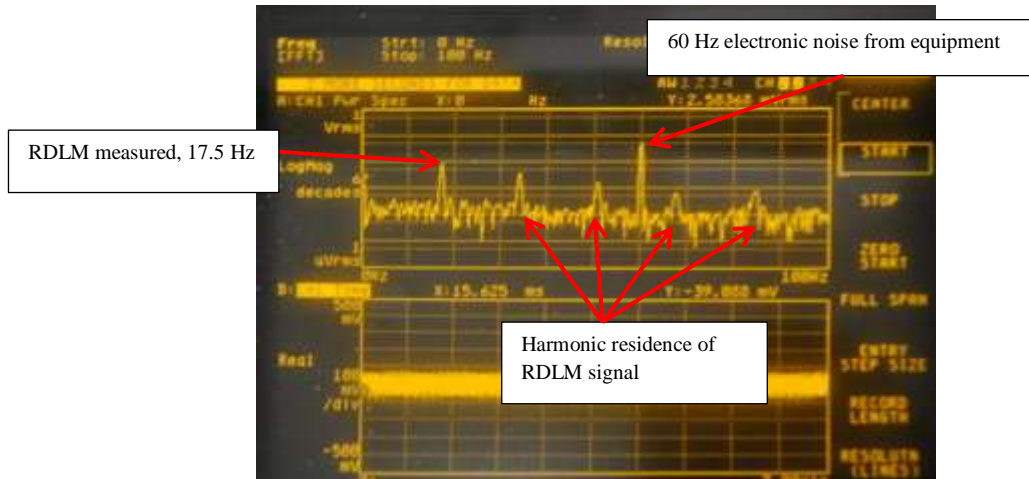


Figure 23: Power Spectral Density recorded from the Right Dorsal Longitudinal Muscle of the *M.sexta*

Theoretical Summary

It is essential to understand how *M.sexta* naturally flaps its wings before determining how to use artificial stimulation to reproduce the flapping motion. The EMG signals are vital for depicting how a muscle is responding to neurological signals and how the muscle contraction is associated with subsequent wing movement. The fundamental biology behind the signal describes how the muscles are reacting at the cellular level. By capturing these signals, more information can be gathered about the muscle response. The signals can be decomposed and processed to help give further insight into how best to simulate the proper wing movement through muscle stimulation. This information helps to guide the experimentation process for gathering data.

III. Experimentation

"Under the most rigorously controlled conditions of pressure, temperature, volume, humidity, and other variables-the organism will do as it damn well pleases."

Harvard's Law (Zera, 2005)

Experimenting with Living Organisms

The key factors in this research are the physiological and behavioral responses of *M.sexta*. As with all living creatures, the only way to provide proper handling and care is to understand the life cycle and the developmental process that occurs naturally. All living specimens used in this thesis were handled with the utmost gentleness and with as much respect as possible, but due to the nature of the experiments, some degree of physical damage was necessary for scientific knowledge. Other than the documented experiments, the subjects were at no time mishandled or abused.

Pilot Study

Initial scientific investigation into the use of EMG to gather flight muscle information took place under the direct supervision of Dr. Mark Willis, Associate Professor of Biology, at Case Western University. Dr. Willis is a well-respected scientist with years of experience in the proper handling techniques of *M.sexta*.

Under his guidance, a tobacco horn worm (the common name for *M.sexta* in its larval stage) was dissected and key organs were identified (Figure 24A). Metamorphic changes that take place through maturation directly impact the neurological processes that are used to stimulate controlled flight. Under the microscope, tubules which provide oxygen throughout the system (Figure 24B), individual ganglia (Figure 24C), the nervous system (Figure 24D), and the brain of the caterpillar (Figure 24E) were clearly seen.

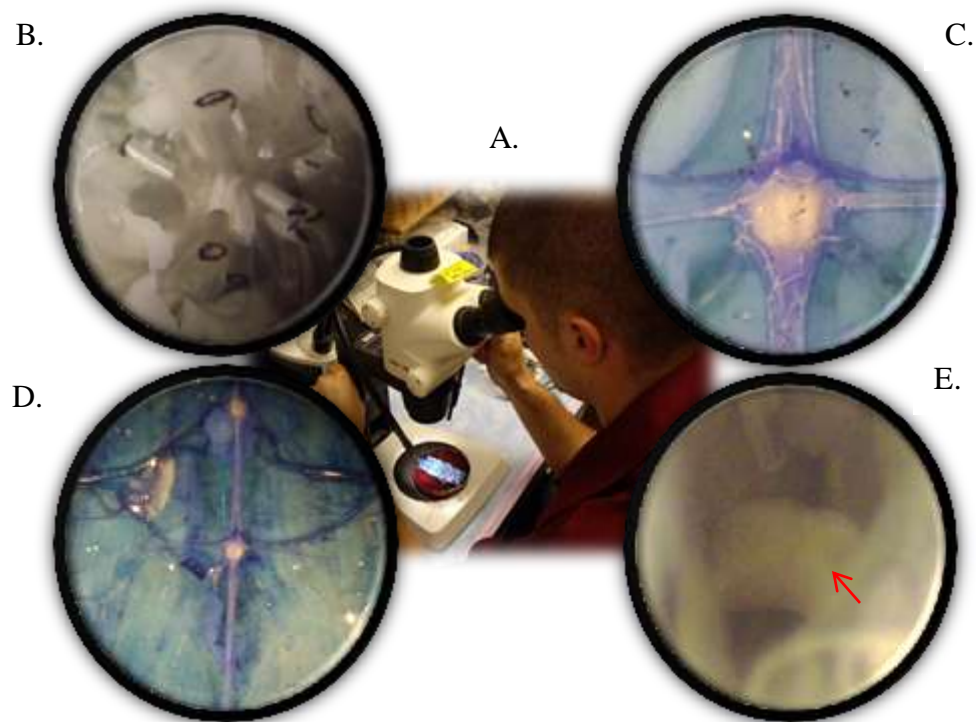


Figure 24: A) Fellow research student, Nate Deleon, observing the dissection of a *M.sexta* larvae; B) Tubules; C) Ganglia; D) Nervous System; E) Brain (indicated by arrow)

In addition to anatomical lessons, Dr. Willis provided a practical and hands-on demonstration in the proper preparation and implantation processes for *M.sexta* (Figure 25A). The process that was demonstrated is as follows:

- First, a male *M.sexta* was cold anesthetized by placing it in a small container and submerging it in a bucket of ice for approximately 15 minutes, until the moth was unresponsive to stimulation.
- Under a fume hood, the scales on the thorax were removed with a can of compressed air and a stiff bristled brush.
- The legs of the moth were removed because it will not fly if it can feel the sting (test fixture) that it is mounted to.

- The moth was then super-glued to a modified metal spatula, between the last two pair of legs, and an accelerator was used to speed up the gluing process.
- When the moth was secure, a small hole was “drilled” through the metathorasic cuticle with a dissection pin being twisted back and forth with fingers. This motion ensured a small hole pierced the cuticle, verses a straight thrust through the exoskeleton, which could cause the cuticle to crack or tear and inflicted more physical damage, which would most importantly reduce the ability of the wires to make proper contact with the underlying muscle.
- The small hole was then enlarged using a teasing needle.
- A two pronged connector pin was used, with each prong soldered to two strands of 0.003”/76.2 μm silver wire coated in Teflon, and held together with dental wax.
- The tip of this wire was bathed in acetone, cut at a slight angle (about a millimeter of the tip was bent at a 90° angle). This is to expose "fresh" clean silver conductor from the wire to the muscle tissue. The wire was then inserted through the enlarged hole so that the cut tip penetrated into the DLM and the rest of the wire lay along the dorsal side of the moth (Figure 25C).

- Heated dental wax was used to secure the implant in place, and wax was also used to secure the wire to the sting so that it was out of the way of wing motion (Figure 25B).

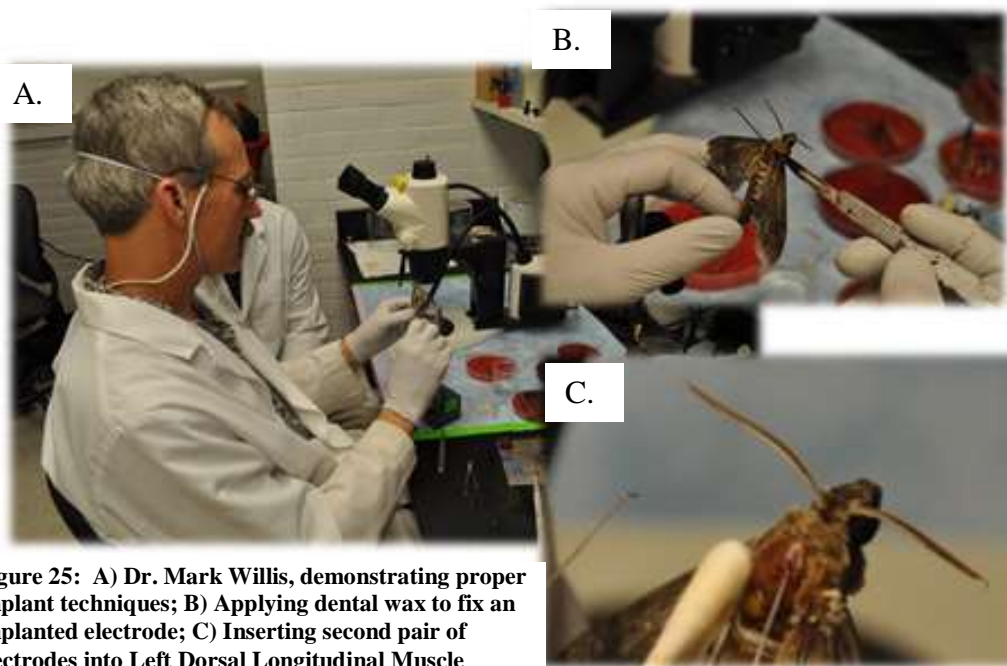


Figure 25: A) Dr. Mark Willis, demonstrating proper implant techniques; B) Applying dental wax to fix an implanted electrode; C) Inserting second pair of electrodes into Left Dorsal Longitudinal Muscle

Under the guidance of Dr. Willis, it was demonstrated that biological EMG signals could be recorded using a sound recording device, such as an analog to digital converter. The device of choice was the M-Audio Fast Track Pro. The Fast Track Pro has the ability to record two audio channels at the same time, and the ability to selectively increase the gain of the incoming signal. This brand was

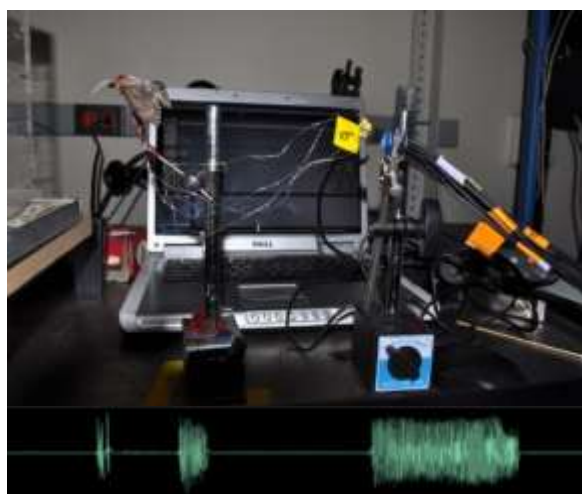


Figure 26: EMG signals from a *M.sexta*, using fine wire implants; the recorded signals are superimposed below the picture

chosen based on numerous positive product reviews (Wize, 2010) and the relative inexpense of the device.

The implanted wires were connected to a 100x amplifier with a low pass filter, which was then connected to the Fast Track Pro using a custom designed wire. Using the supplied software, Ableton Live Light (v. 8.1.4), the bioelectrical signals were able to be recorded when the moth flapped its wings (Figure 26). The signal was only recorded from the right DLM during this initial test.

Initial Development

Case Western provided multiple specimens to study and experiment with. One area of interest for the development of pupal implants was determining the exact location of the muscle groups in the emerged adult *M.sexata*. In order to gather this information, a Computed Tomography (CT) scan was performed on an anesthetized adult *M.sexata*. The CT images clearly show the desired muscle structure's shape and location (Figure 27).

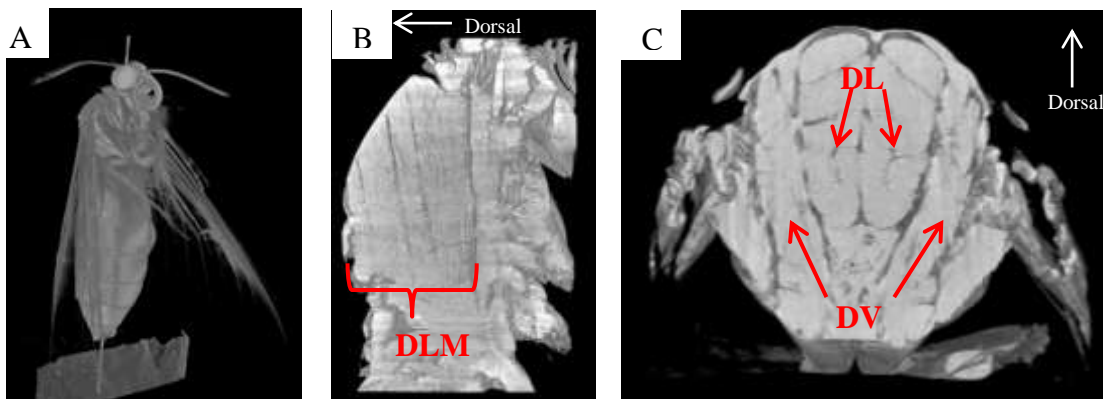


Figure 27: A) Computer Tomography of a *M.sexata*; B) Side view showing the Dorsal Longitudinal Muscle; C) Cross section showing the Dorsal Longitudinal Muscles (DLMs) and Dorsal Ventral Muscles (DVMs)

The CT scan provided excellent internal information about *M.sexta*. In addition, the three-dimensional data was also used in graphical computer simulations and in three dimensional printing (on the rapid prototype machine located at AFIT) for demonstration purposes (Figure 28). The



Figure 28: Rapid prototype of the CT scan of the *M.sexta*

simulations and the 3D models have been of great value during conference presentations, and in open public forums, where current MAV research is being presented.

The Implant

As stated earlier, the implant was designed with express permission from Dr. Alper Bozkurt's basic design (Figure 29). The chip was manufactured with the intention of being able to solder an adapter onto it.

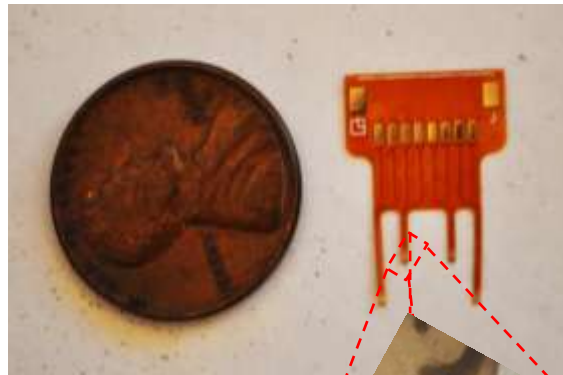


Figure 29: Pupae implant, based on Dr. Bozkurt's design; the fly-out shows the tip at 200x magnification

Electromyography and *M.sexta*

It has been shown that it is possible to implant specially designed devices into *M.sexta* during the pupation phase. Bozkurt, holds multiple patents for insect implants and has proven their viability in his research (Bozkurt, Gilmour, & Lal,

2009). Tsang proved that a device implanted during pupation can be used to change the direction of flight by adjusting the abdomen (Tsang, et al., 2010).

During pupation, the neurological and muscular pathways of the moth are reconfigured and undergo dramatic structural and physiological changes. A device that is surgically implanted correctly during this time is able to take advantage of this anatomical reconstitution, and the muscles are actually able to attach to it. This forms a biological bond that not only increases the sensitivity of the EMG signals, but also strengthens the physical connections to the implant. This removes the need for artificial glues, and decreases the errors encountered during muscle movement.

The primary power producing muscles (DVMs and DLMs) were of primary interest for this investigation, due to their relative ease of location and because they actually produce the force needed for flight; therefore, a pupal implant was chosen that could be imbedded into these four muscle groups. The design was commercially manufactured, ensuring uniformity and standardization of the implant. The copper traces (200 μ m) on the probe body match a Flat Flex Cable (FFC) connector, soldered to a FFC that connects to standard BNC (Bayonet Neill-Concelman) output ports. The implant was designed to be surgically inserted into the insect during the pupal stage, where the wire electrodes are located in the tissue and the FR-4 board body is exposed outside. When the adult insect emerges, the control electronics are connected to the implant through the FFC connector.

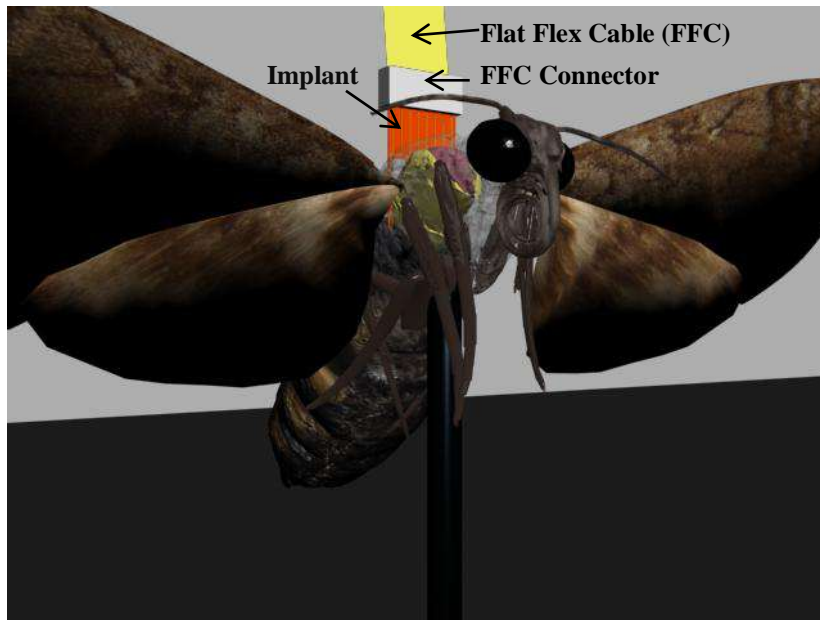


Figure 30: Computer simulated depiction of the pupae implant location on the adult *M.sexta* after emerging from the pupal stage; the components used for testing are listed

Initial Failures

As stated earlier, Willis Labs supplied the pupae for this research. The first attempts at implanting, during the pupal stage, resulted in unreliable results. The initial implant process was accomplished by following the methods demonstrated by Dr. Willis, but instead of using fine wire electrodes, the pupal implants were used. Six pupae were implanted, and three were left as control groups. Four of the implanted moths survived, but none were able to inflate³ their wings. The control group also proved to have problems, because only two survived, and again, none were able to inflate their wings. This indicates that there was a greater problem than just the implants: there had to be something wrong with either the environment that they were currently being raised in, or there was a problem during the larval stage.

³ Pumps blood into the veins after emerging

To establish a more closely controlled environment, hornworm larvae were raised (again sent from Willis Labs, along with hornworm diet). The decision to raise the larvae was made to establish a more precise timeframe of when the pupal stage began so that the implant could be inserted at the desired time (7 days before emerging from the pupal stage as an adult moth).

M.sexta larvae (20) were originally sent, but a clear problem was observed. The larvae would initially follow normal growth patterns, but during the traveling phase, (the prepupation stage), the caterpillars would begin to turn purple and become unresponsive until they died. This problem was also observed at the Willis lab. Additional symptoms (not being able to inflate their wings or having inflated wings still being unable to fly) were also observed.

Only four caterpillars successfully transitioned into the pupal stage. Two were implanted 11 days after pupation, and two were left as control groups. All four emerged, and none were able to successfully inflate their wings. This again resulted in inconclusive data about whether the implant was having significant detrimental effects on the implanted moths, or if there was an underlying reason for the moths to not develop correctly. Some clear problems that were observed with the implanted moths was that their movement was restricted, and the implant appeared to be too heavy for them to cling to the wall while trying to inflate their wings. The mass of *M.sexta* is about 3.64 g while the mass of the implant was 0.157 g with the USB connector soldered to the implant which is about 4.3% of *M.sexta*'s mass. Because of these problems, a new adaptor method was devised without the USB connector attached which had a mass of 0.136 g, which was only 3.7% of *M.sexta*'s mass, reducing the implant mass by ~0.5%.

Rising Moths

Difficulties in quality control of the rearing process resulted in early failures of implantation, so it was decided to make an attempt to raise the research's moths. All the necessary equipment and supplies were purchased from Carolina Biological Supply Company, including ~100 eggs, 24 larvae, and 12 pupae. Appendix B contains information on the rearing process and observations.

Better Implant Methodology

Due to the high failure rate with the implant, the moths were allowed to eclose (emerge) naturally to ensure proper wing development. The ability to fly was verified, and then data was collected using the fine wire method discussed previously. This process proved to be a valid and useful technique. The results were recorded and can be seen in the following chapter.

The implants were reattempted using a new process. This involved gluing four dissection needles that were sandwiched between two pieces of paper towel and two pieces of plastic (Figure 31). The implant tool was then used to puncture the exoskeleton in-between the head and thoracic ridge on the pupae (Figure 32 and Figure 34). Initial evidence suggested that this was a much more reliable location and methodology, with three successful emergences and one able to fully inflate its wings (Figure 33).

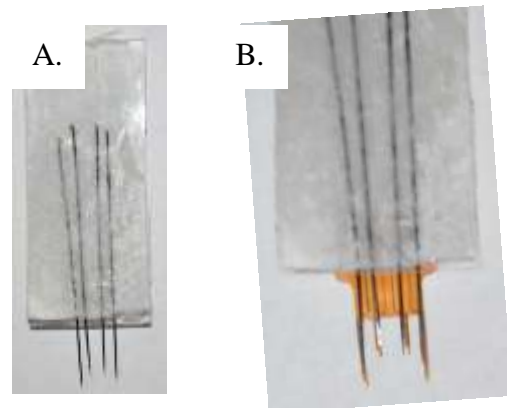


Figure 31: Improved implant tool used to consistently produce small holes in the *M.sexta* exoskeleton at a consistent separation distance apart; B) The tool is overlaid on top of an implant to ensure proper tip spacing



Figure 32: Surgically puncturing the pupae shell with the implant tool



Figure 34: A closer view of where the implant is being inserted



Figure 33: The only successful emergence of a *M.sexta* with the pupae implant attached

EMG signals were attempted to be recorded from the single moth that fully developed (Figure 38 and Figure 35); unfortunately, only one recording was able to be made before the implant pulled out of the muscle. It appeared that the implant and muscle never bonded together as had been expected. The resulting signal did not contain EMG signals, most likely due to poor muscle attachment (see Chapter IV).



Figure 38: Attempting to record EMG signals using pupae implant

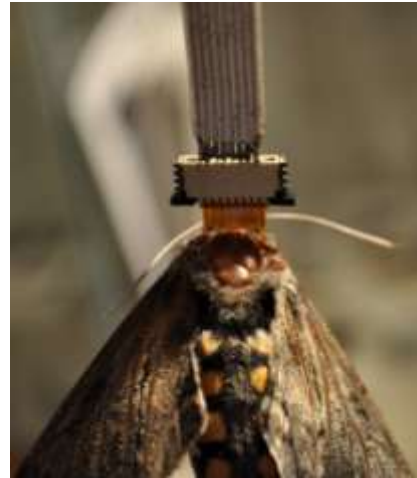


Figure 35: Only successful moth to emerge attached to FFC

The implant procedure was repeated on multiple pupae (Figure 37), with adjustments made to temperature, the light/dark cycle, stabilization methods of the pupae after implant, and the estimated number of days before emergence, but another moth never emerged with an implant in place. When examining the failed pupae, it is evident that the muscle failed to attach to the implant and began to deteriorate, most likely causing death through infection before emergence as an adult (Figure 36).



Figure 37: Multiple pupae were implanted with very limited success



Figure 36: Cross section of a pupae that failed to emerge, the black portion is evidence of muscle decay

Fine Wire Implants

Due to the failures of the pupal implant, it became necessary to use fine wire implants that were placed directly into the flight muscles of *M.sexta*. Prior to testing, the moths were allowed to fly in order (Figure 39) to ensure the capability of sustained flight. Even though the moth was glued to a fixed stand and unable to actually fly during the test, it was assumed that the depicted signals and corresponding wing movement were similar to the signals generated during flight. All EMG signals that were analyzed were of continuous full flapping for longer than five seconds; this helped to ensure that these signals were as similar to those in flight as possible.



Figure 39: Screen shots of *M.sexta* flight using a Casio Exilim FC-150 HS camera

Electrodes were placed in the four different muscle groups, as demonstrated by Dr. Willis (Figure 40 and Figure 41). The silver wire electrodes (Figure 42) were then connected to a low-pass filtered amplifier, and the differential was then recorded using the analog to digital converter, NI USB-6229, which was connected to the computer. The amplified signal was split off and sent to the Fast Track Pro box, which was connected to the computer speakers as well, so that the signal could be heard and recorded using different software.

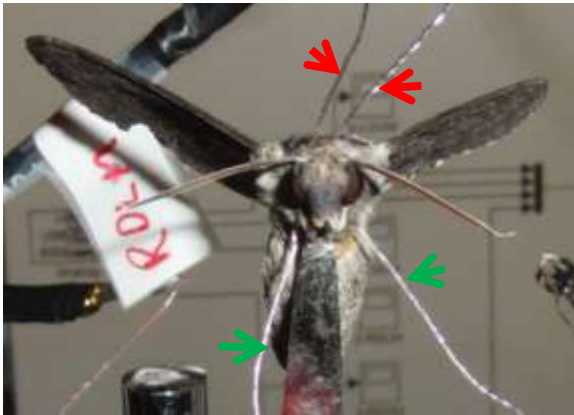


Figure 40: Implanted *M.sexta* in the DLM (red arrows) and DVM (green) using 0.008" silver fine wires coated with Teflon

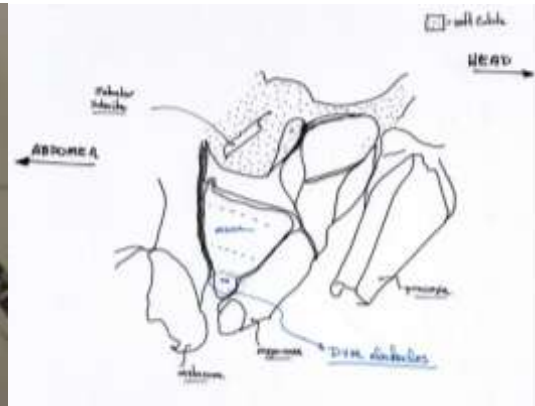


Figure 41: Diagram used by Dr. Willis to demonstrate proper DVM implant location

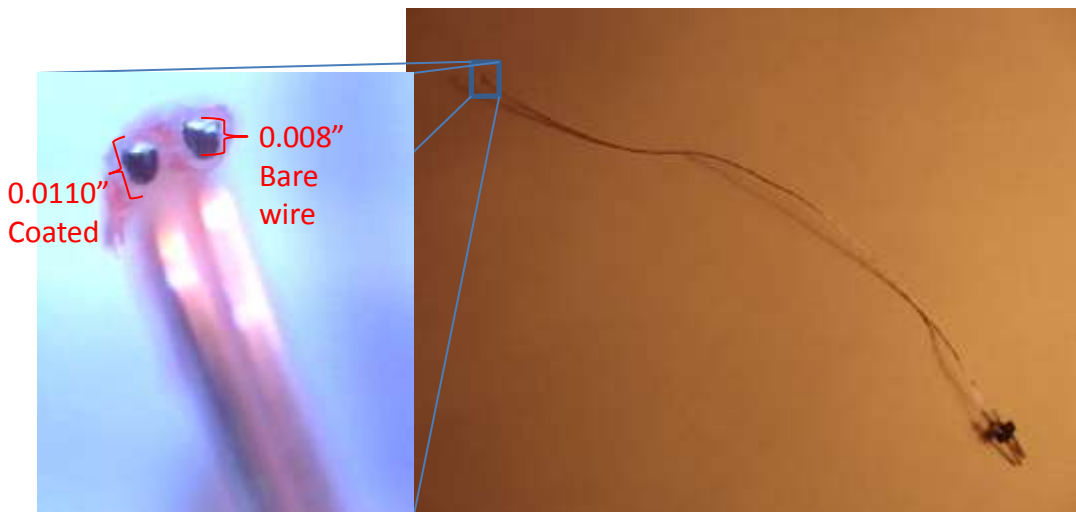


Figure 42: The silver fine wire used to collect EMG signals; fly-out shows a close up of the actual wire and the Teflon coating at 400x magnification

Matlab's Simulink program was used for recording (Figure 43) and sending (Figure 44) signals. The signals were recorded, processed, and sent back into the appropriate muscle. High speed video was taken to record wing movement, whenever signals were transmitted to the moth, as a means to categorize the muscle response. Initially, the recorded EMG signals were sent to the appropriate muscles as a means to determine if EMG recorded signals could illicit similar muscle responses. Next, multiple

different signals and frequencies were transmitted in an attempt to assess wing response due to changes in electrical signal conditions. The results are discussed in Chapter IV.

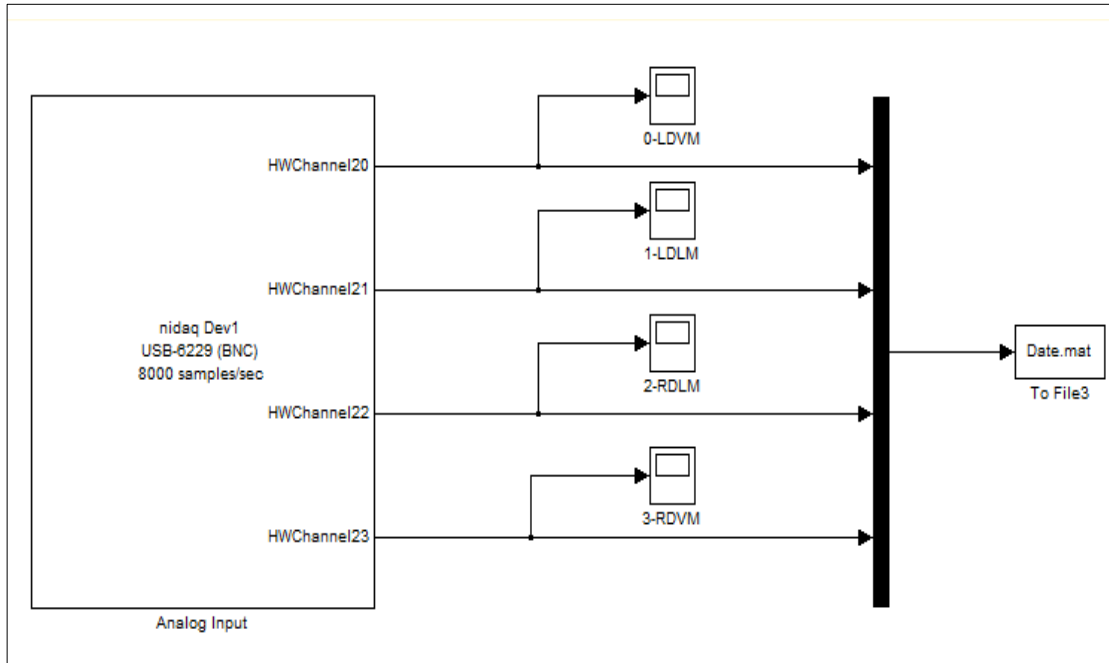


Figure 43: Simulink used to record EMG signals from *M.sexta*

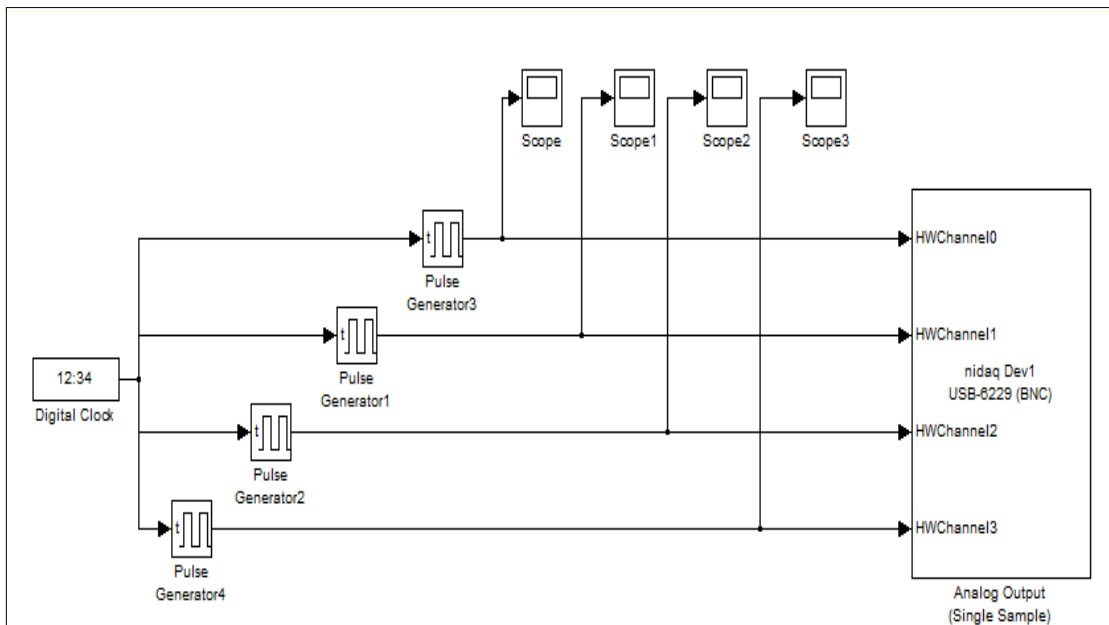


Figure 44: Simulink used to transmit EMG signals to *M.sexta*

The amplified signals were split off and collected using Fast Track Pro, connected to a laptop. The software supplied with Fast Track Pro was Ableton Live 8.1.4 (Avid Technology, Inc., 2011), and was used to record the signals. In addition, Audacity 1.3 Beta, a free cross-platform sound editor, was used to record EMG signals from Fast Track Pro (Audacity, 2011). Recording the signals multiple ways demonstrated consistency in the signal collection process, and served to validate the methodology. A depiction of the setup can be seen in Figure 45

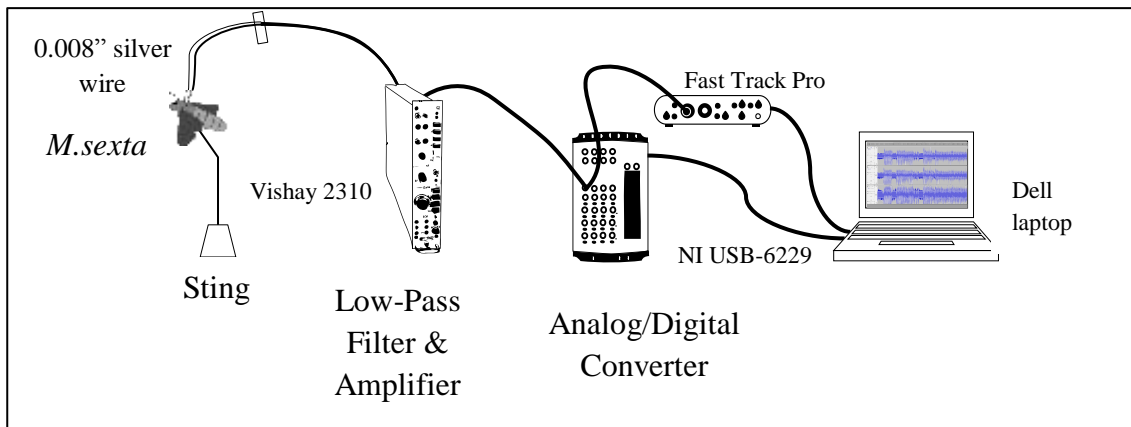


Figure 45: EMG signal collection and transmission process

EMG and Flapping Motion

Collecting the EMG signals provided information on the muscular movement internal to the moth, but this information needed to be associated with structural wing movement, because monitoring the actual wing movement is essential to understanding flight characteristics. High speed video taken during tethered flight, and associated with the EMG signals, could provide data concerning to the causal relationship of the neuromuscular signals and wing movement.

The EMG signals were recorded and reapplied to the muscles. This enabled a comparison between the observed “natural” wing movement that the moth produced

during flight and the artificial induced signals that could be applied to the muscle. The differences between the flight patterns were of primary interest.

After sending the recorded EMG signals into the respective muscles an attempt was made to determine the wing response to a simple impulse signals. To associate the EMG signal and artificial stimulating signal with wing movement the position of leading edge was measured and the difference between the leading edge position and the resting wing position was recorded as the wing flapping angle. Because this is an initial investigation it was determined that measuring the change in the wing angles was sufficient to verify the process.

The importance of this work is to demonstrate control over wing movement. This ability to induce known wing responses provides the potential capability of controlling free flight behavior of a moth, in essence making it a biological MAV. This control could aid in studying manufactured wings, which could be attached to the moth and analyzed. Understanding how to control wing movement could also provide insight into the design and control of synthetic MAVs. But, before wing control can be established a clear connection between signal input and wing movement must be identified

High Speed Wing Angles

To calculate the leading edge wing angle to associate with the recorded EMG signals and the transmitted signals, high speed photography at 420 frames per second (fps) was used throughout the research. The process was to first find the resting position of the leading edge of the wing when no signals were being sent. Adobe After Effects CS3 software (Adobe Systems Incorporated, 2011) provided the ability to place a blue dot on the pivoting joint, where the wing meets the thorax, of the forewing in a layer

superimposed on top of the video frames. A video frame, with the wing at a stable rest, was selected and a red dot was placed on top of the leading edge. The line formed between the joint (blue dot) and the leading edge at rest (red dot) marked the base line by which all other wing measurements were taken.

The Adobe After Effects software provides the ability to track high contrast areas throughout the video, so the leading edge wing tip was marked with a green dot and tracked throughout a video sequence. Often, the pixels were lost during the tracking process, so hours were spent processing the data (frame by frame) to mark the wing tip. This process could have been greatly improved with a higher contrasting background.

When the video sequence was marked appropriately, the background video was removed so that only the three colored dots were visible. The three dot video was rendered at 29.97 fps which is the standard for television, and the video was then pulled into the Matlab software. Using Matlab's Red, Green, Blue (RGB) layering system (which breaks colors into their own data set), and the centroid of each colored dot was able to be calculated. With the centroid calculated for each dot, the angle between the baseline (blue and red dots) and the wing tip (blue and green) was able to be calculated for each sequenced frame (Figure 46). Despite the time this took, the process proved invaluable for measuring the leading edge wing angle and associating it with the recorded and transmitted signals.

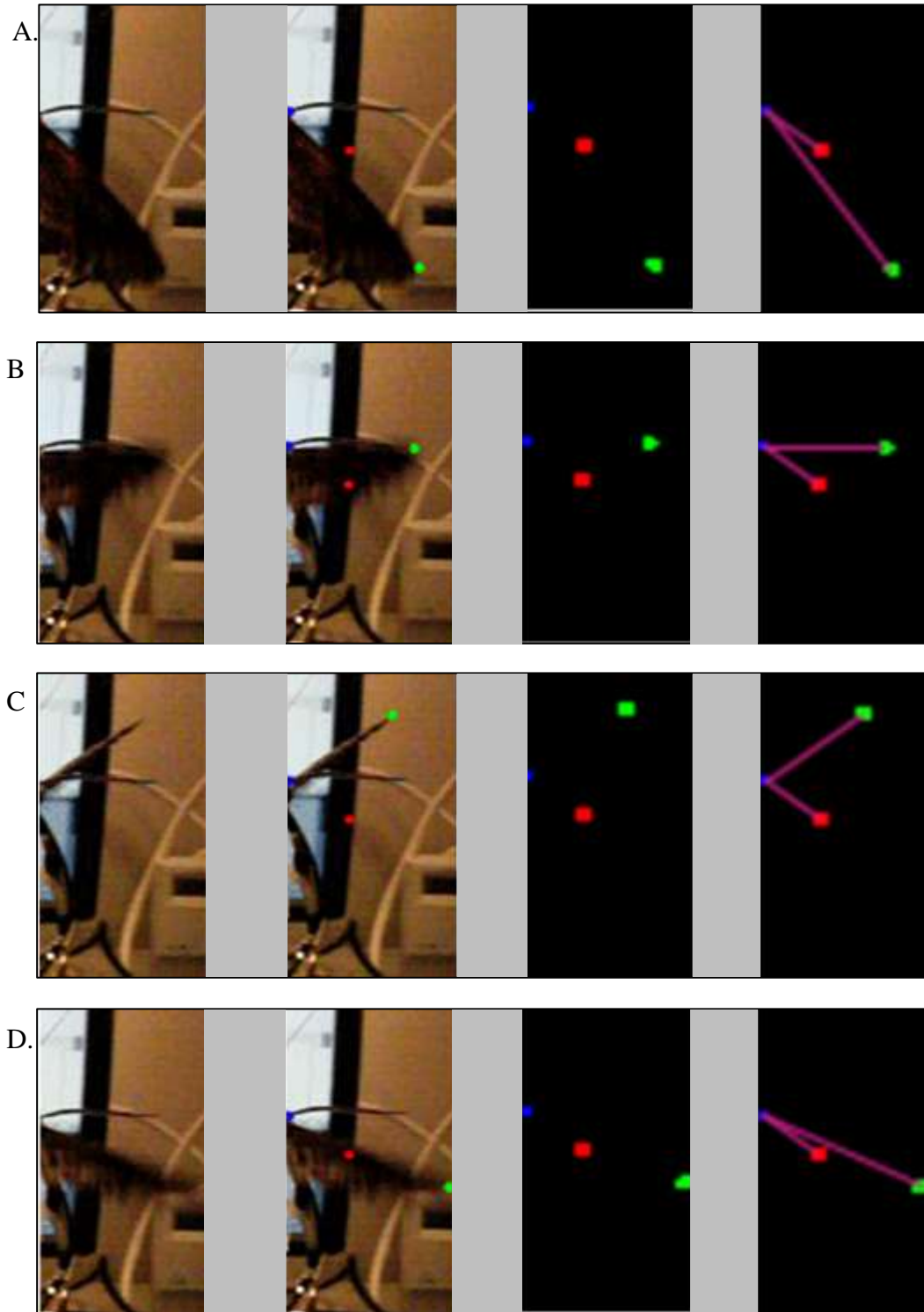


Figure 46: Four sequences of images being processed through Adobe After Effects and Matlab; A) Lowest point in the down-stroke; B) Moving through the up-stroke; C) Highest point on up-stroke; D) Moving through the down-stroke

Potential Energy Process

Once the wing angles were established an attempt was made to determine the muscular force responsible for the wing movement. This information gives a simple linear reference by which to compare measurable anatomical characteristics, like wing length and tergum displacement, with expected muscular energy and to provide some understanding of the energy requirements that will be required when designing bio-type MAVs. The energy necessary to generate wing movement in the biological system is important for MAV development as a way to determine the energy requirements needed to produce lift. In order to find a rough potential energy estimation associated with the flapping motion, the weight and displacement of the center of gravity needed to be found. The weight of the wing was found to be 6.2×10^{-4} N by simply multiplying the weight (63.3 mg) by the pull of gravity (9.8 m/s^2). To find the geometric center of gravity, a *M.sexta* wing was scanned and converted to a black and white image so that the clearly define the edges could be observed.

Using Matlab, the centroid was found to 304.45 pixels (px) away from the joint (Figure 47). The distance from the joint to the tip (520.05 px) was also measured to determine the pixel to distance ratio. For this picture, the scale was found to be $1 \text{ mm} = 12.09 \text{ px}$. The centroid was found to be 25.17 mm from the joint. The displacement was found by overlaying two

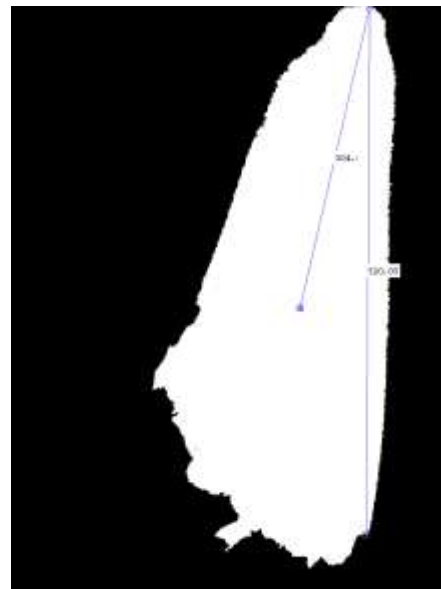


Figure 47: Centroid of wing found using Matlab

be

images of wing movement on top of each other and measuring the same distance to the centroid between the wing positions. The ration of mm/px for this image was found to be 1 mm/20.50 px.

When the DVMs contract they pull the tergum down, this displacement is responsible for wing elevation. A general idea of the force required to raise the wing a known distance was calculated by first using the same ratio calculation process as previously discussed to determine tergum displacement between a wing at rest and one that is elevated. The tergum displacement was found to be 0.30 mm.

The wing displacement was then found by measuring the angle between what was calculated to be the correct distance for the center of gravity from Figure 47. It was understood that this was a rough estimation because the measurements were taken at the leading edge instead of the geometric center of gravity; however, for this thesis, this can be justified because the mass of the wing is disproportionately distributed in the leading edges. With Photoshop's (Adobe Systems Incorporated, 2011) measurement tool, the angle was found to be 24.4° (Figure 48). A geometric depiction was constructed to show the determined lengths (Figure 49).

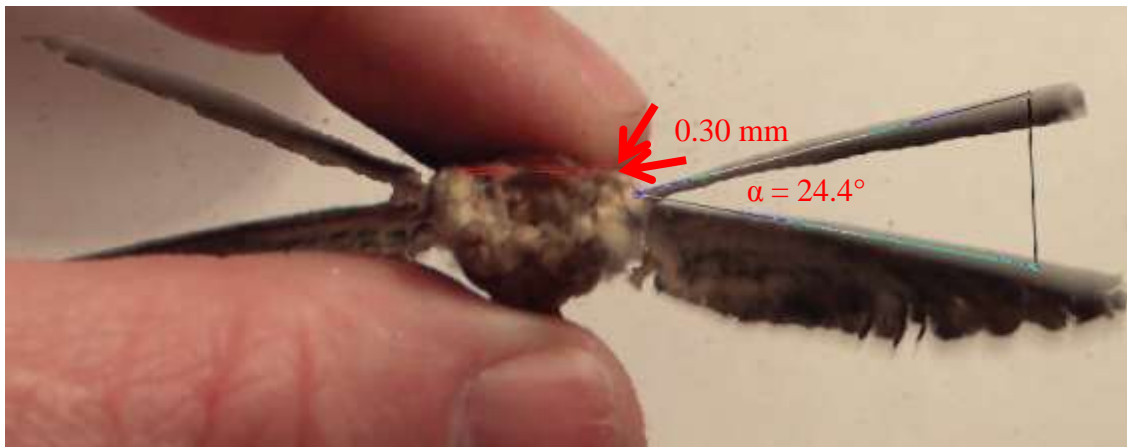


Figure 48: Two images superimposed to find the wing angle (α) associated with tergum displacement as indicated by red arrow

Using trigonometry the following distances were found:

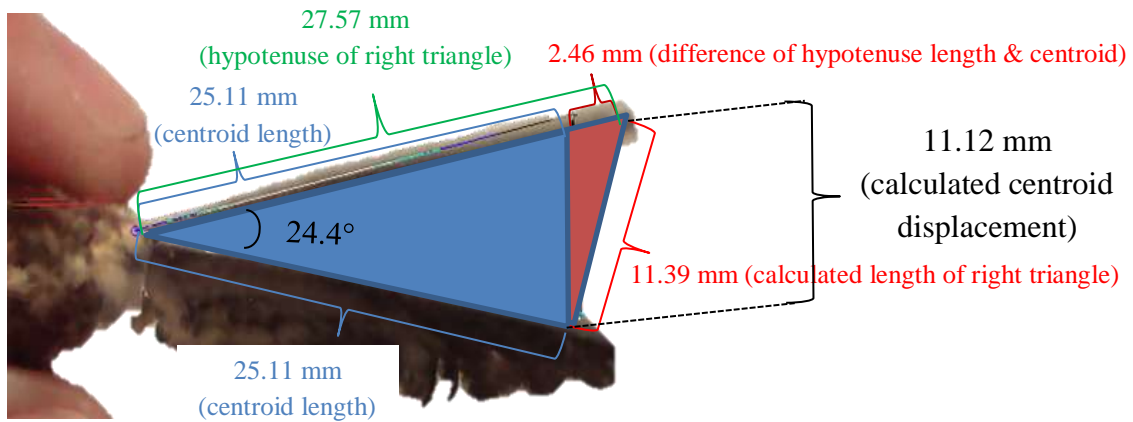


Figure 49: A graphical representation of the calculated triangles and the associated lengths to determine the centroid displacement

The mathematical process used is as follows:

Using the equation:

$$\cosine = \frac{adjacent}{hypotenuse} \quad (1)$$

$$\frac{25.11mm}{\cos(24.4^\circ)} = 27.57mm = \text{hypotoneuse length} \quad (2)$$

From Pythagorean's theorem:

$$A^2 + B^2 = C^2 \quad (3)$$

$$\sqrt{27.57mm^2 - 25.11mm^2} = 11.39mm \quad (4)$$

The difference between the hypotenuse length and centroid length was found:

$$27.57mm - 25.11mm = 2.46mm \quad (5)$$

Then Pythagorean's theorem was used again to find the total center of gravity displacement between the two photographs:

$$\sqrt{11.39mm^2 - 2.46mm^2} = 11.12mm$$

This distance was verified using Photoshop measuring tools. From this displacement potential energy can be calculated using the formula:

$$E = W * \delta \quad (6)$$

Where $W = \text{weight (N)}$ and $\delta = \text{displacement of the center of gravity}$.

The potential energy was found to be:

$$E = 6.2 * 10^{-4} N * 0.01112m = 6.89 * 10^{-6} J \quad (7)$$

This indicates that $6.89 * 10^{-6} J$ was used to displace the tergum by 0.30 mm.

This process demonstrates that an estimation of the muscular forces associated with wing movement can be calculated. This information can provide valuable insight into the forces necessary to develop MAV flight. Knowing the forces associated with wing movement could also help with modeling and simulating MAV flight characteristics.

This equation is only relevant for determining the energy needed to lift the wing due to gravity and does not take into account any energy associated with the spring-like characteristics found in the thorax. It is believed the spring forces play a much larger role

in the energy requirements associated with wing movement when compared to the energy due to gravity.

Experimental Summary

The experimentation process was critical for gathering accurate results and useful data. This chapter has described, in detail, the methodology and equipment used to collect and transmit EMG signals from *M.sexata*, with the intention of reproducing the biological flapping motion using artificial stimulation. The experimental process was based on the observations and directions provided at Case Western under the guidance and tutelage of Dr. Mark Willis. An attempt was made to use the pupal implants patterned after those designed by Dr. Bozkurt, but for currently unknown reasons, this process failed. The pupal implant was determined to not be a viable option, so the fine wire method was adopted.

By using the fine wire implants, EMG signals were captured from an adult *M.sexata* during tethered flight. These signals were then processed and reapplied to the respective muscles. The wing motion was captured with slow motion photography, and the wing angles were measured. A number of different signals were also transmitted to determine the associated wing response. The results are discussed in Chapter IV

IV. Results and Discussion

Implant Results

This section will discuss some of the different results that were gathered throughout this investigation, and discuss why this information is significant. The mortality rate of the implanted pupae (Figure 50) was very high. When consulting with Dr. Bozkurt, he believed that our process was sound and that we seemed to be implanting the pupae correctly (Bozkurt A. , 2011). The pupal implant resulted in high pupae mortality: 41 out of 47 (87%) moths failed to emerge successfully. In addition, 5 out of 6 (83%) of the emerged moths were unable to inflate their wings. Only one moth managed to inflate its wings, but the implant pulled out after just one test. Despite having survived the implant process, the muscle did not appear to have been able to successfully graft onto the implant.

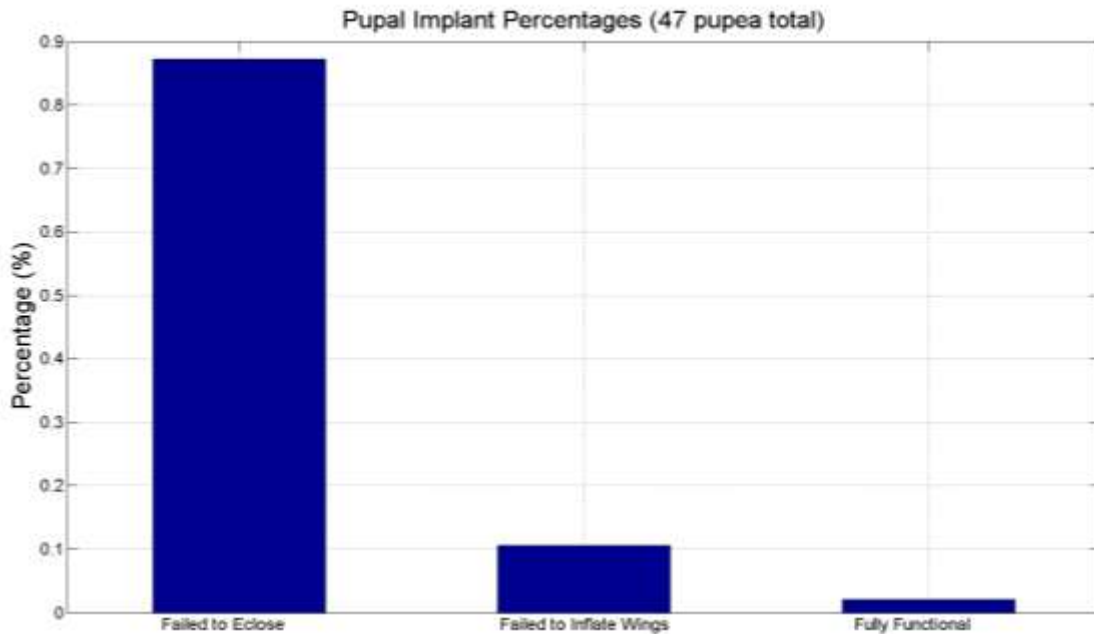


Figure 50: Chart depicting implant mortality rate

No EMG signal information was able to be collected from the one implanted test subject that survived the implant process (Figure 52 and Figure 51). After this initial test, the implant pulled out of the muscles of the moth.



Figure 52: A photograph of the surviving pupae implant moth while the signals are being recorded

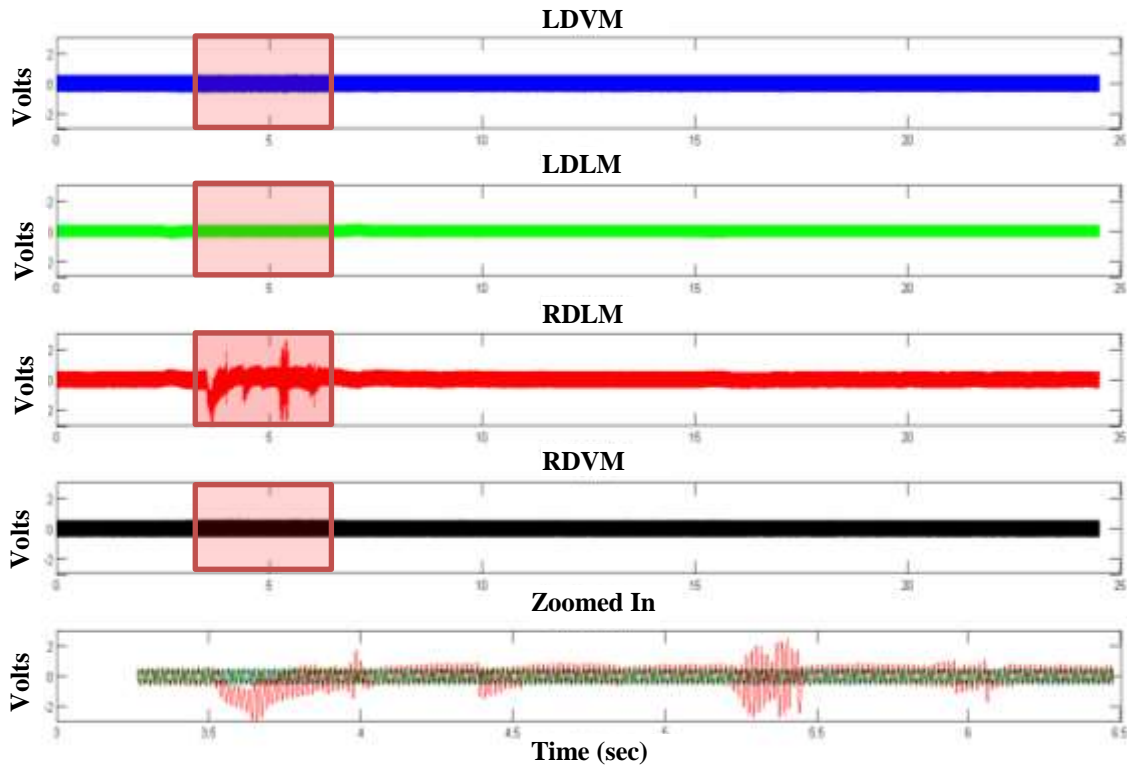


Figure 51: Matlab graph showing the only EMG recording made with a pupae implant, the highlighted area in red can be seen in the 'Zoomed In' section of the graph

There were a number of possible reasons for the lack of EMG signal. The most likely ones are:

1. The implant became defective during the pupae development, possibly because of tissue growth or the natural healing process of the moth coating the leads.
2. The connection between the implant and the Flat Flexible Cable was not correctly established.
3. The noise of the setup masked any signal produced.

More research needs to be conducted on this process. There were many advantages to having an implant directly attached to moth muscles, like making the signals clearer to read and analyze. Using the pupal implant made the process much more standardized, and removed the problem of wires moving during the testing. The implants have been shown to work in other research, and should lead to additional free flight studies.

Fine Wire EMG

Fine wire electrodes were used to record EMG signals when the pupal implant supply was exhausted. It was more laborious to get the electrodes in the correct location, but the signals were fairly clear and valuable data was obtained. One of the more difficult problems was wire movement during the recording process. The connection that soldered the fine wire to the amplifier cable broke many times during EMG testing, primarily due to the small diameter of the fine wire.

Some examples of captured EMG signals captured can be seen in Figure 53. This figure shows four EMG channels, two recorded from right and left DVM, and two from

the right and left DLM. The red shaded areas are indications of a where flapping motion was occurring. The zoomed in section at the bottom is a better indication of the signals' quality. The LDLM (green) is out of phase from the other three muscles, was expected. The RDLM (red) appears to be incorrectly recording DVM muscle activity, because it is superimposed on the other two signals (blue and black), when it should be in phase with the LDLM to provide the down-stroke. Unfortunately, the ability to detect this problem was not available during the collection of this data.

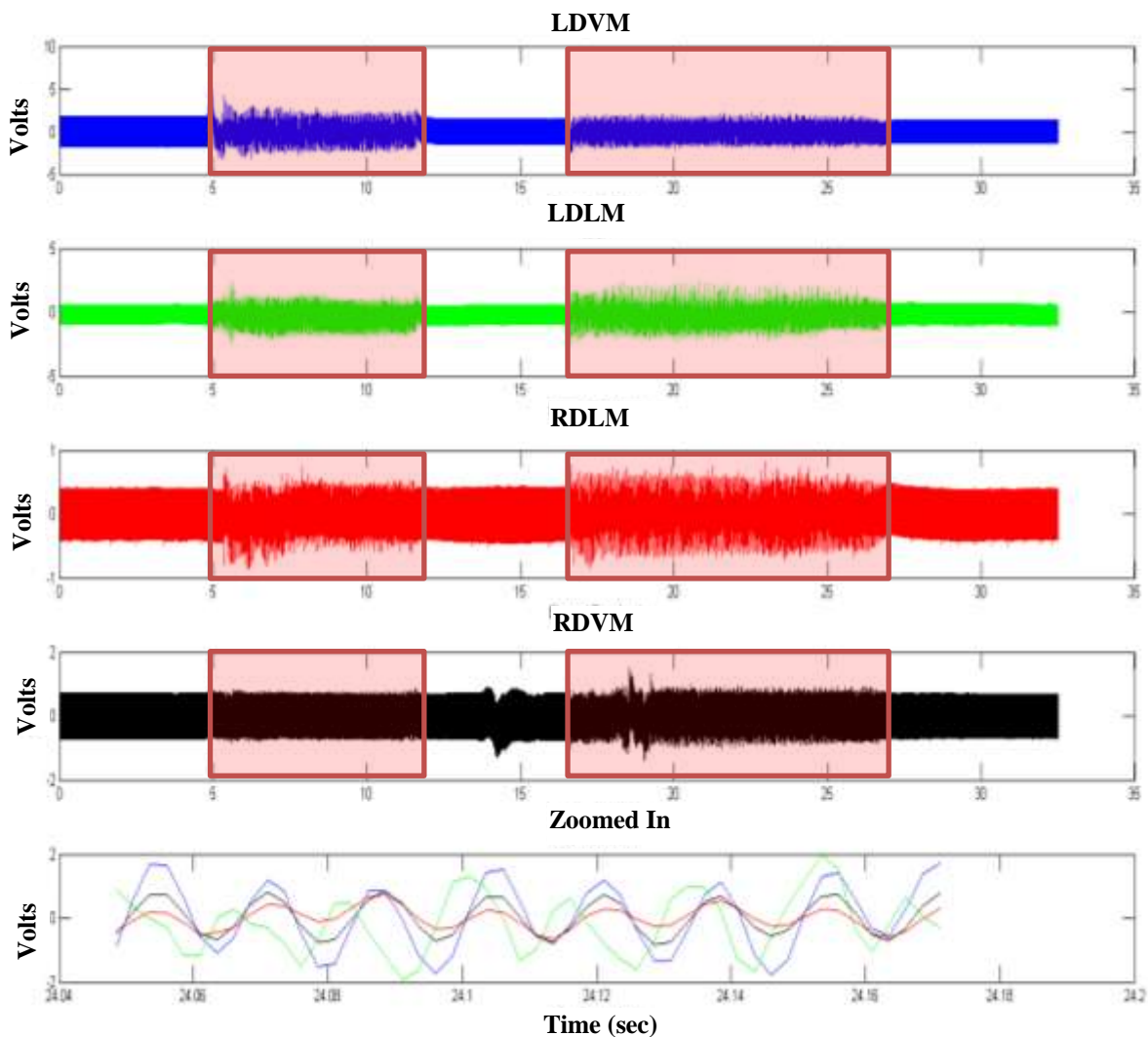


Figure 53: One complete recording of EMG signals. Two periods of flapping motion can be seen

Natural Unstimulated Flapping Angle

The flapping angles were then calculated from high speed video footage, taken during the associated EMG signal acquisition, using the process discussed in Chapter III. The flapping angles were plotted over time (Figure 54) to determine if the flapping angle was similar among those with the fine wire electrode implanted moths to those found in published literature.

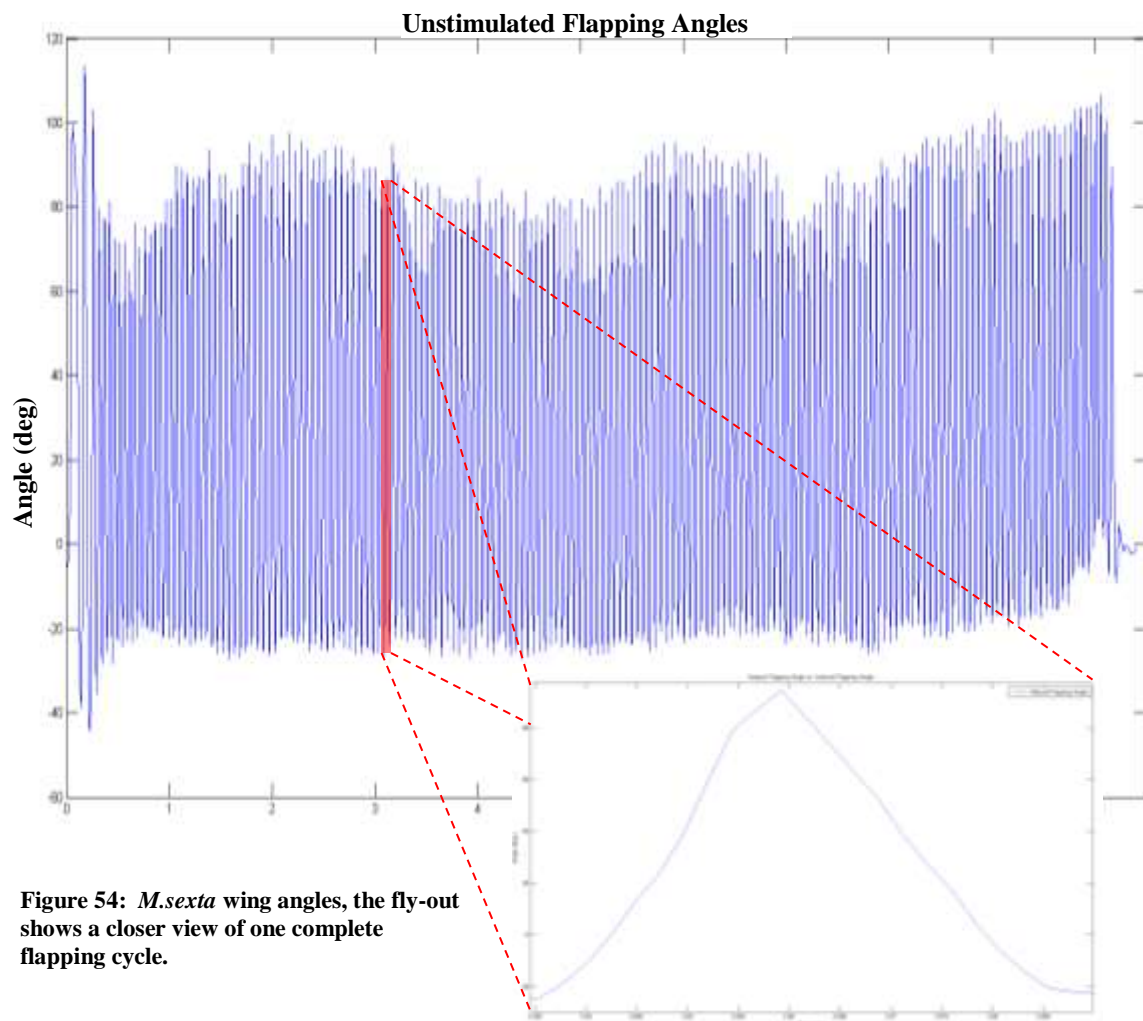


Figure 54: *M.sexta* wing angles, the fly-out shows a closer view of one complete flapping cycle.

A random cycle of the flapping angles found during this research was overlaid on the experimental data found from Lui et al. (Liu, Ellington, Kawachi, Van Den Berg, & Willmott, 1998), and appeared to be very similar (Figure 55). The data suggests that the tested moth in this study was not depressing its wings as much as experimental data would suggest. There are many different explanations for this. Some possible reasons could be: variability between individual specimens, implanted with fine wires versus a moth that was unimplanted, different angle measurement processes, fixed versus free flight flapping, atmospheric or environmental factors, or muscle fatigue.

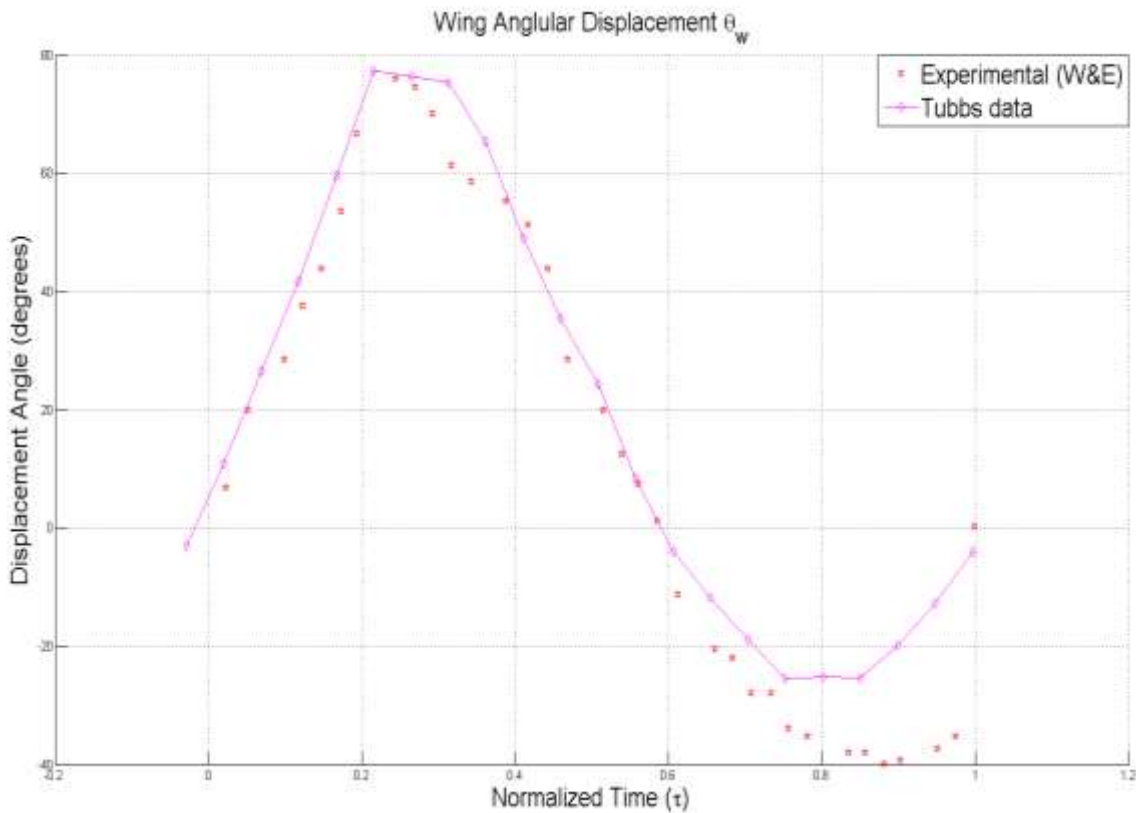


Figure 55: Overlay of found flapping angles with those found experimentally from Wilming and Ellington

EMG Signal Analysis

The EMG signal frequency of the left dorsal longitudinal muscle (LDLM) was then analyzed using Matlab, with a locally devised interface by Dr. Richard Cobb (Cobb R. , 2011). By using the fast Fourier Transform, it was evident that the LDLM was primarily contracting at 23.44 Hz which is was perfectly in line with previously published findings concerning the flight for *M.sexta* (Willmott & Ellington, 1997). This information was valuable for determining frequency response times (Figure 56). The multi colored peak at zero a baseline noise of the system, and the peak at ~60Hz is noise produced through electrical devices.

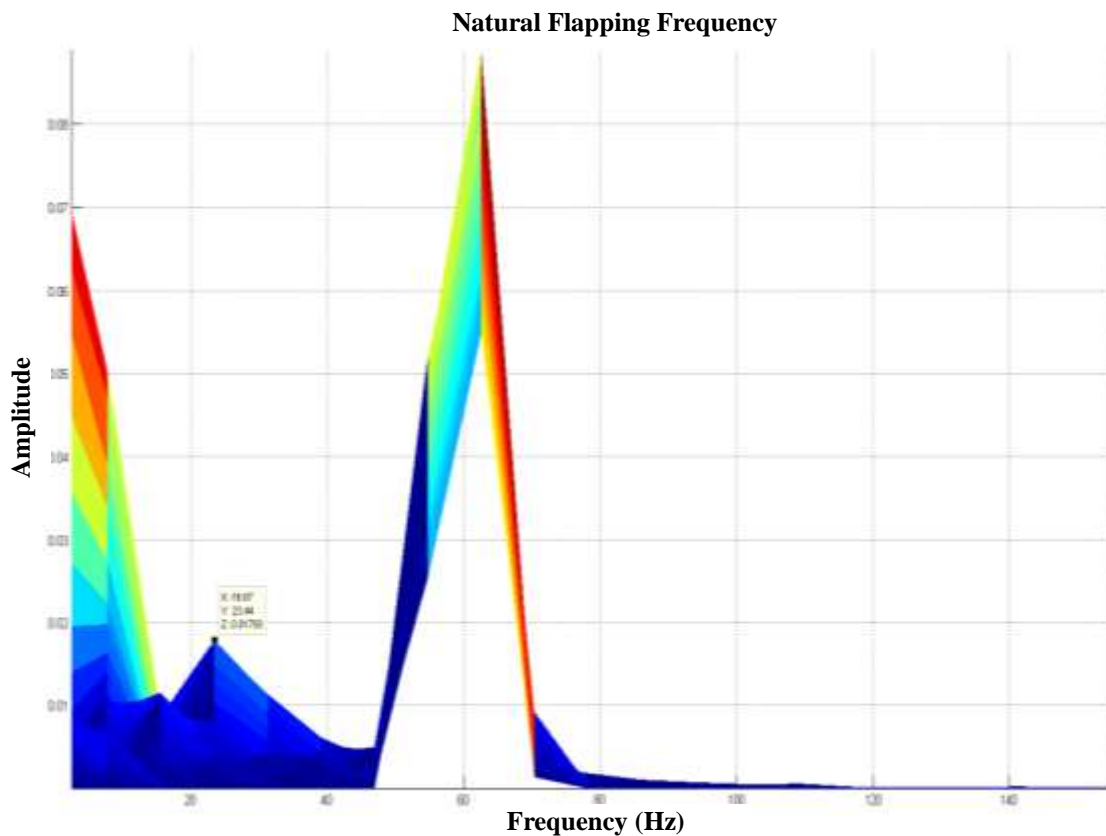


Figure 56: A chart indicating the frequency responsive components of the signals

The signals recorded from *M.sexta* during flight-like flapping were recorded and cropped to capture only the flapping signals (Figure 57). A buffer of zeros was added to the beginning and to the end of the signal to ensure that only the signal was causing stimulation, rather than background noise.

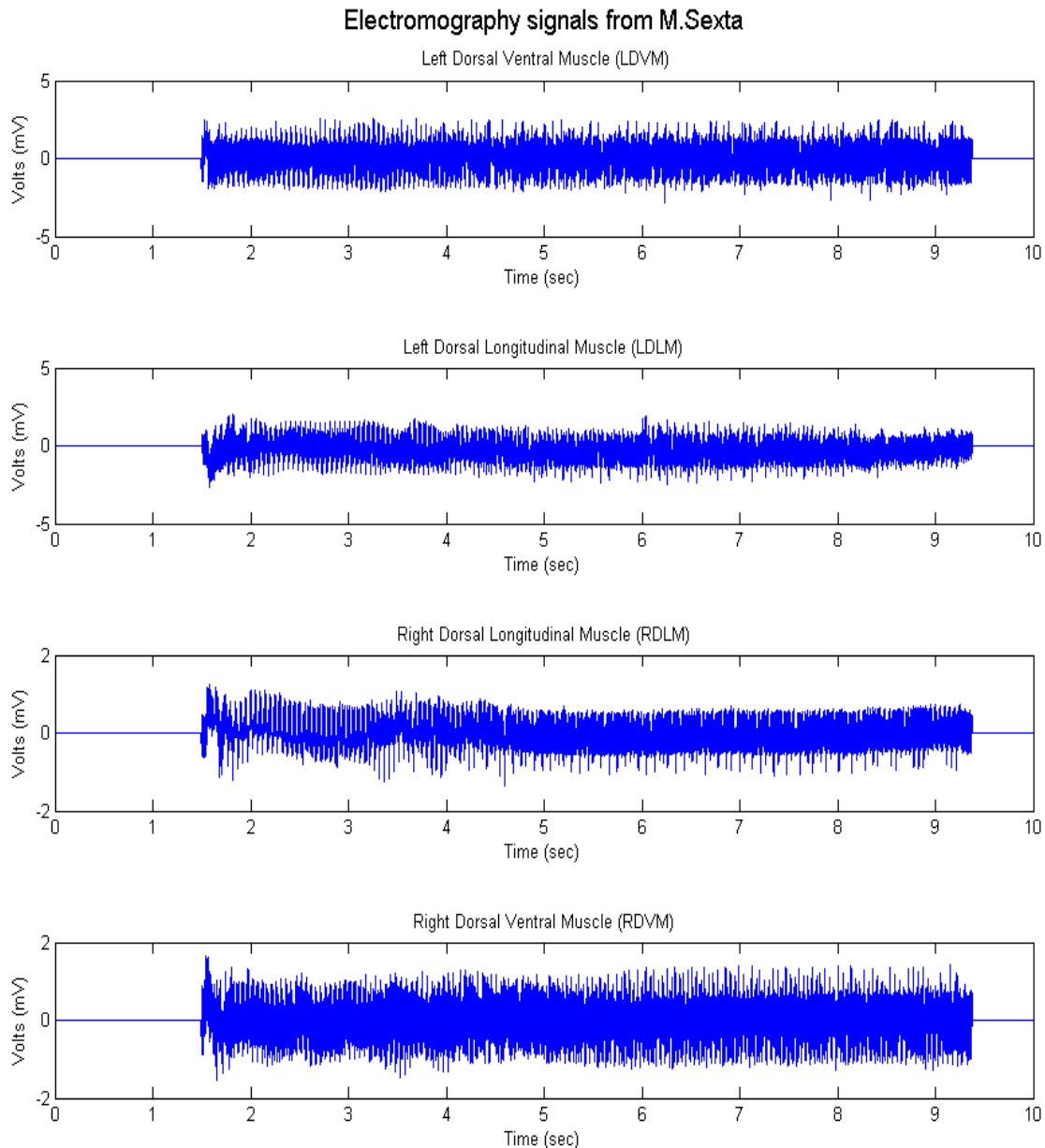


Figure 57: The cropped EMG signals from the primary flight muscle of the *M.sexta*

Transmitted EMG Signal

The signals found in Figure 57 were sent into the corresponding muscles of the previously implanted moth, the only configuration was the BNC cable were moved onto the output ports of the NI USB-6229, and the flapping angle was measured (Figure 58). Based on these findings, it appeared that the overall input caused a greater net force in the DLMs because all of the angles were measured below what was deemed the resting angle. This indicated that *M.sexta* would respond to input signals, but clearly not in a similar fashion as it did when the EMG signals were collected. The moth would not perform the same flapping motion that generated the EMG signal when that same signal was reapplied to the muscle.

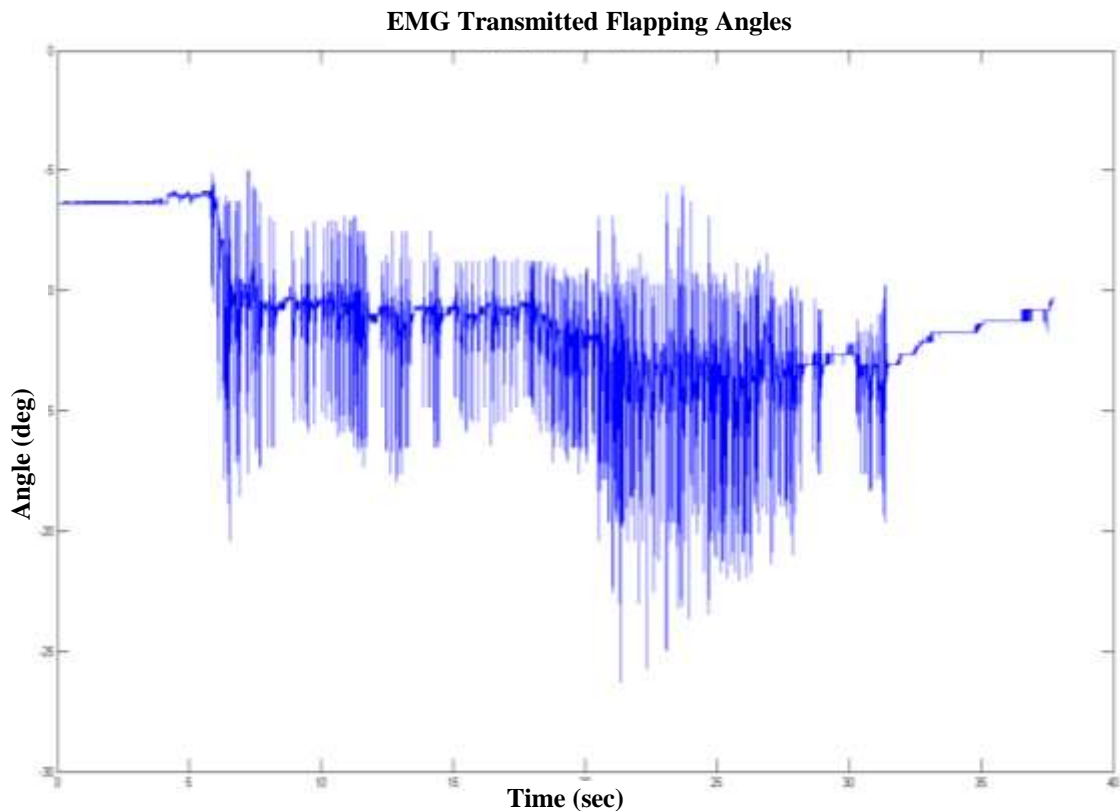


Figure 58: Flapping angles found when stimulated with previously recorded EMG signals

It is not surprising that the EMG signals transmitted back into the muscles did not produce the same flapping angles because insect muscle fibers do not propagate the depolarization Action Potential like motor neurons (Keeley, n.d.). The EMG signal supplied by the electrodes was a localized stimulation, versus using the distributive properties of multi-terminal innervation and the transvers tubular system to ensure that the entire muscle was reacting to the signal. Another reason it might have responded differently could have been attenuation through the muscle, as well as the noise that was inherited through the collection process.

Transmitted Impulse Signals to Individual Muscles

It was understood that for insects, the entire muscle would not react to the EMG signal because of their inability to propagate the depolarization signal. So, a known signal was supplied to the individual muscles in an attempt to assess what the muscle response was in that signal. A 5V impulse signal with a period of 1.9 seconds and a signal length of 0.19 seconds was transmitted from the computer, using Simulink through the NI USB 6229 hardware, out through the fine wire electrodes into the left dorsal ventral muscle (LDVM). Using the wing angle process mentioned in Chapter III, the responding wing movement was collected. The 5V impulse signal was generated asynchronously and the timing was adjusted to correspond with suspected transmit time. The signal was superimposed upon the responding wing angle (Figure 59). This graph showed direct muscular response to the signal which indirectly induced wing movement. By using Matlab to offset the resting angle to zero and then averaging the maximum

angle between each pulse (beginning after the initial flapping, between 0 and 3 seconds), the average angular wing displacement was found to be about 5.2 degrees.

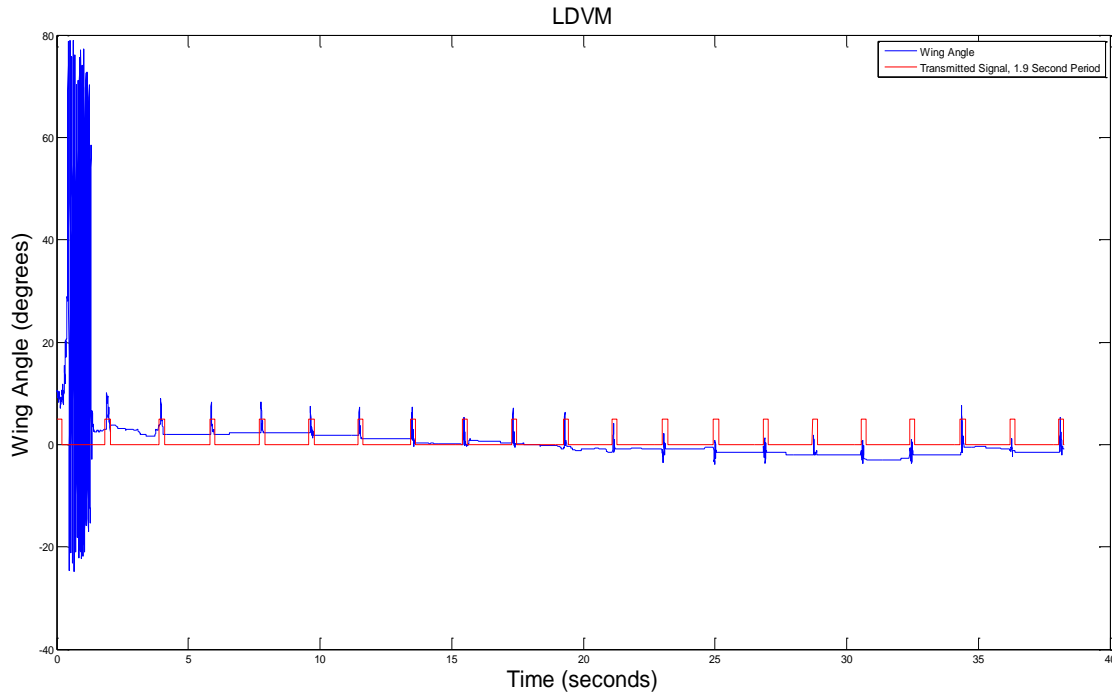


Figure 59: 5V signal directed into the LDVM at a 1.9 second interval; the impulse was 0.19 seconds long

This process was repeated for each of the primary flight muscles. The average wing angular response, from a 5V signal directed into the left dorsal longitudinal muscle (LDLM), was found to be -17.9 degrees (Figure 60). This information was again found using Matlab by offsetting the resting angle to zero, and then averaging the minimum angle between each pulse, beginning after the initial flapping between 0 and 4 seconds. The DLM muscles were the depressor muscles, and it was evident that they caused a much greater wing response when stimulated with the same signal.

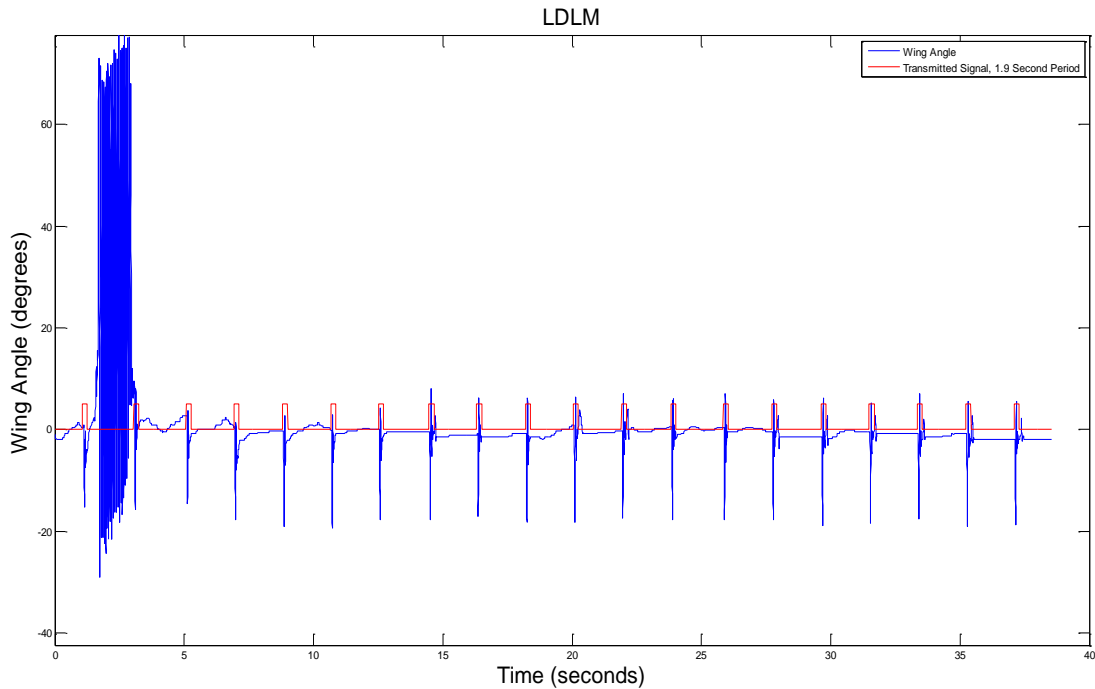


Figure 60: 5V signal directed into the LDLM at a 1.9 second interval; the impulse was 0.19 seconds long

A large response was seen when the right dorsal longitudinal muscle (RDLM) were stimulated (Figure 61). The 5V signal with a 1.9 second period and a 0.19 second signal length, was transmitted to the muscle, but the response was unique because it caused *M.sexta* to flap its wings in the down stroke position twice for each impulse signal transmitted. The most likely reason for this was that one flap was caused when the signal began, and the second flap was for when the signal stopped. The double flap with each signal could also have to do with the electrode location, which was previously seen to be in the wrong location in Figure 53.

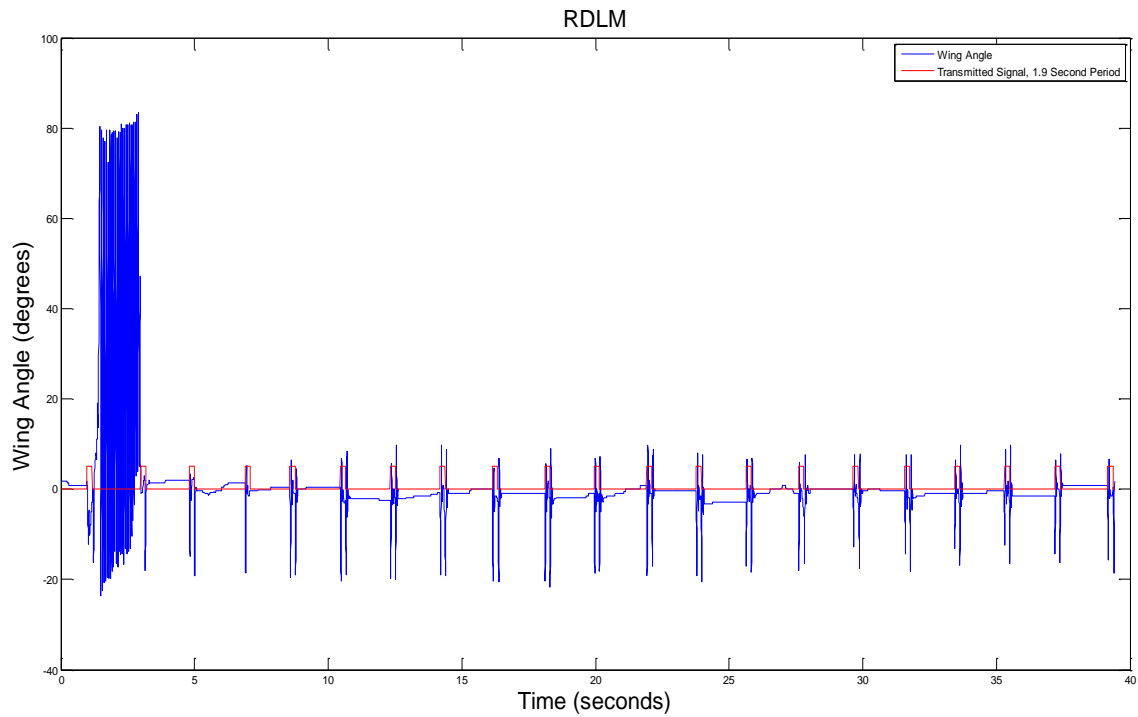


Figure 61: 5V signal directed into the RDLM at a 1.9 second interval; the impulse was 0.19 seconds long

Again using Matlab to offset the resting angle to zero, then averaging the minimum angle between each pulse (beginning after the initial flapping between 0 and 4 seconds), the average wing angular response was found to be -18.8 degrees.

The last muscle group to be tested independently with the 5V signal was the right dorsal ventral muscle (RDVM). By averaging the maximum angle between each pulse (beginning after the initial flapping, between 0 and 3 seconds), the wings were elevated to an average of 5.7 degrees with each corresponding impulse (Figure 62). This appeared to be consistent with the LDVM and with the literature, which indicated that the DVMs were not as powerful as the DLMs (Tu & Daniel, 2004).

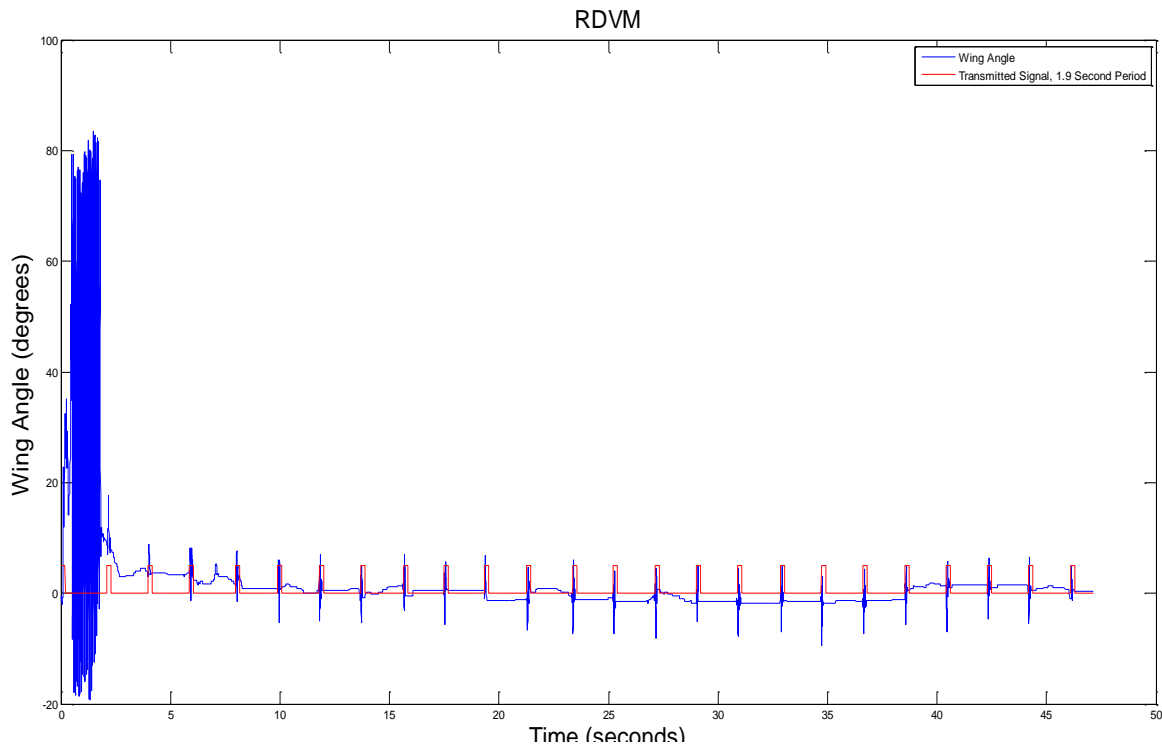


Figure 62: 5V signal directed into the RDVM at a 1.9 second interval; the impulse was 0.19 seconds long

Transmitted Impulse Signals to DLMs and DVMs

Once the individual muscle responses were isolated and recorded, the same signal was sent to all four of the muscles being studied (Figure 63). The DLM signal was delayed by 0.5 seconds so that the different signals could be detected. The graph shows the angular response of two different impulse signals being supplied to the two main muscle groups. The red line represents the two 5V signals, with a 1.9 second period (pulse width of 0.19 seconds), that were generated asynchronously and the timing adjusted to correspond with suspected time that the signals were transmitted into the DVMs. For demonstration purposes these signals was superimposed upon the responding wing angle. The green line represents the same signal, with a phase delay of 0.95 seconds supplied to the DLMs.

There were two periods of time when the moth flapped under its own volition. The first was at the beginning of the graph, when the signals first arrived at the muscle and *M.sexta* immediately responded. This immediate flapping response when the signal first arrived has been seen on the previous four graphs. The second unstimulated flapping occurred around the 49 second mark. After the initial flapping, the beginning of the graph showed a very distinct angular reaction for the two different muscles that were being stimulated. The magnitude of the DLM response gradually became less pronounced over time. This graph clearly indicates that the DLM and DVM muscle groups can be stimulated separately to achieve different wing movements.

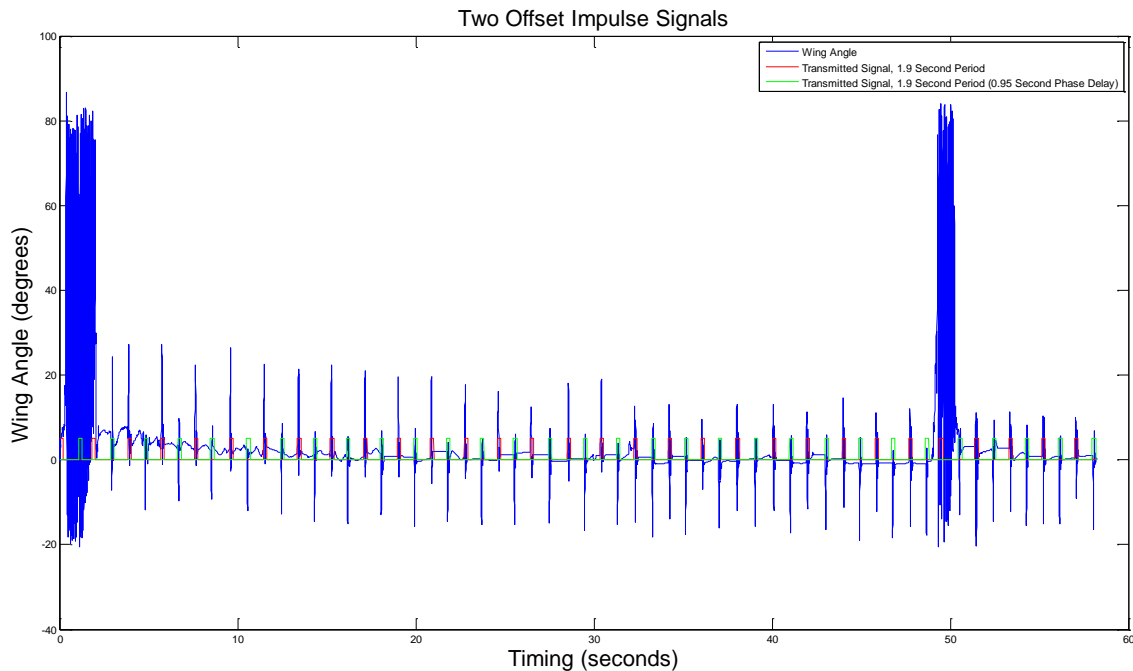


Figure 63: Wing angle response with two different 5V signals, the DLM impulse signal was 180 degrees out of phase

Faster Transmitted Signals

The 5V impulse signal with a 1.9 second period was useful for depicting what each muscle was stimulated to do. However, this was not the rate at which *M.sexta* flapped its wings. To encourage the more realistic flapping movement, the signals were transmitted at a faster rate (Figure 64).

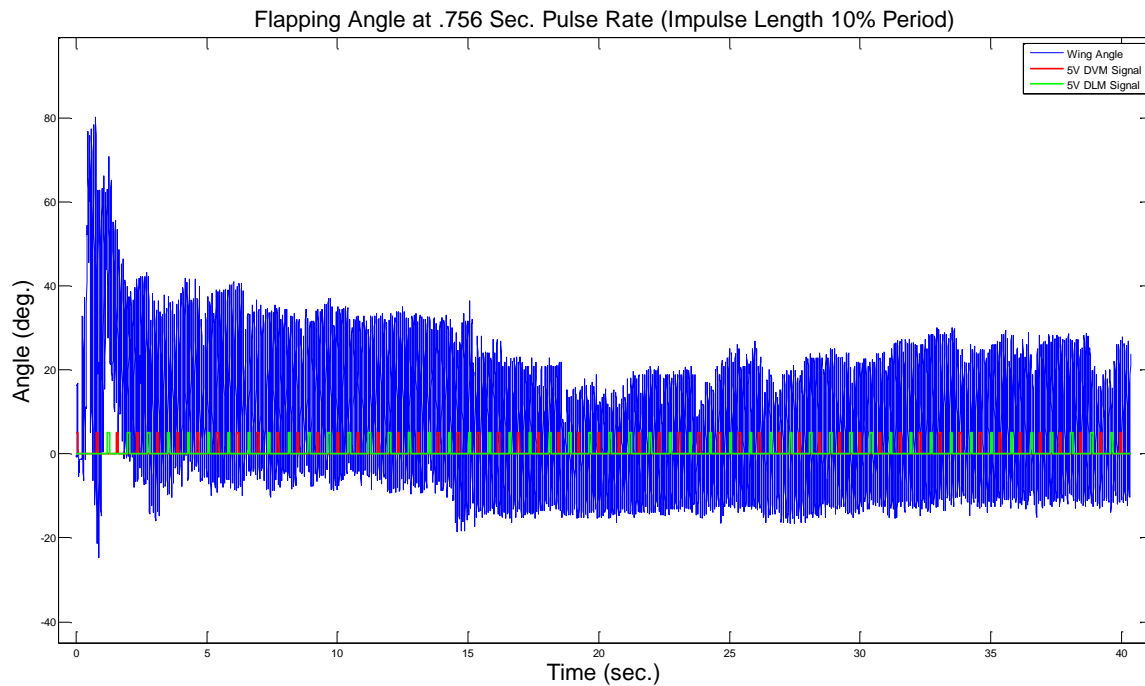


Figure 64: Two different 5V signals supplied with a 0.756 second period and a 0.0756 second signal length; the red is supplied to the DVM and the green is supplied to the DLM

This graph shows the wing angles when supplied with a 5V signal, with a 0.756 second period and a signal length of 0.0756 seconds. The wing movements became much more similar to those observed during independent flapping, when no signal was being supplied, but the range of motion was not as great. The disparity between the two signals still needs to be analyzed to determine what changes could induce the wing to achieve the full range of motion. As with the other signals, the red line was being

supplied to the DVMs, and the green line is being directed into the DLMs. This graph justifies the belief that predictable and near natural wing motions can be supplied with artificial signals.

The wing angles appeared to be very similar to natural wing movement when superimposed upon the unstimulated wing movement (Figure 65). The artificially induced wing movement (**Error! Reference source not found.**), seen in green, was superimposed upon the natural wing movement produced without external electrical

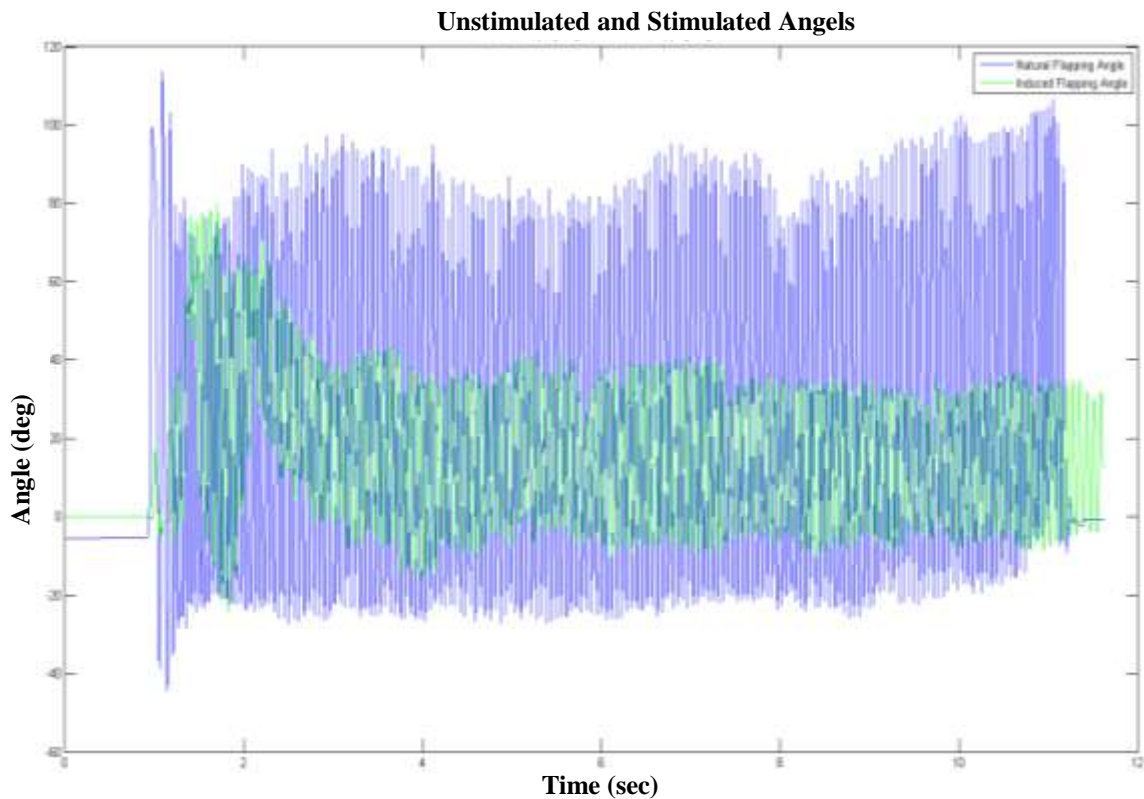


Figure 65: The natural flapping angle from the M.Sexta (blue) and the artificially stimulated signal (green), overlaid to show the differences

stimuli (Figure 54), as seen in blue.

This graph shows the angular difference that the moth produced naturally (blue) versus what was stimulated (green). It was evident that the stimulated wing did not have

the full range of motion when compared to natural wing movement. The signal did appear to be similar in cycle length, the time between the down and up-stroke. The most likely reason for reduced wing motion was caused by incomplete contraction of the DLMs, which indirectly increase the wing angle. It could also be because the need to stimulate additional flight muscles which was not examined in this research.

As a means to demonstrate that the artificially transmitted signal caused the flapping motion, the same signal (seen in Figure 64), which was a 5V signal with a 0.756 second period and a signal length of 0.0756 seconds) was transmitted to *M.sexata*. During this test, the transmitted signal was randomly stopped (Figure 66). The flat green line

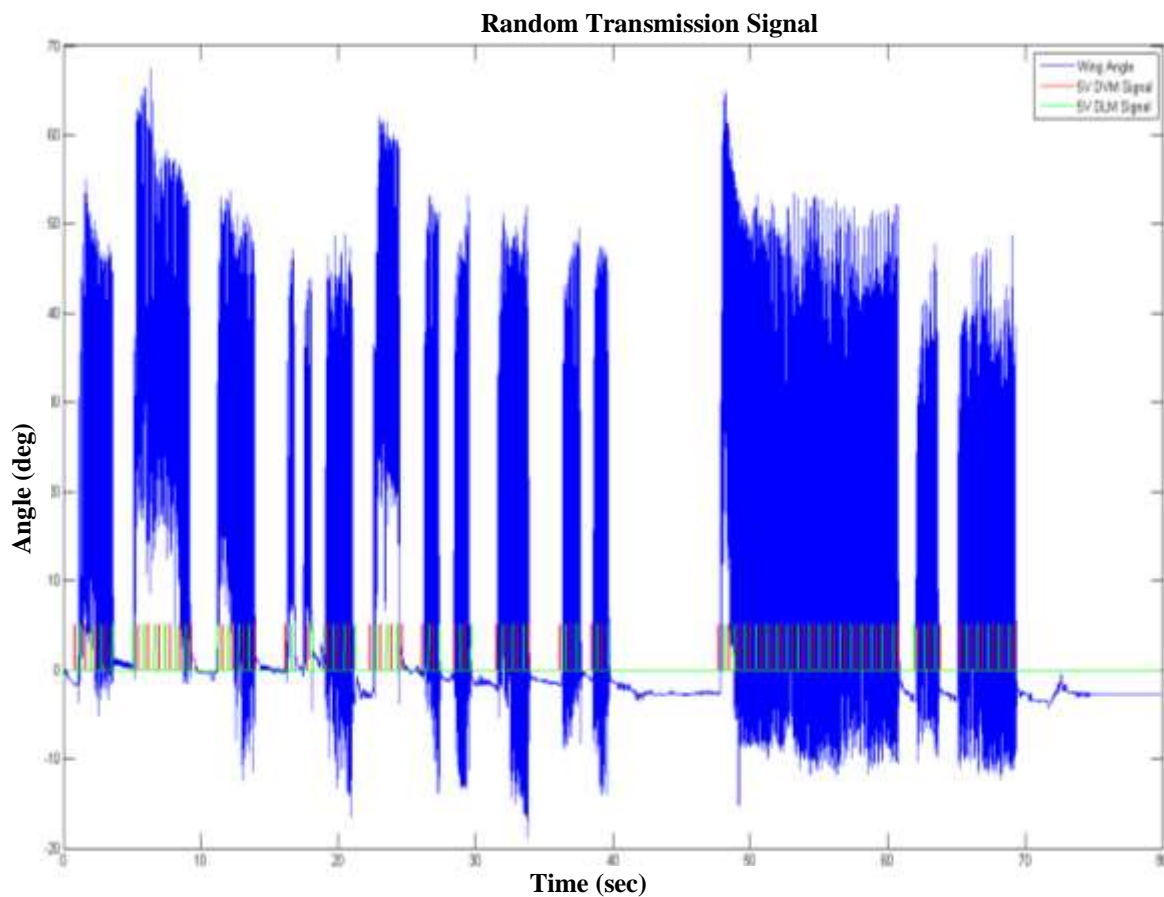


Figure 66: Two different 5V signals supplied with a .756 second period and a .0756 second signal length; the red is supplied to the DVM and the green is supplied to the DLM; during this test, the signals were randomly removed from the test subject to indicate that the supplied signal was in fact causing the motion.

indicates the times when no signal was being supplied. It is evident that the signal was driving wing movement. When the signals were removed, no wing motion took place. This once again justifies the fact that artificial signals can be used to induce known and expected wing movement.

Using Matlab's spectrogram function, a graphical representation of *M.sexta*'s natural flapping frequency components over time was shown (Figure 67). The primary component of the beat frequency occurred at an average of 18.05Hz. The natural frequency had many harmonics associated with the wing movement, as indicated by the arrows; this could be caused by additional muscles being used that were not tested.

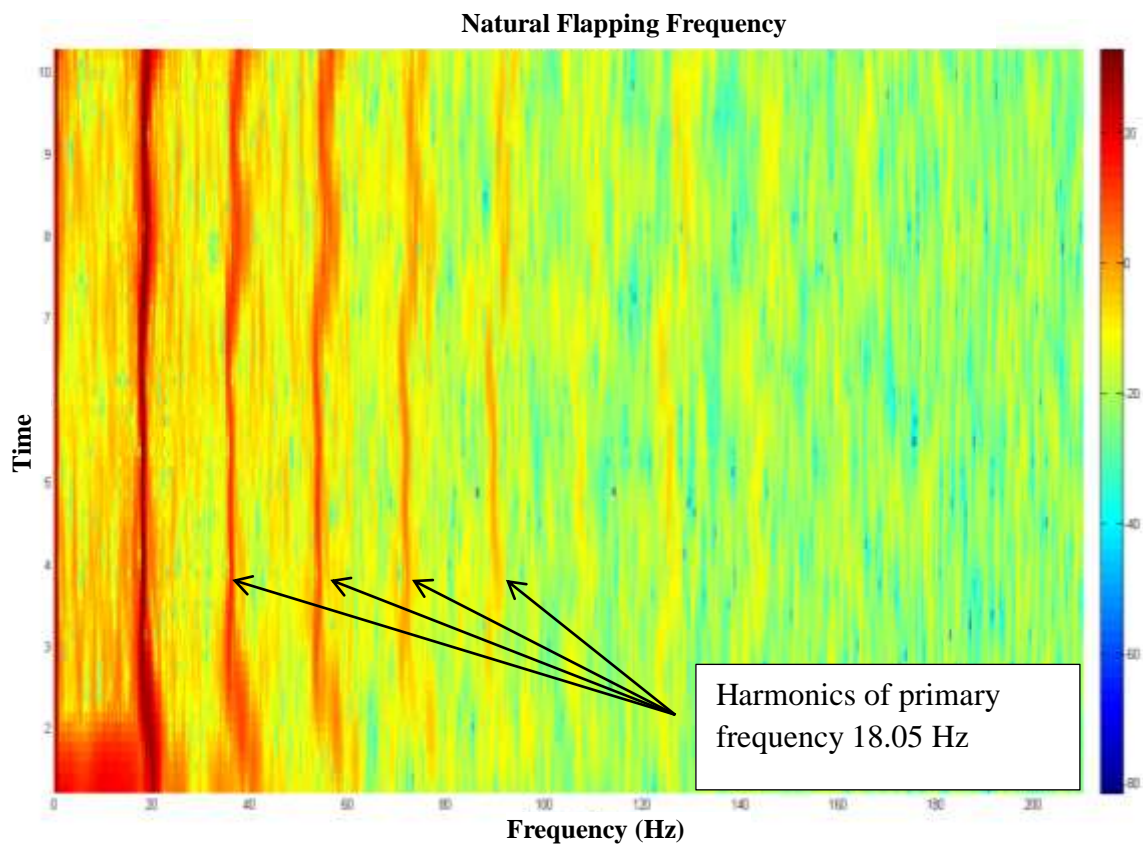


Figure 67: Matlab's spectrogram function showing the natural wing beat frequency over time

Matlab's spectrogram function showed that the Fourier transform of the stimulated frequency had less pronounced harmonics (Figure 68). This was likely due to the fact that only a few muscles were being caused to move, where natural flapping most likely included several other muscle movements. This data also indicates that *M.sexta* would flap at the supplied signal versus one that might have been more natural, because the primary component of the stimulated beat frequency occurred at an average of 13.54Hz. The artificially induced flapping frequency was much slower than what the *M.sexta* naturally flaps, which is between 20 and 27 Hz (Willmott & Ellington, 1997).

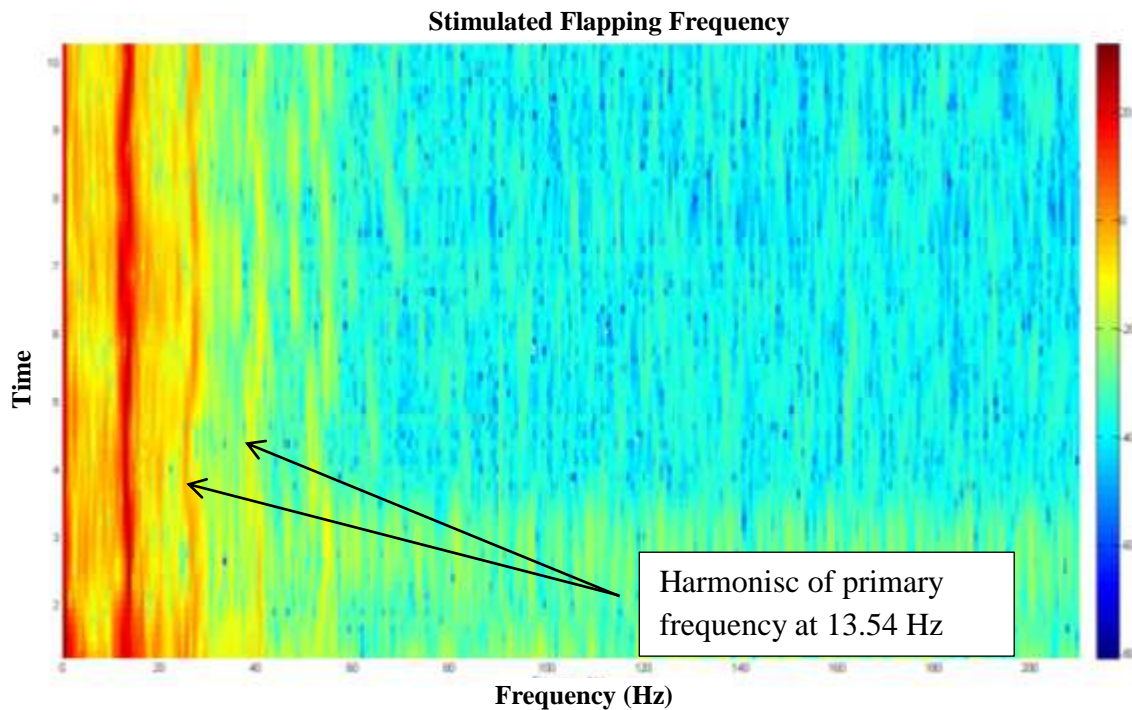


Figure 68: Matlab's spectrogram function showing the artificially stimulated wing beat frequency over time

Clear Frequency Response

The wing angle response directly correlated with the transmitted signals. To demonstrate this relationship the HP 3312A 15 MHz function generator was used because of the ease in adjusting the transmitting frequency. The function generator was connected to the fine wire electrodes and inserted into the DLMs of the moth. A 1 volt signal was used and the frequency was incrementally increased from 1Hz to 22Hz. As the frequency increased the magnitude of the wing response became smaller, therefore at higher frequencies the wings would appear to vibrate.

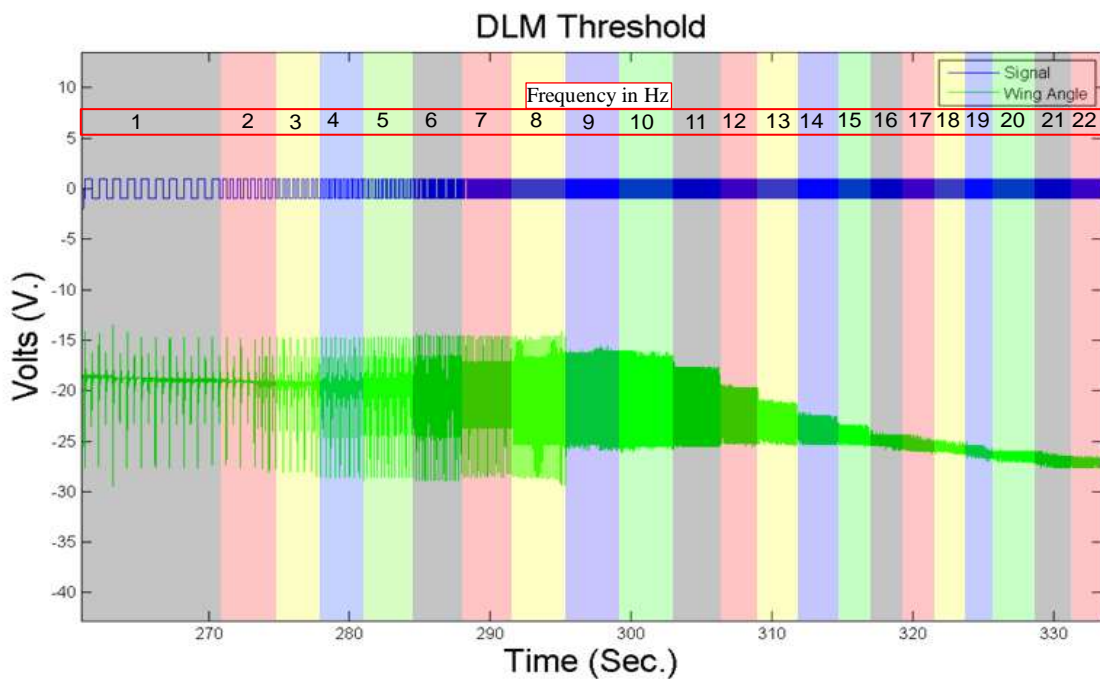


Figure 69: Incrementally increasing the transmitted frequency. The different colors were added using Photoshop to indicate the different frequencies. The numbers in the red box indicate the frequency in Hz associated with that color.

Using the spectrogram script in Matlab, and the aid of Dr. Richard Cobb, the frequency changes transmitted by the signal generator (Figure 70) and the responding wing frequency (Figure 71) were able to be graphed. These graphs show a clear relationship between the transmitted signal and the wing angle response.

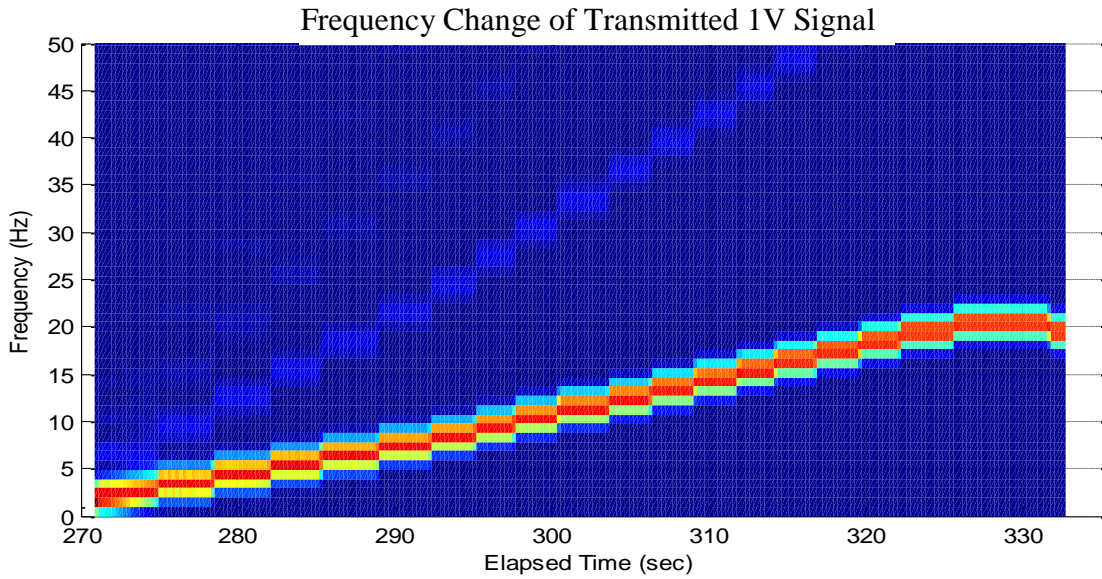


Figure 70: Matlab spectrogram depicting the frequencies transmitted to the DLMs by the function generator

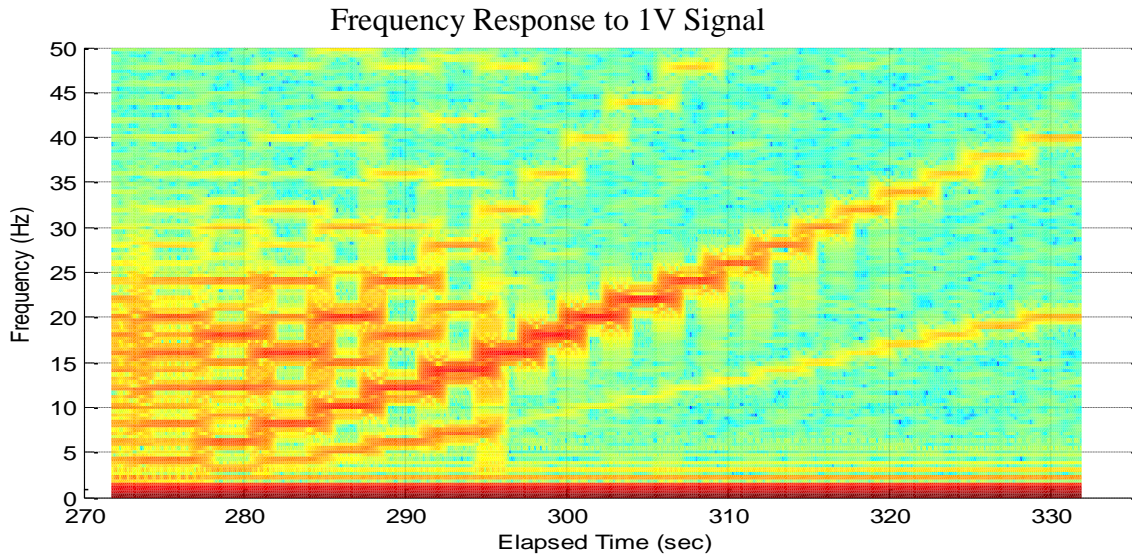


Figure 71: Matlab spectrogram depicting the frequency response of the transmitted signal in Figure 70

Voltage Response

The HP 3312A 15 MHz function generator was used to incrementally increase and decrease the voltage that was transmitted into the DLMs. The voltage threshold was established using a 1 Hz square wave. A clear wing movement response was observed at 240 mV, the wings depressed about 7.12 degrees from its resting angle. During this test the voltage was then increased incrementally to 10 Volts then decreased back down to 1 Volt. The wing response (green) was superimposed to show the changes over time. Throughout this test the resting angle, or the angle at which wing would return to when not moving, shifted significantly. This resting angle is can be seen in Figure 72 as the dark green area that begins centered at zero but drifts lower as the voltage increases. This shifting of the resting angle indicates that the moth's wings did not return to the same resting position at higher voltages.

Only the DLMs were being stimulated during this test so only the depression of the wings were considered in relation to the transmitted signals not the elevation. Once the threshold was reached (~240 mV) the magnitude of the response was 7.12 degrees from its resting angle. At 700 mV the magnitude that the wings depressed became about 16.75 degrees from its resting angle. It is believed that the higher signal was able to excite more motoneurons which in turn were able to retransmit the signal back into the muscles resulting in a more complete DLM contraction. At 2V the wings were again able to depress even more, about 24.23 degrees from the resting angle. This was the largest increase from the resting angle observed. The wings did not depress below 30 degrees

and the depth of depression from 2 V to 10 V remained relatively consistent with what was observed in the unstimulated flapping in Figure 54.

The resting angle of the *M.sexta* appeared to follow the voltage pattern, as the voltage increased the resting angle paralleled the negative portion of the signal. This trend continued until the voltage signal was again decreased. For some unknown reason the resting angle continued to trend downward but as expected the actual difference between the resting angle and the wing depression angle decreased.

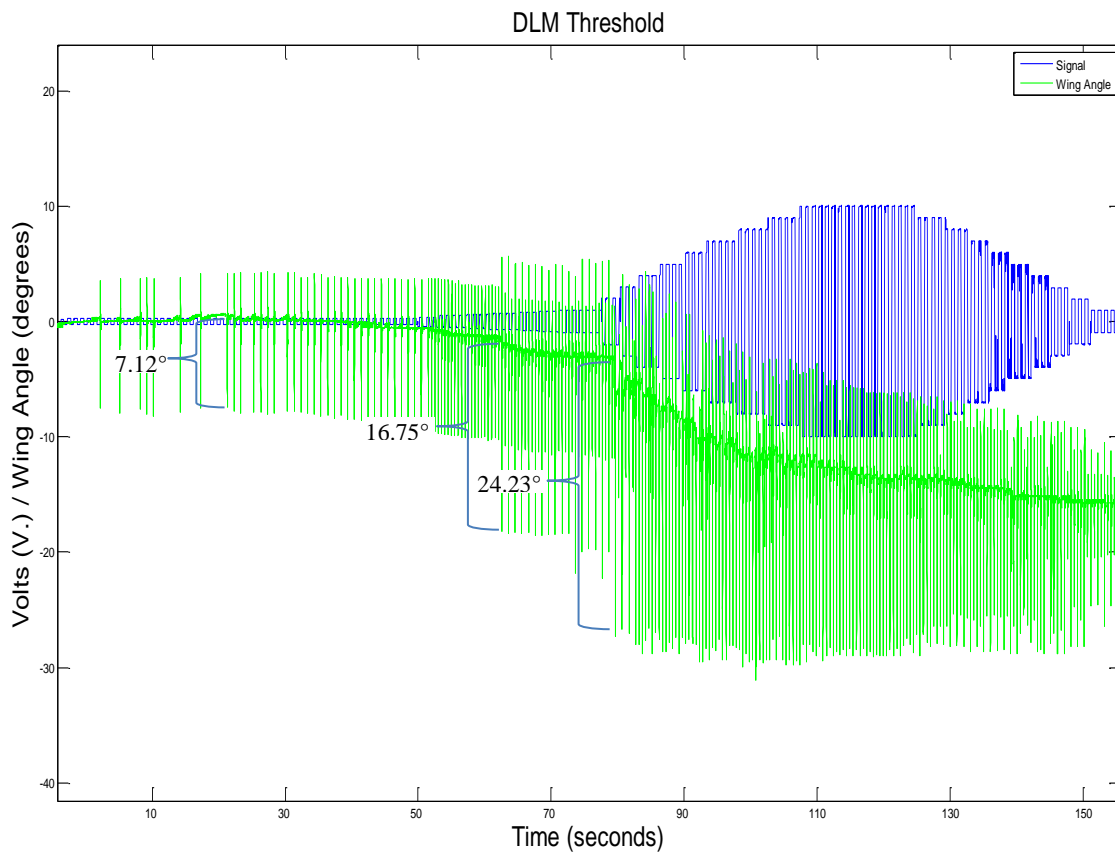


Figure 72: The transmitted voltage incrementally increased and decreased and associated wing response

Pulse Width Modulation

Pulse width modulation (PWM) is a technique used to control power to modern electronic circuits. The basic idea is to send a signal rapidly enough that the receiving system only responds to the average voltage. The average voltage can be digitally adjusted by varying the duration of the pulse. A simple test was conducted using pulse width modulation (PWM), where the width of the impulse signal was changed (Figure 73). It was observed that the total magnitude of the wing angles varied significantly by changing the pulse width.

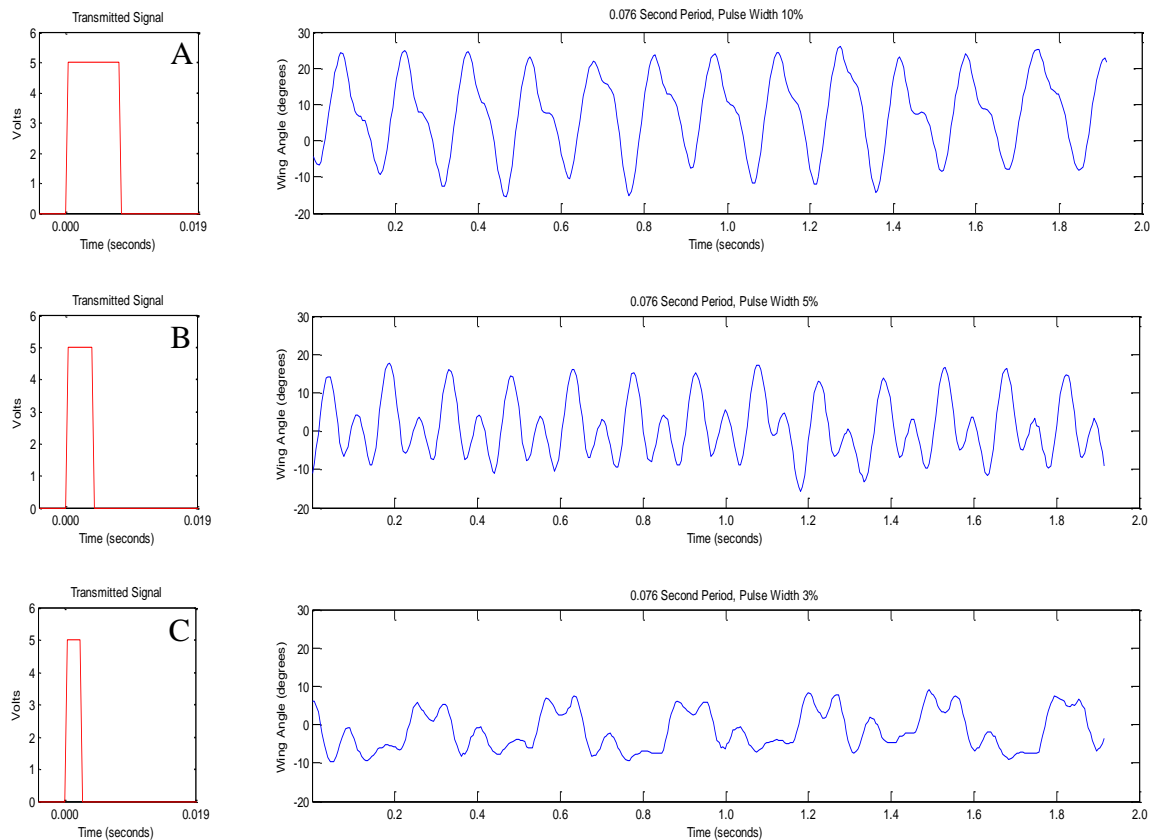


Figure 73: Pulse width modulation test, three different tests were conducted with all the variables consistent except the pulse width. The top transmitted signal had a pulse width of 0.0076 seconds; the middle transmitted signal had a pulse width of 0.0038 seconds; the bottom transmitted signal had a pulse width of 0.0023 seconds

A square wave with a 0.076 second period was transmitted into the DLMs. The width of the signal was varied at 0.0076 seconds (A), 0.0038 seconds (B) and 0.0023 seconds (C). The pulse width of 0.0076 seconds resulted in a range of ~38.2 degrees. The pulse width of 0.0038 seconds resulted in a range of ~27.5 degrees. The pulse width of 0.0023 seconds resulted in a range of ~12.8 degrees. The width of the pulse directly corresponded to the range of wing movement, the larger the pulse width resulted in larger total angular wing motion. This is significant because it demonstrates that the biological flight system of the *M.sexta* can be directly controlled with the electronic technique of PWM which could have significant MAV control implications.

Results Summary

The pupal implant resulted in high mortality and no usable data. In contrast, the results generated from the fine wire process proved that collecting EMG signals from the primary flight muscles is possible with relatively inexpensive equipment. Transmitting the collected EMG signals into *M.sexta* muscles did not reproduce the natural flapping angles, as was expected. However, using impulse signals at rapid frequencies did produce similar wing angles, but with reduced range of motion. These results indicate that EMG signals were able to be recorded and electrical signals were able to be transmitted back into the muscles to establish predictable wing movement. This provides evidence that it is possible to control *M.sexta*'s wing movement in a predictable fashion. This process aids biological MAV work by developing a clear connection between supplied

signals and wing response. This evident muscular control may be used to directly control moths in the future or to test different wing designs under biological flapping conditions.

V. Summary and Conclusion

Flapping Angle Data

The intent of this investigation was to determine if the flapping motion of *M.sexta* could be artificially induced. Based on the experimental data, it is evident that electrical signals supplied to the different muscle groups can cause predictable wing behaviors. The idea of using electricity to induce muscle movement has been around for hundreds of years. However, technology has just now advanced sufficiently enough to allow basic EMG signal capturing capabilities outside of the medical community, and to then be able to transmit specific electrical signals back into the designated muscle.

The desire to produce reliable Micro Air Vehicles (MAVs) is driving an extensive amount of research. By developing the three phase iterative operational plan under the direction of Dr. Palazotto, the need to focus upon flight muscle research was established using the iterative development process. The moth, *M.sexta* had previously been established as the natural template by which AFIT MAV research would be patterned, because of its unique characteristics which satisfy the Defense Advanced Research Projects Agency's (DARPA) MAV specifications. To investigate the biological mechanism of interest, the functionality of the flight muscles, it became necessary to develop the ability to accurately capture the bioelectrical signals that stimulate the muscle powered flight of *M.sexta*. This research provides a better understanding about the signals responsible for biological flight at the MAV level.

With the help of Dr. Willis, a logical process was outlined for preparing *M.sexta* for study, and a system was designed to capture EMG signals from the primary flight

muscles. These EMG signals provide valuable information about the electrical signals being used to stimulate the muscle naturally. These signals are also useful to ensure proper implant placement into the appropriate flight muscles.

The pupal implants failed to produce usable data and resulted in a high mortality rate for the pupae. There are potential benefits with a functioning pupal implant. First, it has potential to provide a more standardized process for recording EMG signals. Second, the implant would streamline the EMG recording process by removing the multiple separate wires that were required to capture EMG signals. Lastly, implanting during the pupal stage could allow the muscles to heal around the implant. The muscle tissue would directly attach to the implant, making the signals much clearer and removing the problem of wires moving during the testing. This could lead to free flight studies where the implants have been shown to work in other research. For these reasons, it is recommended that the pupal implant process continue to be tested and evaluated to determine what the specific problems are in the process.

EMG Signals

The EMG signals that were recorded are a measurement of the ionic difference between two electrodes, due to the neuromuscular Action Potential (AP). In *M.sexata*, the AP has a direct one-to-one relationship with muscle contraction, which indirectly leads to wing movement. This study was designed to induce this muscular response, in a known fashion, with the intent to illicit a clear and predictable response. As indicated in the results section, each muscle was stimulated in a repeating pattern, and the wing angle was measured in each instance. A direct causal relationship can be seen. This being an initial

study, the full range of motion was not able to be achieved. However, strong evidence indicates that stimulated full flapping motion *is* achievable with improved techniques and procedures.

Reapplying the EMG Signal

Analyzing and experimenting with living organisms with artificial constraints may introduce possible errors because these conditions are not found in the natural environment. It is impossible with current technology to record EMG signals without affecting the natural movement of *M.sexata*. The fine wire technique used in this research was chosen because of the availability and functional capabilities of the equipment. The results generated from the fine wire process are acceptable and prove that this technique can reproduce expected neuromuscular signal responses, as measured by the wing angles.

When the actual EMG signals were reapplied to *M.sexata* muscle, the wing angle demonstrated disjointed and erratic behavior. This was due to the multiple motoneuron signals that were recorded during the EMG process. Another problem with reapplying recorded EMG signals is that the muscle fibers do not react the same way that motoneurons do because the electrodes affect only a localized area, rather than distributing the signal throughout the muscle. One reason that the voltage needs to be increased is to induce more muscle fibers to reach their threshold, which in turn will increase muscular contraction the signals transmitted to the moth during this investigation most likely were activating the motor neurons which then activated the muscles. The EMG signals that are recorded give a basis of understanding about how the muscles are

working to generate lift; these signals can then be processed into a simpler impulse signal that can be used to stimulate wing movement.

The recording of EMG signals from a *M.sexta* is an intrusive process; as technology improves, it may be possible to gather this information in a different way which will not affect the natural movement of *M.sexta*. This could be done with some device that is so sensitive that the muscle movement could be detected from a distance, removing the need for implants or any equipment touching the test subject. Despite the problems in collecting them, the EMG signals proved to be very valuable in determining the electrode placement, phase shift, and flapping frequency. Based on this EMG information specific impulse signals were selected and reapplied to the flight muscles.

Transmitting Impulse Signals

A variety of impulse signals were transmitted into the DLMs and DVMs of the moth, *M.sexta*. The resulting wing movement provided a basis of understanding of how the signal stimulated muscle contraction. Figure 72 demonstrated the voltage threshold that was required to induce muscle contraction and how voltage variation changed the wing angle range of motion. Figure 73 showed that the technique of PWM can be used successfully on a biological system and that wing angle range will directly be affected by the pulse width. These tests clearly demonstrate that electrical control of the flapping mechanism of *M.sexta* can be achieved and with further study improved upon.

Experimental Limitations

This thesis was limited by the amount of specimens that were able to be tested. The initial failures of the supplying colony, as discussed in Chapter III and the high

mortality rate caused by the implant reduced the number of samples that could be analyzed in the time allotted. A limited number of pupal implants halted any further study on that aspect of the research because the supplies were exhausted. The constraint of the life cycle of the species also made it difficult to conduct as much research as expected, because it took about 48 days from the time a larvae hatched before it could be tested as an adult.

Another limiting factor of the research was the inability to standardize the fine wire placement within the flight muscles. The amount of time it took was longer than expected to successfully implant a moth with the fine wires. These limitations were anticipated to be greatly reduced with the pupal implant.

Sample Size Limitations

The results of this thesis were limited to *M.sexta* from Willis Labs at Case Western University and Carolina Biological Supply Center. As stated earlier, the scope of this investigation was limited in quantity of specimens that were tested using fine wire implants. This was due to the majority of them being tested with the pupal implant. It is recommended that additional research be conducted to quantitatively determine the results of wing movement through artificial stimulation, and to determine the extent by which this information can be applied across species.

Relevance of the Current Investigation

There are three main benefits with having the ability to categorically induce known wing movement through artificial stimulation. First, using *M.sexta* as the flapping mechanism maintains the biological integrity under which MAV research at AFIT is

conducted. Secondly, this provides quantitative data that can be used in artificial MAV designs. Lastly, this research could evolve into the ability to successfully control the movements of *M.sexta* as a biological MAV. This thesis establishes procedures for fixed wire EMG signal acquisition and signal transmission into *M.sexta* muscles. It also acquired preliminary data associating wing angle responses with a known signal.

There are many different flapping designs and mechanisms that attempt to simulate wing movement. The best way to ensure that the variables remain constant is to avoid changing them. The best way to see how a *M.sexta* would move its wings under a given condition is to induce the desired movement in *M.sexta*. How the wings of a *M.sexta* function and react in their natural environment (attached to the insect) is more precisely understood by studying wing movement from a known impulse. The data in this thesis proves that it is possible to generate wing movement with simple impulse signals sent into the muscle. This process also removes the time variable condition of the wing desiccation that was seen previously in Figure 13.

An estimate of the energy necessary to induce wing movement was calculated in Chapter III. This section gave the expected energy requirements that are needed for wing movement, and this information can help in the testing of flapping MAVs of similar dimensions. By studying the biological system of *M.sexta*, additional information could be generated. For example, the amount of deformation each bioelectrical signal induces on the thorax due to muscular contraction, and other quantitative data, can be used in mechanical MAV designs.

This research is intended to evolve and grow to incorporate some form of control mechanism that could be adapted and incorporated into a free flying *M.sexta*, with the

aim to directly control flight through human supplied signals. This would be a biological MAV. This has been successfully accomplished with beetles (Sato, et al., 2008) and has been tested on *M.sexta* (Bozkurt, Gilmour, & Lal, 2009) with promising results, but with no free flight capability yet. The data presented in this paper is intended to assist with or inspire the pursuit of the effort.

This research has great application for MAV research. Currently, there is very little understanding about how to power MAVs with the constraints that have been established. It is believed that further insight into this problem will be generated by studying the flight muscles and their impact on wing movement.

Final Statement

This thesis successfully accomplished its objective, which was to determine the possibility and benefit of reproducing the biological flapping motion of a *Manduca sexta* with artificial stimulation for the purpose of MAV development. This investigation has clearly shown that it is possible to generate specific flapping movement of *M.sexta* through direct muscle stimulation with fine wire electrodes. The ability to accurately reproduce biological movement has three primary benefits, which are to maintain the integrity of wing and joint during testing, provide useful data for MAV design, and to create the possible design of living *M.sexta* MAVs. This research directly applies to the future of biologically inspired MAV work, and with further study, could greatly improve current understanding about wing movement.

Appendix A.

Scientific Instrument Used

This section contains a brief description of the equipment used throughout this research.

NI USB 6229

This National Instrument hardware has 16 differential BNC analog inputs (16-bit, 250 kS/s) and 4 BNC analog outputs (16-bit, 833 kS/s), which were needed to supply signals to the four muscle groups of interest. The instrument is designed for signal streaming for sustained high-speed data streams, transmitted over USB. This equipment is compatible with Matlab, which made programing it much easier.



HP 3312A 15MHZ Function Generator

The function generator was used to ensure that the connectivity of devised EMG recording system (Figure 45) was functioning and accurate. The function generator also worked well for supplying a known signal to the moth's muscles quickly and easily.



Instruments Division-Signal Conditioning

Amplifier 2310

Four of these multifunctional signal amplifiers and filters were used during this research. Each muscle group was wired into one of the amplifiers so that the low EMG signal produced in the muscle could be amplified, and all of the high frequency signals could be filtered out with this equipment.



Eyeclops

This was a simple toy digital microscope that was modified to aid in minute and detailed work. The Eyeclops was disassembled and mounted onto a more stable platform, enabling it to be much more controllable and reliable. This equipment was also hardwired into a computer so that it could stream video, which was used to capture *M.sexta* eggs hatching.



Lux Thermostat

The Lux thermostat was a quick and easy fix to environmental control of the rearing environment for the larvae and pupae. The temperature was digitally set and the heater was plugged into the outlet on the bottom so that when the predefined temperature was reached, the heater would shut off.



Repticare Heat Emitter

The Repticare is an infrared heat lamp designed for reptile habitats. This worked well for this research because it maintained the correct temperature, when used in conjunction with the Lux thermostat, but it did not change the lighting conditions for which the moths were so sensitive, and it did not blow hot air onto them, which was one of the reasons why the system had to be redesigned because so many pupae got too hot.



Tektronix TDS 420 A

The oscilloscope was more useful at the beginning of the setup so that all of the equipment could be tested to insure proper function and expected results. But once everything was correctly calibrated, it was not used as much.



Microsoft LifeCam

This little webcam proved to be very useful throughout the entire research process. It was easy to use, had nice picture quality, and was very versatile in its abilities. It was first used as a microscope video camera. It was simply taped to the microscope and it provided a very good



picture. It was then connected to the computer and left running to create time lapse videos showing changes over time. There were some compatibility issues on the computer-sometimes the video would cause the computer to restart but for the most part, it was a very simple and useful tool.

Stemi SV 6 Zeiss

This was a good microscope but, it had limited functionality because it did not have a camera and its magnification range was limited. It did provide very nice footage of a *M.sexta* hatching, but having more magnification would make it much more useful.



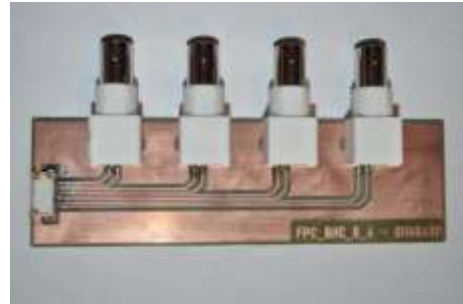
Casio Exilim EX-FC 150

This camera did exactly what it said it would. It was essential for this research, and it came through with no problems. There were many features that made this a very nice camera, but the most attractive was the affordability. This was a nice high speed camera that provided a wide range of options for this research.



The Implant FFC to BNC Adapter

This was a specially designed adapter for recording from the pupal implant. It was designed by Maj. Ryan O'Hara, but was not able to fully be tested, due to the mortality rate of the pupae



Appendix B.

Manduca Sexta Background

The majority of this process is found in the *Teacher's Manual for the Tobacco Hornworm Nursery Kit* (Carolina Biological Supply Company, 2001). Tobacco hornworms are considered economic pests, and there have been extensive studies about how to control them. At the same time, they are often studied in research environments such as AFIT and other universities because of their large size and simplified anatomy. Hornworms are used as "model systems" for studying nervous systems. They are excellent fliers, so a great deal of time is devoted to understanding this process as well.

Hornworms are relatively easy to raise, and are often used in schools and classroom settings to present life studies to students. According to the teachers manual that was supplied with the eggs the tobacco hornworm range throughout South America, Central America, Mexico, the West Indies, the United States, and southern Canada.

The average life cycle, in a properly controlled environment, lasts about 30-40 days. The two most critical factors that must be correctly monitored are lighting and temperature. A malfunction with the temperature controller resulted in complete loss of 40+ pupae.

The lighting that was used during this experiment was on a 18 hour light/6 hour dark cycle, and it appeared to work well. The time was originally offset so that the hours of dusk fell for the pupae around 10:00 am, so that when they emerged they would be most active during the day. It became easier to work with them at night during their normal schedule, so this was adopted after the first batch emerged.

Eggs

Pale green hornworm eggs are shipped in a vial with a foam plug. Each smooth egg is about 1 mm in diameter, its color fading slowly to white as hatching approaches. The hatching chamber should be placed in an area with a relative humidity of 40-50% and a temperature of around 80°F. The hatching time varied, but most eggs hatched about three days after arrival.

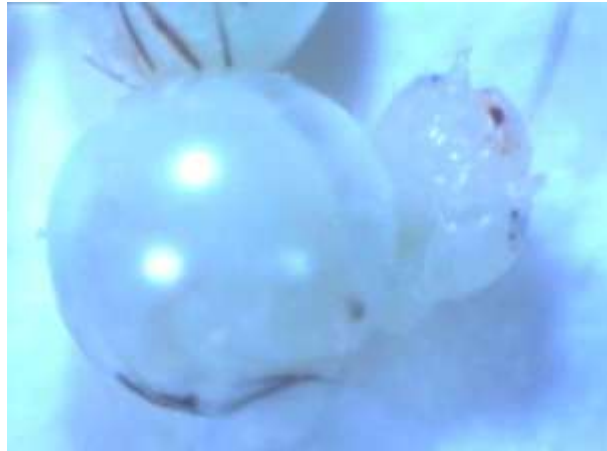


Figure 74: *M.sexta* hatching from its egg at 400x magnification

The last observed hatching was as late seven days. Figure 74 is an image from video taken of the hatching process using the Eyeclops microscope (Appendix A).

Larvae

The larvae (caterpillars) appear white or a pale yellow-green, with a long black horn at the posterior end when they first hatched (Figure 75). They gradually turn green over the first few days. Like all insects their bodies are divided into three parts: head, thorax, and abdomen. According to the included literature, the hornworms have compound eyes, three pairs of



Figure 75: Newly hatched *M.sexta* on the edge of a penny

thoracic legs, five pairs of prolegs, and a segmented abdomen. They breathe through openings, called spiracles, along the sides of their bodies.

The larvae pass through five larval instars (stages between molts) before the pupal instar is formed. The shedding of their exoskeleton marks the instar stages. It was very apparent that the most larval growth occurs in the fourth and fifth instars, as the literature stated, because the food consumption also increases dramatically during this time. A mature larvae weighs 10 grams on average, and is 7-10 cm long (Figure 77). Two quarts of hornworm diet were purchased for the larvae but this was not enough. Dr. Willis sent some diet just in time to sustain the larvae that were being raised. It is recommended to have at least four or five quarts on hand before raising another batch of eggs.



Figure 77: Mature larvae eating hornworm diet

Pupae

A pupa's cuticle, or exoskeleton, is transparent at first, revealing its bright green inner tissues (Figure 76). During this time, the pupa is soft and can be easily damaged or killed. Gradually, the cuticle turns reddish-brown, becomes opaque, and hardens. This hardening process is known as sclerotization.



Figure 76: *M.sexta* larvae becoming a pupae

Changes begin at the posterior end and move toward the anterior. The color of the pupa continues to deepen to a dark brown or black as adult emergence approaches.

Typically, the pupa is about 5 cm long and weighs over 4 grams. Within the pupal case, all appendages are tightly fused to the body; the tongue is also encased, and if broken, the pupa will die-this was particularly a problem when the pupae were mailed. On average, 1-2 would arrive with a broken tongue case. The abdomen is the only moveable part of the body. It is during this stage that you can determine the sex of the hornworm by observing the ventral (bottom) of the abdomen at segments.

Adults (Manduca sexta)

The adult emerges in early summer, weighing about 2 grams. The pupal case splits across the dorsal thorax and down the sides as the moth struggles out (Figure 78). Mottled dark gray with two parallel rows of yellow spots along the sides of its abdomen, the adult climbs to a vertical surface and spreads its wings (Figure 79). Its wingspan is 10-12 cm. The moth is a strong flier and performs most of its activities in the dark. In flight, its wings can beat rapidly, allowing it to hover in place. The adult has the ability to maintain an elevated



Figure 78: *M.sexta* pupae emerging as an adult

thoracic temperature during flight. This heat is an advantage as muscle operates more efficiently at higher temperatures. In fact, the moth often shivers its wings for a few minutes before take-off to increase its body temperature.

Preparation

Hatching Chamber

1. The hatching chamber was an 8-ounce cup containing the hornworm diet (about half inch deep at the bottom); a yellow plastic netting was placed inside to allow the baby hornworms to climb to the food.
2. The hatching chamber was inverted so that the lid was on the bottom and the food was on the top.
3. The lid from the hatching chamber had four holes punched through it with a hole punch. This was to allow air to circulate into the chamber and to help prevent mold from developing on the food.
4. The lid was placed on the table and one paper towel was placed on top of it.
5. The eggs were placed on the paper towel, and the chamber containing the food was then placed on top of the lid. The lid was tightened onto the chamber without inverting the cup and spilling the eggs onto the food.
6. The hatching chamber was placed, lid down, a temperature controlled aquarium with the temperature set to 80°F. The eggs began to hatch in about 3 days.



Figure 79: Adult *M.sexta* inflating its wings

Rearing Chamber

1. The larger larvae were transferred with a paint brush to large plastic containers that had been prepared with 1/5 of food. The unused portion of the diet was stored in a refrigerator or freezer depending on the amount.
2. A lattice was placed over the food and used to allow the larvae to climb upon, but it got soggy and did not work very well.
3. Many containers were kept and the larvae were transferred around to different containers depending upon their size, because the larger ones would hold onto the smaller ones and eventually kill them.
4. The food was checked daily and if mold began to form, it was remove immediately. In addition, the fecal material was removed daily.
6. When the worms stopped eating, and the dorsal aorta (a black pulsating line) was visible, they were transferred to a different container to begin pupation. It took approximately 3 weeks for each hornworm to go from an egg to the fifth instar, when the larvae were ready to begin pupation.

Pupating Chamber

1. Some of the pupae were placed in the supplied clear plastic pupating chamber (vial). Each container was loosely filled with pupating medium (bark chips), but the material was not packed down.
2. A foam plug was placed in the end of each pupating chamber, and the plastic cap was placed on the end of the chamber to secure the pupating hornworm.
3. The vials were then put in a dark box, giving them the sense of being underground.

4. The pupating hornworm were kept at 80°F.
 5. When the pupae have turned completely brown, they were then transferred back to the aquarium for observation.
 6. In a addition, so many larvae survived that there were not enough vials for each one.
- Therefore the process used in the Willis Labs was used here: a 4X6 board was cut approximately 6 inches long. One side had a 0.5 inch piece removed to act as the lid, and 4-6 holes were drilled with a diameter of 1.25 inches, to a depth of about 3-4 inches. The pupae were placed in the holes and the lid was held in place by rubber bands back on the top. This became the preferred method and clearly had the highest success rate for larvae becoming pupae without abnormalities.

Moth Cage

1. The white mesh moth cage was hung from the ceiling.
2. Approximately 10-12 days after pupation began, when they turned darker, the pupae were placed in the bottom of the moth cage. Most moths successfully emerged and their wings developed correctly in the moth cage.
3. A 40% sugar solution was made by mixing 40 g of sugar with 100 mL of water. The feeding solution had a few moths land on it, but they were never observed to actually drink. The adults could live up to 14 days under the right conditions.

Bibliography

- Adobe Systems Incorporated. (2011, n.d. n.d.). *Adobe After Effects [computer software]*. Retrieved Feb 28, 2011, from Adobe After Effects CS5:
<http://www.adobe.com/products/aftereffects/>
- Adobe Systems Incorporated. (2011). *Adobe Photoshop [computer software]*. Retrieved Feb 28, 2011, from Adobe Photoshop CS5:
<http://www.adobe.com/products/photoshop/compare/>
- Alexander, D. E. (2002). *Nature's Flyers; birds, insects and the biomechanics of flight*. Baltimore: The Johns Hopkins University Press.
- Audacity. (2011, n.d. n.d.). *Audacity*. Retrieved Feb 28, 2011, from Audacity:
<http://audacity.sourceforge.net/>
- Avid Technology, Inc. (2011, n.d. n.d.). *M-Audio*. Retrieved Feb 28, 2011, from M-Audio: http://www.m-audio.com/products/en_us/FastTrackPro.html
- Bayline, R. J., Duch, C., & Levine, R. B. (2001). Nerve–Muscle Interactions Regulate Motor Terminal Growth and Myoblast Distribution during Muscle Development. *Developmental Biology*, 348–363.
- Bertrand, T., Regnier, M., & Daniel, T. (2008). A spatially explicit model of muscle contraction explains a relationship between. *The Journal of Experimental Biology*, 180-186.
- Bozkurt, A. (2011, Jan 6). Email Correspondence. (T. Tubbs, Interviewer)
- Bozkurt, A., Gilmour, R., & Lal, A. (2009). Balloon-Assisted Flight of Radio-Controlled Insect Biobots. *IEEE Transactions On Biomedical Engineering*, 2304-2307.
- Braithwaite, W. (1853). Experiment in animal electricity. *Retrospect of Medicine: Containing a Retrospective view of every discovery and practical improvement in the medical sciences.*, 428.
- Cambell Neil A, Reece, J. B., & Mitchell, L. G. (1999). *Biology-5th Edition*. Menlo Park, CA: Benjamin/Cummings.
- Carolina Biological Supply Company. (2001, n.d. n.d). Tobacco hornworm Nursery Kit. *Teacher's Manual*. USA: Carolina Biological Supply Company.
- Chapman, R. F. (1998). *The Insects, 4th edition*. Cambridge: University Press.

- Chung, A. J., & Erickson, D. (2009). Engineering insect flight metabolics using immature stage implanted. *The Royal Society of Chemistry* , 669–676.
- Cobb, M. (2002, May). Exorcizing the Animal Spirits: Jan Swammerdam on Nerve Function. *Nature Reviews Neuroscience*, pp. 395-400.
- Cobb, R. (2011, Jan 18). Ezspectrum, personalized Matlab interface code. Dayton, OH, USA.
- Cranshaw, W. (2008, December). *Bacillus thuringiensis*. *Home & Garden, insect series*.
- De Luca, C. J. (1997). The use of surface electromyography in biomechanics. *Journal of Applied Biomechanics*, 135-163.
- Dondelinger, R. M. (2011, Jan 4). *Tools Of The Trade The Fundamentals Of Electromyography—An Overview*. Retrieved Jan 25, 2011, from Biomedical Instrumentation & Technology: <http://www.aami-bit.org/doi/xml/10.2345/0899-8205-44.2.128>
- Downs, T. (2009). *Ends of the Earth*. Nashville, Tennessee: Thomas Nelson, Inc.
- Evers, J. H. (2007). Biological Inspiration for Agile Autonomous Air Vehicles. *Defense Technical Information Center*, (p. 12).
- Geddes, L., & Roeder, R. (2002). The First Electronic Electrocardiograph . *Cardiovascular Engineering* , 13,14.
- Hinterwirth, A. (2010 , Jul 30). *Country diary: Shetland*. Retrieved Mar 12, 2011, from The Guardian: <http://www.guardian.co.uk/environment/2010/jul/30/country-diary-shetland>
- Johnston, R., & Levine, R. (1996). Locomotory behavior in the hawkmoth *Manduca sexta*: kinematic and elektromyographic analyses of the thoracic legs in larvae and adults. *J Exp Biol*, 759-774.
- Jungnickel, C., & McCormmach, R. (1999). *Cavendish: the experimental life*. unknown: Bucknell University Press.
- Kammer, A. E. (1971). The motor output during turning flight in a hawkmoth, *Manduca sexta*. *Journal of Insect Physiology*, 1073-1086.
- Keeley, L. (n.d.). *Vertebrate and Insect Muscle Innervation*. Retrieved Jan 21, 2011, from Department of Entomology Texas A&M University: <http://entochem.tamu.edu/VertInvertContractswf/index.html>

- Keithley, J. F. (1999). *The story of electrical and magnetic measurements: from 500 B.C. to the 1940s*. Piscataway, NJ: Wiley-IEEE Press.
- Knight, E., & Kinesiology, H. (2003, Aug 2). *Best Workout Exercises*. Retrieved Jan 25, 2011, from myfit.ca:
<http://www.myfit.ca/archives/viewanarticle.asp?table=fitness&id=28&subject=Best+Workout+Exercises>
- Kondoh, Y., & Obara, Y. (1982). Anatomy of motoneurons innervating mesothoracic indirect flight muscles in the silkworm, *bombyx mori*. *Journal of Experimental Biology*, 23-37.
- Liu, H., Ellington, C. P., Kawachi, K., Van Den Berg, C., & Willmott, A. P. (1998). A Computational Fluid Dynamic Study of Hawkmoth Hovering. *The Journal of Experimental Biology*, 201, 461–477.
- McGill, K., Lateva, Z., & Marateb, H. (2005). EMGLAB: an interactive EMG decomposition program. *J. Neurosci Methods*, 121-133.
- Medicine, U. N. (2010, August 28). *Electromyography*. Retrieved September 28, 2010, from National Library of Medicine - Medical Subject Headings:
http://www.nlm.nih.gov/cgi/mesh/2011/MB_cgi
- Mezoff, S. P., Takesian, A., & Trimmer, B. A. (2004). The biomechanical and neural control of hydrastatic limb movements in *Manduca Sexta*. *Journal of Experimental Biology*, 3043-53.
- Mohseni, P., Nagarajan, K., Ziaie, B., Najafi, K., & Crary, S. (2001). An Ultralight Biotelemetry Backpack for Recording EMG signals. *Transactions on Biomedical Engineering*, 734-737.
- Mohseni, P., Nagarajan, K., Ziaie, B., Najafi, K., & Crary, S. (2001). An Ultralight Biotelemetry Backpack for Recording EMG Signals in Moths. *IEEE Transactions on Biomedical Engineering*, 734-736.
- Nation, J. L. (2002). *Insect physiology and biochemistry*. Boca Raton, FL: CRC press LLC.
- Reeder, M. (2009). Editorial. *International Journal of Micro Air Vehicles*, i.
- Robertson, D. H. (2004). *Research Methods in Biomechanics*.
- Sato, H., Berry, C., Casey, B., Lavella, G., Yao, Y., VandenBrooks, J., et al. (2008). A cyborg beetle: Insect flight control through an implantable, tetherless

- microsystem. *IEEE 21st International Conference on Micro Electro Mechanical Systems*, (pp. 164 - 167). Tucson, AZ.
- Sauer, E. (n.d, n.d n.d). *Pine hawk moth sitting on conifer bark*. Retrieved Feb 12, 2011, from Corbisimages: <http://www.corbisimages.com/Enlargement/42-15315063.html>
- Sims, T. W., Palazotto, A. N., & Norris, A. (2010). A Structural Dynamic Analysis of a Manduca Sexta Forewing. *International Journal of Micro Air Vehicles*, 121.
- Talwar, S., Xu, S., Hawley, E., Weiss, S., Moxon, K., & Chapin, J. (2002). Rat navigation guided by remote control. *Nature*, 37-8.
- Tsang, W., Stone, A., Aldworth, Z., Otten, D., Akinwande, A., Daniel, T., et al. (2010). Remote control of a cyborg moth using carbon nanotube-enhanced flexible neuroprosthetic probe. *Micro Electro Mechanical Systems (MEMS), IEEE 23rd International Conference*. Wanchai, Hong Kong: IEEE.
- Tu, M. S., & Daniel, T. L. (2004). Submaximal power output from the dorsolongitudinal flight muscles of the hawkmoth *Manduca sexta*. *The Journal of Experimental Biology*, 4651-4662.
- Tubbs, T. B. (2010). Bio-Inspired research for Manufacturing Purposes. *ASC 25th Annual Technical Conference and the 14th US-Japan Conference on Composite Materials*. Dayton: DEStech Publications, Inc.
- unknown. (n.d, n.d n.d). *Pterodactyl (Pterodactylus antiquus), Jurassic, Germany*. Retrieved Feb 12, 2011, from Super Stock: <http://www.superstock.com/stock-photos-images/1566-0109989>
- Vaughn, C. L., Davis, B. L., & O'Connor, J. C. (1992). *Dynamics of Human Gait*. Howard Place, Western Cape, South Africa: Kiboho Publishers .
- Wang, H., Ando, N., & Kanzaki, R. (2008). Active control of free flight manoeuvres in a hawkmoth, *Agrius convolvuli*. *The Journal of Experimental Biology*, 423-432.
- Wang, H., Ando, N., & Kanzaki, R. (2008). Active control of free flight manoeuvres in a hawkmoth, *Agrius convolvuli*. *The Journal of Experimental Biology*, 423-432.
- Watson, J. T., & Ritzmann, R. E. (1995). Combined intracellular stimulation and high speed video motion analysis of motor control neurons in the cockroach. *Neuroscience Methods*, 151-157 .

- Willmott, A. P., & Ellington, C. P. (1997). The mechanics of flight in the hawkmoth *Manduca sexta*. *Journal Experimental Biology*, 2705–2722.
- Wize. (2010). *M-Audio Fast Track Pro External Sound System Reviews*. Retrieved March 23, 2009, from Wize, reporting the best & worst products: <http://wize.com/sound-cards/p1760-m-audio-fast-track-pro-external-sound-system>
- Zachry, T. (2004, n.d. n.d). *Historical Perspective of EMG*. Retrieved Jan 2, 2011, from University of Nevada, Las Vegas: <http://faculty.unlv.edu/jmercer/Seminar%20presentation/History.ppt>
- Zera, R. S. (2005). *Business Wit & Wisdom*. Washington DC: Beard Books.
- Zhongying, M. (2007, Mar 10). *China Science And Technology-Newsletter*. Retrieved Jan 27, 2011, from The Ministry of Science and Technology: http://www.most.gov.cn/eng/newsletters/2007/200703/t20070319_42154.htm

REPORT DOCUMENTATION PAGE			<i>Form Approved</i> <i>OMB No. 0704-0188</i>	
The public reporting burden for this collection of information is estimated to average 1 hour per response, including the time for reviewing instructions, searching existing data sources, gathering and maintaining the data needed, and completing and reviewing the collection of information. Send comments regarding this burden estimate or any other aspect of this collection of information, including suggestions for reducing this burden to Department of Defense, Washington Headquarters Services, Directorate for Information Operations and Reports (0704-0188), 1215 Jefferson Davis Highway, Suite 1204, Arlington, VA 22202-4302. Respondents should be aware that notwithstanding any other provision of law, no person shall be subject to any penalty for failing to comply with a collection of information if it does not display a currently valid OMB control number. PLEASE DO NOT RETURN YOUR FORM TO THE ABOVE ADDRESS.				
1. REPORT DATE (DD-MM-YYYY) 24 03 2011		2. REPORT TYPE Master's Thesis		3. DATES COVERED (From — To) Aug 2009-Mar 2011
4. TITLE AND SUBTITLE Title in Title Case Biological investigation of The stimulated flapping motions of the moth, <i>Manduca sexta</i>			5a. CONTRACT NUMBER	
			5b. GRANT NUMBER	
			5c. PROGRAM ELEMENT NUMBER	
6. AUTHOR(S) Tubbs, Travis B. Capt, USAF			5d. PROJECT NUMBER 212/127	
			5e. TASK NUMBER	
			5f. WORK UNIT NUMBER	
7. PERFORMING ORGANIZATION NAME(S) AND ADDRESS(ES) Air Force Institute of Technology Graduate School of Engineering and Management (AFIT/ENY) 2950 Hobson Way WPAFB OH 45433-7765			8. PERFORMING ORGANIZATION REPORT NUMBER AFIT/GSS/ENY/11-M04	
9. SPONSORING / MONITORING AGENCY NAME(S) AND ADDRESS(ES) Air Force Office of Scientific Research, AFOSR Dr. Douglas Smith, (douglas.smith@afosr.af.mil), (703) 696-6219 875 North Randolph St. Suite 325, Rm 3112, Arlington, Va. , 22203 Air Force Research Lab, AFRL Dr. Richard Snyder, (richard.snyder@wrpafb.af.mil), (937) 785-8473 2210 8 th St, B146 R220, WPAFB, OH			10. SPONSOR/MONITOR'S ACRONYM(S) AFOSR, AFRL	
			11. SPONSOR/MONITOR'S REPORT NUMBER(S)	
12. DISTRIBUTION / AVAILABILITY STATEMENT APPROVED FOR PUBLIC RELEASE; DISTRIBUTION UNLIMITED				
13. SUPPLEMENTARY NOTES This material is declared a work of the U.S. Government and is not subject to copyright protection in the United States.				
14. ABSTRACT An investigation was conducted assessing the possibility and feasibility of reproducing the biological flapping motion of the wings of the moth, <i>Manduca sexta</i> (hawkmoth) by artificially stimulating the flight muscles for Micro Air Vehicle research. Electromyographical signals were collected using bipolar intramuscular fine wire electrodes inserted into the primary flight muscles, the dorsal longitudinal and dorsal ventral muscles, of the adult <i>M.sexta</i> . These signals were recorded and associated with wing movement using high speed video. The signals were reapplied into the corresponding muscle groups with the intention of reproducing similar flapping motion. A series of impulse signals were also directed into the primary flight muscles as a means of observing muscle response through measured forewing angles. This study pioneered electromyographic research on <i>M.sexta</i> at the Air Force Institute of Technology with tests conducted with pupal implants and fine wire electrodes. Through this process, the research showed the deformational structural changes that take place when a wing is removed from an insect and proved that muscular stimulation is a viable means of measuring wing movement while still attached to the moth. This study also assisted in developing an understanding related to the role that a thorax-like fuselage could play in future micro aircraft designs. This study has shown that partial neuromuscular control of the primary flight muscles a <i>Manduca sexta</i> is possible with electrical stimulants which could be used to directly control insect flight.				
15. SUBJECT TERMS Manduca sexta, M.sexta, Micro Air Vehicle, MAV, Biological, Electromyography				
16. SECURITY CLASSIFICATION OF:			17. LIMITATION OF ABSTRACT UU	18. NUMBER OF PAGES 125
a. REPORT	b. ABSTRACT	c. THIS PAGE		
U	U	U	19a. NAME OF RESPONSIBLE PERSON .Dr.Anthony Palazotto, Professor, AFIT, (ENY)	
			19b. TELEPHONE NUMBER (Include Area Code) (937)255-3636, ext 4599 Email: Anthony.palazotto@afit.edu	

Standard Form 298 (Rev. 8-98)
Prescribed by ANSI Std. Z39.18